Synthetic Biology for Enhanced Protein Secretion

to Valorize Biological and Synthetic Polymers

by

Apurv Madhusudan Rachana Mhatre

A Dissertation Presented in Partial Fulfillment
of the Requirements for the Degree
Doctor of Philosophy

Approved May 2023 by the
Graduate Supervisory Committee:

Arul M Varman, Chair
David Nielsen
Rajeev Misra
Brent Nannenga
Cesar Torres

ARIZONA STATE UNIVERSITY

August 2023

ABSTRACT

Polymers have played a pivotal role in building modern society. Polymers can be classified as synthetic and natural polymers. Accumulation of both synthetic and natural polymer waste leads to environmental pollution. This dissertation aims at developing one-pot bioprocesses for a breakdown of natural polymers like cellulose, and hemicellulose and synthetic polymers like polyethylene terephthalate (PET).

First, a one-pot process was developed for hemicellulose breakdown. A signal peptide library of native SEC pathway signal peptides was developed for efficient secretion of endoxylanse enzyme. Furthermore, *in situ,* the process was successfully created for hemicellulose to xylose with the highest reported xylose titer of 7.1 g/L. In addition, *E. coli*: *B. subtilis* coculture bioprocess was developed to produce succinate, ethanol, and lactate from hemicellulose in one pot process.

Second, a one-pot process was developed for cellulose breakdown. *In vitro* enzyme assays were used to select SEC pathway signal peptides for endoglucanase and glucosidase secretion. Then, the breakdown of carboxymethyl cellulose (CMC), a cellulose derivative, was conducted in *in situ* conditions. U-^{13}C fingerprinting study showed carbon enrichment from CMC when cultures were cofed with CMC and [U-^{13}C] glucose. Further, Whatman filter paper sheets showed a change in shape in recombinant cocultures. SEM images showed continuous orientation in the case of two enzymes confirmed by fast Fourier transform (FFT), suggesting higher crystallinity of residues. Similarly, in microcrystalline cellulose breakdown in *in situ* conditions, a 72% reduction of avicel cellulose was achieved in a one pot bioprocess. SEM images revealed valleys and crevices on residues of coculture

compared to smoother surfaces in monoculture residues pressing the importance of the synergistic activity of enzymes.

Finally, one pot deconstruction process was developed for synthetic polymer PET. First, the PET hydrolase secretion strain was developed by selecting a signal peptide library. The first bis(2-hydroxyethyl) terephthalate (BHET) consolidated bioprocess was developed, which produced a terephthalic acid titer of 7.4 g/L. PET breakdown was successfully demonstrated in *in vitro* conditions with a TPA titer of 4 g/L. Furthermore, PET breakdown was successfully demonstrated in *in situ* conditions. Consolidated bioprocesses can be an invaluable approach to waste utilization and making cost-effective processes.

ACKNOWLEDGMENTS

TABLE OF CONTENTS

LIST OF TABLES

LIST OF FIGURES

CHAPTER 1

BACKGROUND AND MOTIVATION, RESEARCH AIMS, AND DISSERTATION

ORGANISATION

1.1 Background and Motivation

Polymers are an integral part of our day-to-day life. Different types of polymers are present, from a plate of food to the cell phone we use; they are everywhere, and their impact on humankind cannot be neglected. However, these polymers, which make our lives easier, can also contribute to environmental pollution if their waste is not mitigated. The simplest way to classify polymers can be synthetic polymers and natural polymers. Natural polymers contribute to environmental pollution in the form of agricultural waste, which is often burned in different parts of the world contributing to environmental pollution.

Similarly, synthetic polymers like plastics contribute to ocean pollution and clogging of other small water bodies (Lee & Li). These wastes are a rich source of carbon that can be untapped by different thermochemical treatments. Thermochemical treatments are energy intensive and can also lead to corrosive streams. Enzymatic hydrolysis is an excellent alternative to it with milder conditions and high specificity. One major demerit of enzymes being a viable alternative is that they are expensive, and 20% of total bioprocess cost can come from purified enzymes (Raftery & Karim, 2017). A solution to a costly enzyme is exporting enzymes in the fermentation media by the growing cultures and conducting hydrolysis and fermentation in one single step. To make this effective

alternative, it is essential that the concentration of enzymes in the media is at par with the purified enzymes used in bioprocesses. To achieve this, enzyme export machinery in the bacterium system should be studied and used to export enzymes of our interest in high concentrations. In the present work, signal peptides were analyzed to link them with enzymes to facilitate enzyme export. Signal peptides are short polypeptide chains recognized by membrane proteins (Bendtsen et al., 2004; Hemmerich et al., 2016; Schneewind & Missiakas, 2012). Signal peptides can play an essential role in efficient enzyme export. *Bacillus subtilis* is the host organism used in the present study due to its ability to export enzymes. There are three enzyme export pathways in *B. subtilis*: the SEC, TAT, and ABC. A significant portion of the enzymes are exported via the SEC pathway; hence, SEC pathway signal peptides were explored for this work. SEC pathway signal peptides were linked with hydrolytic enzymes of interest to export them in the *B. subtilis* system. There is significantly less information on how signal peptide enzyme combination work, and signal peptide-enzyme combinations are unique (Brockmeier et al., 2006). Hence, signal peptide enzyme libraries were developed and further screened using enzymatic assays to select the best-performing strain. The present study was conducted to explore two plant waste polymeric components of hemicellulose and cellulose and a synthetic polymer polyethylene terephthalate. The *in situ* processes were developed for one-step hydrolysis and carbon utilization in plant and plastic waste.

1.2 Aims and Objectives

The project aims at three primary objectives to increase the difficulty level.

1) Developing a one-pot hemicellulose breakdown process

Hemicellulose is the second most abundant component in plant biomass. Hemicellulose breaks down into C5 sugars using one single hydrolytic enzyme. The primary hypothesis was that by efficiently exporting endoxylanases, we could achieve a high extracellular concentration of endoxylanase to break down hemicellulose to xylose efficiently. The project aimed at:

a) Developing endoxylanase secretion strain

b) One pot of hemicellulose breakdown into C5 sugar xylose

c) Assimilation and metabolism of xylose to produce industrially viable products

2) Developing a one-pot cellulose breakdown process

Cellulose hydrolysis involves a hydrolytic enzyme cocktail wherein more than one enzyme work together for a complete breakdown of cellulose. In this study, an engineered *B. subtilis* coculture was to be developed to export two enzymes, primarily endoglucanase and glucosidase. We hypothesize that efficient secretion and increase in enzyme concentration in supernatant will lead to will further lead to complete enzymatic hydrolysis of cellulose

a) Developing endoglucanase and glucosidase secreting strains

b) Selection of best exporters using enzymatic assays

c) Developing one pot cellulose breakdown process

3) Developing a one-pot process for PET plastic

PET plastic substrate is different than the previously explored substrate. It is highly crystalline and hydrophobic. Different known PET hydrolyzing enzyme candidates were chosen and linked with signal peptides to develop a signal peptide enzyme library. We hypothesize that efficiently exporting PET hydrolyzing enzymes can increase enzyme

concentration in extracellular media to conduct PET hydrolysis efficiently. The project aimed at the following

a) Developing PET hydrolytic enzyme secreting strain

b) Develop a strategy to increase the bioavailability of PET surface

c) Demonstrating one-pot deconstruction of PET components

1.3 Organisation of Dissertation

The thesis aims to showcase our work on developing bacterial platforms for efficiently utilizing synthetic and natural polymers as a source of untapped carbon for producing useful chemicals. In Chapter 2, we extensively discuss available literature in the field of research, which covers all three aims of the project. Chapter 3 demonstrates synergistic hemicellulose breakdown, assimilation, and product formation in a coculture process. It discusses the development of consolidated bioprocess wherein *B. subtilis* and *E. coli* cocultures are used to break down hemicellulose into xylose and use xylose to produce succinic acid. In Chapter 4, we further demonstrate β glucosidase secreting *B. subtilis* strains depolymerize and assimilate cellobiose and plan to construct cellulose depolymerizing strains. Cellulose depolymerization to glucose needs the operation of at least two cellulases. In this chapter, we developed a *B. subtilis* coculture which synergistically depolymerizes cellulose to glucose. This coculture was used to explore different types of cellulose substrates like CMC, Whatman filter paper, and avicel cellulose. Chapter 4 explores synthetic polymer PET and aims to develop a signal peptide PETase/ cutinase small library to develop a PET breakdown system. This project aims to

develop a *B. subtilis* strain that can efficiently depolymerize PET polymer into terephthalic acid and ethylene glycol. After selecting the best performing strain from the library developed. The potential of UV treatment was explored to study the bioavailability of the PET surface.

Furthermore, the first *in situ* BHET deconstruction process was demonstrated. At last, in Chapter 6, we discuss conclusions generated in all the chapters and the scope of possible future works. Hemicellulose can be completely depolymerized using one enzyme, whereas cellulose needs an enzyme cocktail for a complete breakdown. PET is highly hydrophobic, and enzyme surface contacting needs to be attained efficiently in this process.

CHAPTER 2

CRITICAL REVIEW OF RESEARCH

2.1 Polymers: a blessing or a curse!

Humankind has relied on crude oil for fulfilling its energy needs for over a century. Crude oil provides energy and is used for making plastics, cosmetics, naphtha, organic solvents, etc. Although crude oil is a significant resource for providing fuels and building block chemicals, it has adverse environmental impacts. Other than petroleum, crude oil is the major source of different polymers used in everyday products. Polymers can be classified as synthetic and natural polymers. Bakelite was the first synthetic polymer developed using polymerization reaction; a surge in synthetic polymers' production soon escalated. Some commonly used synthetic polymers are polyethylene terephthalate, polyethylene, polystyrene, etc. Due to their malleability, lightweight, tensile strength, low cost, high-temperature stability, etc (Reinert and Carbone, 2008). Synthetic polymers are used in almost every modern equipment, gadget, textiles, household product, etc.

Mass production of synthetic polymers also came with the mass accumulation of non-biodegradable waste. Polymers are also present in nature in different forms. These are referred to as natural polymers; some examples are alginates, rubber, carrageenan, xantham, etc (Kulkarni et al., 2012). The utilization of these polymers (synthetic and natural) can help explore untapped resources to produce useful chemicals. Thermochemical and biological methods have been investigated for the breakdown of polymers (Lynd et al., 2005; Öhgren et al., 2007; Wu et al., 2017; Xu and Huang, 2014). Production of fuels and chemicals by bioprocessing synthetic and natural polymers is a promising alternative to

non-renewable fossil fuel resources. The most abundant source of natural polymers is stored in the form of lignocellulosic biomass.

2.1.1 Natural polymers

Natural polymers range from silk secreted by silkworms to DNA and protein molecules. Natural polymers can be characterized as plant origin and animal origin polymers. Animal origin polymers include chitin, alginates, silk, xanthan gum, etc. Plant-based natural polymers are cellulose, hemicellulose, glucomannan, agar, etc. (Kulkarni et al., 2012). Lignocellulosic biomass is one of the most common natural polymers found in nature.

Lignocellulosic biomass

Lignocellulosic biomass is one of the most abundant carbon feedstock available on earth. Different lignocellulosic biomass sources include energy crops, forest residues, algae, wood processing residues, municipal waste, and wet waste. Agricultural crop residues are one of the most abundant and low-cost lignocellulosic waste available and hence is a valuable resource for making low-cost products like fuels. Biomass mainly constitutes cellulose and hemicellulose polymers bundled inside a lignin sheet (Figure 2). Cellulose is a long chain biopolymer containing glucan subunits linked together using β-1,4 glycosidic linkages and comprises 35 to 55% of the total lignocellulosic biomass (Zhang et al., 2011). Unlike cellulose, which has only glucose subunits, hemicellulose comprises several pentose sugars. The most abundant pentose sugar in hemicellulose is xylose. Rhamnose, mannose, galactose, and arabinose are the other monomers that make up hemicellulose. Also, hemicellulose is not a single chain structure but is branched

7

together into sheets forming plant cell walls. Hemicellulose is available in different forms, mainly as xylan, glucuronoxylan, arabinoxylan, glucomannan, and xyloglucan. Xylan being the most abundant of them, we have explored it as a carbon feedstock and the work discussed in Chapter 2. Lignin is the third principal component in biomass after cellulose and hemicellulose. Lignin forms a secondary structure in plant cell walls, offering most of its rigidity. Lignin is the primary source of non-fossil carbon among the biopolymer components in plant biomass (Calvo-Flores and Dobado, 2010). Lignin predominantly contains aromatic derivatives, which can be toxic to bacterial cells used in fermentation.
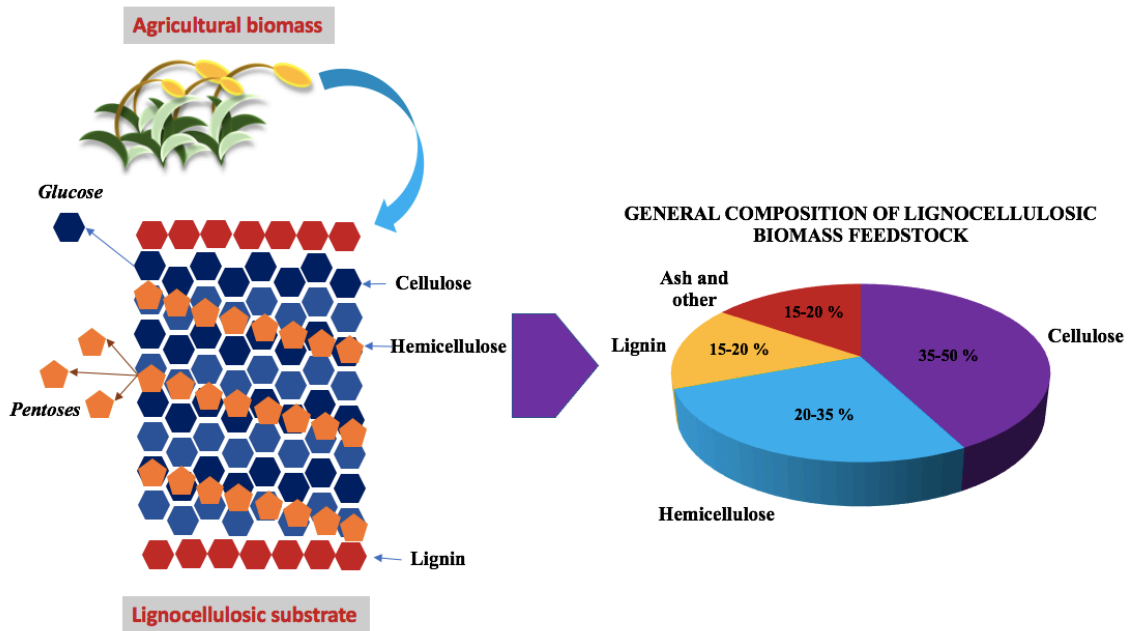
Figure 2.1: Structure and composition of lignocellulosic biomass. Lignocellulosic biomass which can be sourced from agricultural wastes at a low-cost and is mainly composed of the following three components: cellulose (blue), hemicellulose (orange), and lignin (red). Hemicellulose and cellulose polymers are bundled together by recalcitrant lignin and are made up of hexose and pentose sugars.

2.1.2 Synthetic polymers

Synthetic polymers like PET, PVC, PLA, PCL, PDO, polyesters, polyethylene, and polymer blends are widely used to make essential products. For example, polyethylene terephthalate (PET) is the most commonly used polymer in the textile and packaging industry. As a result, more than 70 million tonne production of PET was predicted to be produced in 2020 (Sang et al., 2020).

2.1.2.1Polyethylene terephthalate

Polyethylene terephthalate is a synthetic polymer formed by polycondensation of bis(hydroxyethyl)terephthalate. PET is mainly used in the packaging industry for making PET bottles because of its dimensional stability, resistance to impact, moisture, alcohol, and solvents. PET bottles have 50% recycling efficiency, and a significantly high portion escapes waste recycling systems. PET can only be recycled for a limited number of cycles, so developing technologies for its degradation is essential.

2.2 Methods of polymer treatment

Polymers discussed previously are long-chain structures formed by monomeric units linked together by covalent bonds. Monomeric units obtained after the breakdown of polymers can be utilized as feedstock to produce alternative products or the production of polymers again to bypass recycling.

2.2.1 Photolytic degradation of PET

When Pet is exposed to UV light, chain scission occurs, and the mechanism by which this happens is called chain scission. Chain scission is Norrish type I and type II reactions that involve radicals leading to PET regions' cleaving. Amorphous regions are

more affected by photolysis than crystalline regions. Photolysis of PET depends on oxygen, hydroperoxides, and carbonyls (Sang et al., 2020). UV light in a range lower than 315 nm has shown strong absorption in PET, as shown by Fechine et al., 2002. The Photolysis of a Pet in the presence of UV light reduces mechanical properties.

2.2.2 Chemical Method of PET Depolymerization

Depolymerization of PET is carried out by glycolysis reaction in polyethylene glycol and catalyst at temperatures ranging between 150 to 300 $^{\circ}$C and 2 to 10 hours. Different catalysts used in the PET depolymerization method can be broadly classified as metal-based catalysts and organic catalysts containing nitrogen bases. Flores et al., 2019 demonstrated PET-polylactic acid copolymer hydrolytic breakdown in phosphate buffer. Similarly, PET depolymerization and recycling system in zinc acetate, sodium, and potassium salts are shown by López-Fonseca et al., 2010.

2.2.3 Effect of UV Treatment on a polymer surface

UV treatment can improve the bioavailability of the PET plastic surface. UV exposure to some of the plastic surfaces can lead to movement of photons which further leads to formation of free radicals which in presence of oxygen lead to degradation of plastic surface. UV treatment has been known to improve hydrophilicity of the surface which assists in biodegradation. As shown in table below:

Table 2.1 Effect of UV treatment on biodegradation times of different organisms (Taghavi et al., 2021)

Plastic Type	Strain	Pretreatment	Degradation time (day)	Weight loss %	References
PE	*B. subtilis*	UV (300 nm)	30	9.26	(Vimala & Mathew, 2016)
PE	*B. subtilis*	UV (280-370 nm)	730	8.4	(Roy et al., 2008)
PE	*Penecillium simplicissimum*	UV and acid UV	90	38	(Sowmya et al., 2015)
PE	*Penecillium simplicissimum*	UV(<300 nm)	90	-	(Yamada-Onodera et al., 2001)
PE	*A. pitti*	UV (245 nm)	180	-3.5	(V.Mahalakshmi, 2012)
PE	*Curvularia lunata*	UV (354 nm)	28	26.8	(Montazer et al., 2018)
PE	*A. niger*	UV (245 nm)	90	43.76	(Raut et al., 2015)
PE	*B. borstelensis*	UV (312 nm)	126	29.5	(Arkatkar et al., 2010)
PP	*B. Flexus + P. asotoformans*	UV (225 nm)	365	1.95	(Aravinthan et al., 2016)

2.2.4 Thermochemical methods of lignocellulosic biomass breakdown

Pre-treatment is a process by which the recalcitrance in lignocellulosic biomass is overcome to make biomass components such as cellulose and hemicellulose more accessible by enzymes for hydrolysis (Singh et al., 2015). There is a wide range of pre-treatment methods developed and used in industry, from physical treatments like milling, extrusion, etc., to chemical techniques like acid, alkaline, ionic liquid treatments (Figure 2.2). Physical pre-treatments mainly include milling, extrusion, microwave, and freeze

treatments (Haghighi Mood et al., 2013). As the name suggests, the major physical pre-treatment processes, milling, and extrusion mostly use shear forces to break down biomass components. All the physical treatment methods have the drawback of having low energy efficiency and high cost. Chemical treatment methods in biomass include acid, alkaline, ionic liquids, organic solvents, and ozonolysis. These chemical treatments vary based on the chemicals used in the treatments like acid treatments mainly include sulphuric acid/HCL, alkaline treatments use bases like sodium hydroxide, solvents like methanol, ethanol, etc. in organic solvent treatment, Ozone gas in the oxidation of biomass components, and ionic liquids like 1-allyl-3-methylimidazolium-chloride ([AMIM]Cl), 1-ethyl-3-methylimidazolium-acetate ([EMIM]Ac), 1- butyl-3-methylimidazolium chloride ([BMIM]Cl), etc. (Haghighi Mood et al., 2013; Mesa et al., 2011; Wan et al., 2011a; Zavrel et al., 2009).
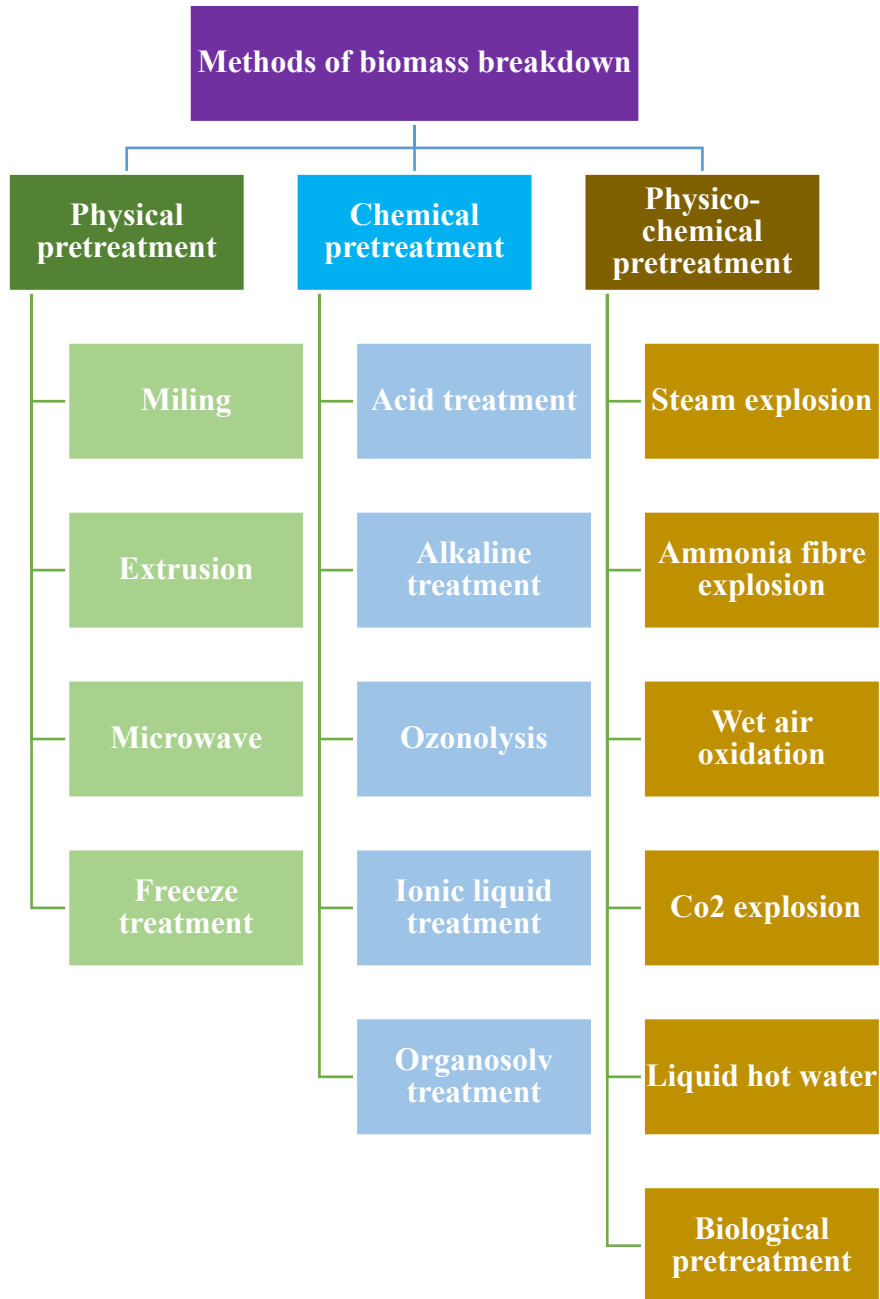
Figure 2.2: Overview of different biomass breakdown methods

Major drawbacks in chemical treatments include corrosiveness to equipment, microbial toxicity, production of fermentation inhibitors like furfurals, the need for neutralization, and incompatibility of the chemicals with hydrolases (Li et al., 2010; Sun

and Cheng, 2002; Taherzadeh and Karimi, 2008; Wan et al., 2011b). Along with using chemicals and physical conditions for the pre-treatment, substantial efforts have been made to combine physical and chemical treatments. Different physiochemical pre-treatment methods include steam explosion, wet air oxidation, CO_2 explosion, Ammonia fibre explosion, biological treatment, and liquid hot water. Steam explosion involves the high-pressure breakdown of biomass in the presence of steam. The Ammonia fibre explosion method consists of the breakdown of biomass in the presence of ammonia, steam, and pressure. As different pre-treatment methods have multiple drawbacks, combining these methods (combination pre-treatment) can be used to overcome the limitation of individual pre-treatment.

2.2.5 Enzymatic hydrolysis of polymers

Thermochemical treatment methods mostly operate in harsh conditions, produce inhibitory-products that can affect the environment. On the other hand, Enzymatic hydrolysis is a promising alternative with milder conditions, high specificity, high reaction rates, and lower operating temperatures. Enzymatic hydrolysis of polymers can be conducted with different types of enzymes like esterase's, peroxidases, cellulases, endoxylanases, lipases, etc.

Enzymatic hydrolysis of polymers

Enzymatic hydrolysis of natural and synthetic polymers follow different mechanisms. Natural polymers are hydrophilic, and hence enzymes can easily absorb on their surface. Hydrolysis of natural polymers like cellulose is not completely known, but these cellulases like cellobiohydrolases cleave cellulose chain at reducing and non-reducing ends (Table 1.3). On the contrary, synthetic polymers are highly hydrophobic,

14

and for efficient reactions to occur, enzymes should absorb on their surfaces. Carboxylic esterases can overcome this obstacle because some have hydrophobic patches on them (cutinases) which or have interfacial activity mechanism to increase activity (lipases).

Table 2.2: Different enzymes having a role in synthetic polymer degradation (Banerjee et al., 2014; Yoshida et al., 2016; Silva et al., 2011; Sulaiman et al., 2012)

Polymer	Key enzyme
Polyethylene glycol	Dehydrogenases
Polypropylene glycol	Dehydrogenases
Polytetramethylene glycol	Dehydrogenases
Polyvinyl alcohol	Oxidases or dehydrogenase or hydrolase
Polycaprolactone	Lipase and cutinase
Polylactic acid	Protease and lipase
Polyethylene terephthalate	Cultinase and PET hydrolase

2.2.5.1 Enzymatic hydrolysis of PET

Enzymatic hydrolysis of PET has been reported by several studies, as shown in table 2.3. Most of the Pet hydrolytic enzymes are cutinases and lipases. Cutinases hydrolyse cutin, an insoluble polyester secreted by plants, and lipases show hydrolytic activities towards insoluble triglycerides. Esterases have also been reported in few cases to successfully hydrolyse PET. In the case of *Bacillus subtilis p*-nitrobenzylesterase enzyme was reported to effectively breakdown PET polymer (Ribitsch et al., 2011). *Ideonella*

sakaiensis was isolated from PET bottles and can hydrolyze and assimilate PET components (Shosuke Yoshida, Kazumi Hiraga, Toshihiko Takehana et al., 2016). *Ideonella sakaiensis* secretes an enzyme called PETase, which can hydrolyse PET.
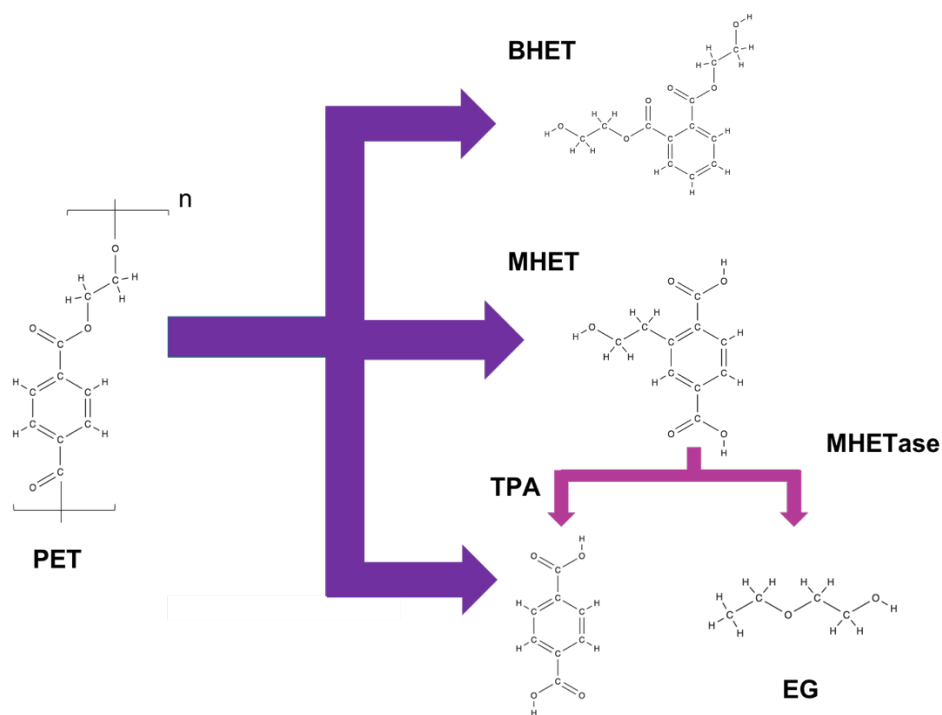
Figure 2.3: PETase hydrolysis mechanism of PET polymer to produce PET derivatives like MHET (mono (2 - hydroxyethyl) terephthalic acid), BHET (bis (2-hydroxyethyl) terephthalic acid), TPA (Terephthalic acid), and EG (Ethylene glycol). PETase can degrade PET at moderate temperature (30 °C) into BHET, MHET, TPA and EG and MHETase breaks MHET into TPA and EG.

PETase from *Ideonella sakaiensis* is considered most efficient and more specific to PET than other PET degrading enzymes (Han et al., 2017). Figure 2.3 shows the PET degradation mechanism by PETase. As shown in the figure, PETase can individually descale PET polymer into its monomeric components, and the PET depolymerization can be further supported by the synergistic effect of MHETase involved in MHET breakdown.

16

Table: 2.3 Reported PET hydrolases

Name	Source	Genbank accession number	Optimal pH, Optimal Temp (°C), acitivity	Substrate	References
TfCut1	*Thermobifida fusca KW3*	CBY05529.1	pH 8; Temp: 55 °C	IcPET film	(Herrero Acero et al., 2011; Roth et al., 2014)
TfCut2		CBY05530.1	pH 8; Temp: 55 °C	IcPET film	(Herrero Acero et al., 2011; Roth et al., 2014)
LC-cutinase	Leaf branch compost metagenome	AEV21261.1	pH 8; Temp: 50 °C ;12 mg/h/mg of enzyme	Amorphous PET film	(Sulaiman et al., 2014, 2012)
Cut1	*Thermobifida fusca* NRRL B-8184	JN129499.1	pH 8, Temp: 55 °C, 318 ± 0.73 (U/ml)	*p* Nitrophenol butyrate	(Hegde and Veeranki, 2013)
Cut2		JN129500.1	pH 8, Temp: 55 °C, 316 ± 0.9 (U/ml)	*p* Nitrophenol butyrate	(Hegde and Veeranki, 2013)
PETase	*Ideonella sakaiensis* strain 201-F6	GAP38373.1	pH 9; 30 °C;	IcPET (1.9%) and bottle grade hcPET	(Tournier et al., 2020; Yoshida et al., 2016)
BsEstB	*Bacillus subtilis* 4P3-11	ADH43200.1	pH 7; Temp: 40 °C; 108 U/mg	3PET; *p*- nitrophenyl butyrate	(Ribitsch et al., 2011)
Fsc	*Fusarium solani* pisi	1CEX	pH: 7.4 Temp 37 °C; 100 U/mg	IcPET (7%) bo-PET (35%); *p*-	(Araújo et al., 2007; Silva et al., 2011)

17

| Hic | *Humicola insolens* | 4OYY | pH 7; Temp 60 ºC | nitrophenyl butyrate IcPET (7%) bo-PET (35%) | (Carniel et al., 2017; de Castro et al., 2017) |

2.2.5.2 Enzymatic hydrolysis of lignocellulosic biomass

Enzymatic hydrolysis involves using enzymes as a catalyst for the hydrolysis and oxidation reaction of biomass components obtained from the pre-treatment process (Mtui, 2009). Enzymes like cellulases attack the β-1,4 glycosidic bonds in the cellulose backbone and breakdown cellulose structure into monomeric hexose sugars (Zhang et al., 2011). Different enzymes cleave different regions in cellulose, hemicellulose, and lignin (Table 2.4). Enzymatic reactions are conducted at milder conditions using lower temperatures and benign chemicals. Enzymatic reactions are precise and have no by-products, which makes them highly atom economic reactions. Hydrolysis is a rate-limiting step in different fermentation processes like anaerobic digestions, ethanol fermentation, butanol fermentation, etc. Enzymatic reactions can be used in the hydrolysis step to improve these fermentation processes (Hosseini Koupaie et al., 2019). Enzymatic hydrolysis is a promising method that uses low energy, greener solvents, and high efficiency, but its high cost is one of its drawbacks. The primary reasons behind the high price of enzymes are the higher purification cost. Methods like consolidated bioprocessing can solve the high-cost problem and reduce unit operations and exogenous enzyme supplementation (Chinn and Mbaneme, 2015; Lynd et al., 2005; Olson et al., 2012; Van Zyl et al., 2007).

Table 2.4: List of enzymes that cleave different regions in lignocellulose biomass components, lignin, cellulose, and hemicellulose (Lynd et al., 2005).

Enzymes	Cleavage site
Cellulases	
Cellobiohydrolase	Hydrolyses cellulose chain at reducing and non-reducing ends
Endoglucanase	Internal glycosidic bonds of cellulose
ß glucosidase	cellobiose and cellodextrin
Phospho ß glucosidase	cellobiose and cellodextrin
Hemicellulases	
Endoxylanases	Glucoronoxylan and arabinoxylan
ß xylosidase	Xylooligosaccharide and xylobiose
Galactosidase	Galactomannan and pectin
Ferulolyl esterase	Ferulolyl esters of arabinoxylan, Xyloglucan
Mannanase	Glucomannan and galactomannan
Xyloglucan	Glucan of xyloglucan hydrolase

2.3 Microbial hosts and protein secretion pathways

When microorganisms were first studied under a microscope, their ability to get stained by crystal violet/ safranin indicated there was some difference in these organisms, which are part of our surroundings for ages. Later, the difference in the staining in the organism was observed because of the peptidoglycan layer (Schneewind and Missiakas, 2012). There are many differences in gram-positive and gram-negative bacteria, like gram negatives having an extra outer membrane. Different bacteria are used in the industry, engineered to metabolize monomeric carbon sources and produce useful chemicals. *Escherichia. coli*, *Bacillus sp*, *Corynebacterium glutamicum,* and *Saccharomyces*

cerevisiae are extensively used in industry due to the availability of genetic manipulation tools.

2.3.1 Bacterial platforms for hydrolase expression

E. coli

E. coli is a gram-negative bacteria which is extensively studied for synthetic biology and metabolic engineering host system. *E. coli* is unarguably the most studied organism for the development of hydrolase expression systems. *E. coli* has been used as a whole-cell catalyst that specifically binds to cellulosic materials (Francisco et al., 1993). *E. coli* cocultures system to utilize hemicellulose and produce ethanol has been explored by Shin et al., 2010. Similarly, *E. coli* has been engineered to biosynthesize a wide variety of chemicals, including fatty acids, isopropanol, alkanes, butanol and isoprenoids (Hasunuma et al., 2013).

Bacillus sp

Bacillus subtilis is gram-positive bacteria that is used in industries for the production of amylases. *B. subtilis* has developed an expression system and has been used previously in exporting hydrolases for depolymerizing biopolymers. *B. subtilis* also has native endoxylanases, nitrobenzylesterase, and endoglucanases which have been expressed for the breakdown of cellulose, hemicellulose, and PET in different research works (Jeong et al., 1998; Ribitsch et al., 2011; Zhang et al., 2011). Synergistic breakdown of cellulose using bacillus megaterium coculture system by expressing endoglucanase (EG11) and cellulase (Cel9AT) was demonstrated by (Kalbarczyk et al., 2018). Similarly, *Bacillus coagulans,* a thermophilic bacteria, have been a promising candidate for lignocellulosic

biomass fermentations. B. coagulans have a unique pentose phosphate pathway active at 50-55 °C and pH five optimal conditions for commercial cellulases. *Bacillus coagulans* though having multiple advantages, is difficult to engineer because of which *B. subtillis* is the preferred host in Bacillus sp.

Corynebacterium glutamicum

C. glutamicum is gram-positive, non-sporulating, non-motile bacteria belonging to order actinomycetes. It's an important organism in the industry because it is utilised to produce amino acids mainly glutamic acid. It cannot metabolize pentose, and hence it is has been engineered to metabolize different types of sugars. Simultaneous cellobiose, xylose, and glucose utilization has been demonstrated in *C glutamicum* by Sasaki et al., 2008 by integrating xylose isomerase, xylulokinase from *E. coli*. *C. glutamicum* has the inherent ability to assimilate aromatics which makes it ideal candidate for exporting cellulases and utilization of lignocellulosic biomass components. Enhanced hydrolysis of cellulosic components by expressing cellulosomes was demonstrated by Hyeon et al., 2011 in *C. glutamicum.*

2.3.2 Protein secretion pathways

One significant difference between gram-positive and gram-negative bacteria is the way protein secretion happens in them. Signal peptide-bearing proteins are exported into the extracellular environment in gram-positive bacteria, whereas on the contrary, in gram-negative bacteria, proteins are localized in the periplasm (Schneewind et al., 1992; Schneewind and Missiakas, 2012). Protein secretion pathways have been extensively studied in *Bacillus subtilis* (a gram-positive bacterium) and can serve as a microbial host

for protein secretion. Major protein secretion pathways include the Sec pathway and TAT (Twin arginine translocation) pathway. Sec pathway is the major protein export pathway and exports more proteins compared to the TAT pathway.

2.3.2.1 Secretion (Sec) pathway

Sec pathway is involved in significant protein export in gram-positive bacteria. There are 173 different signal peptides in *Bacillus subtilis,* which are engaged in exporting extracellular proteins via the sec pathway (Brockmeier et al., 2006; Fu et al., 2018). Signal peptide sequence length varies in gram-positive bacteria (approx. 32 amino acids) compared to gram-negative bacteria (approx. 24 amino acids) (Bendtsen et al., 2004). Sec-dependent protein export mainly has two parts co-translational pathway and post-translational pathway. Co translational pathway involves the export of membrane protein, and the post-translational pathway consists of the export of extracellular protein. Figure 2.4 shows that the SRP protein recognizes the signal peptide sequence, and the signal peptide sequence is cleaved by signal peptidases. Gram-positive bacteria like *bacillus subtilis* have up to 6 signal peptidases native to the organism, which cleaves different signal peptides.
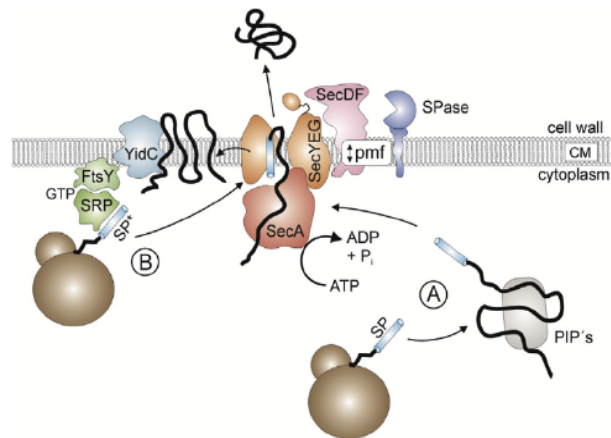
Figure 2.4: General secretion (Sec-) pathway in gram-positive bacteria
(Freudl, 2013) Sec pathway found in gram-negative *E. coli* and gram-positive
B. subtilis follow the same mechanism.

Role of signal peptides in protein secretion

Signal peptides are short peptide chains recognized by membrane proteins that play
an essential role in protein export. Signal peptide structure has a positively charged N
domain, the hydrophobic core, and the hydrophilic signal peptidase region (Brockmeier et
al., 2006; Freudl, 2013). Signal peptide sequences play an essential role in the protein
secretion process, and hence signal peptides have been fused with heterologous proteins to
estimate secretion efficiency (Fu et al., 2018; Hong et al., 2015; Zhang et al., 2011).
Estimation of secretion efficiency of signal peptides and proteins is not yet possible, and it
can be unique. It has been observed that specific signal peptides that work with some
proteins might not necessarily export other proteins. Development of high throughput
libraries has been conducted to select optimal signal peptides, which will show high
translocation efficiency (Degering et al., 2010; Fu et al., 2018; Hemmerich et al., 2016).

2.4   Consolidated bioprocessing (CBP)

The biomass pre-treatment and fermentation process have many challenges. The cost of enzyme, feedstock, and pre-treatment constitu   he total cost. Enzyme co is the largest among all the listed expenses, which leads to high product cost (Bayer et al., 2007). Consolidated bioprocessing helps in reducing the expenditure incurred due t enzymes. Consolidated bioprocessing is a one-pot reaction that includes hydrolysis and fermentation (Chinn and Mbaneme, 2015; Olson et al., 2012). Consolidated bioprocessing has enzyme secretion, enzymatic saccharification of biomass components to sugars, and utilization of produced sugars to produce chemicals like ethanol, lactic acid, etc. (Figure 2.5).
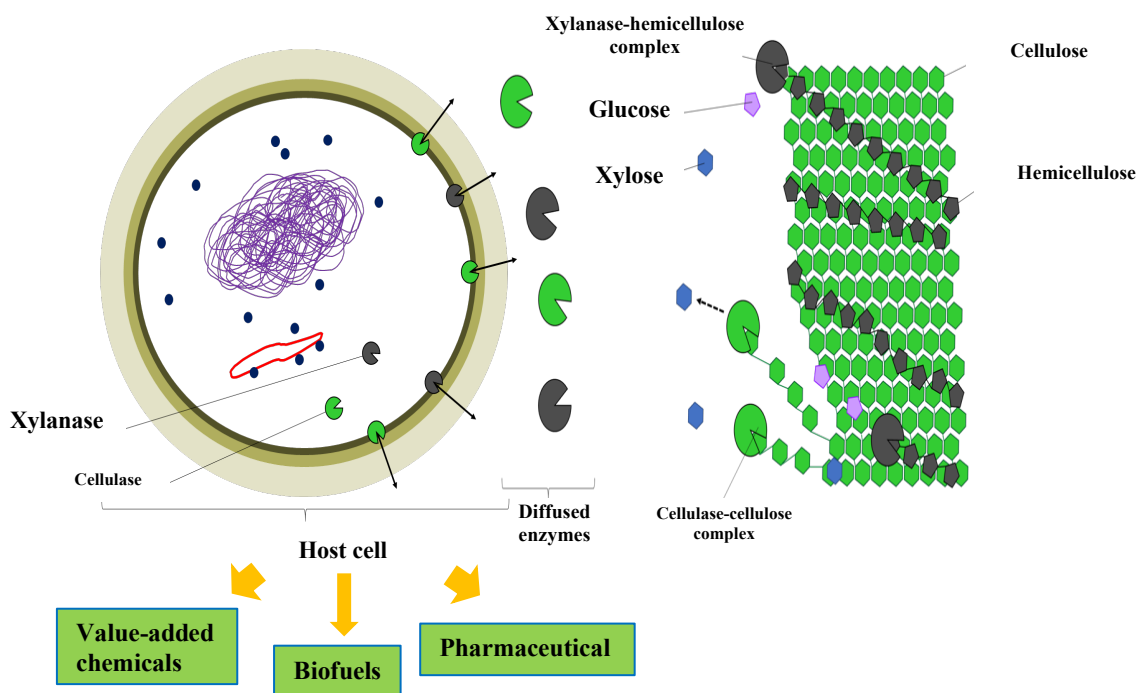
Figure 2.5: Overview of consolidated bioprocessing: Consolidated bioprocess involves exporting extracellular enzymes like cellulases and xylanases, which simultaneously hydrolyse biomass components like cellulose and hemicellulose to glucose and xylose. The host cell further assimilates these sugars to make products like value-added chemicals, biofuels, and pharmaceuticals.

Consolidated bioprocesses have been used to utilize different carbon sources like starch, cellulose, hemicellulose, etc. Some of the consolidated bioprocesses developed using *B. subtilis*, *E. coli,* and *C. glutamicum* systems have been shown in table 2.4.

Advantages of CBP mainly include reducing overall cost, enhancing processing efficiencies, eliminating the need for hydrolytic enzymes, and reducing sugar inhibition of cellulases (Jouzani and Taherzadeh, 2015; Shin et al., 2010; Zhang et al., 2011). Present work involves developing consolidated bioprocesses for depolymerization of different biomass components to produce succinic acid and aromatic chemicals.

Table 2.5 Consolidated bioprocesses reported using *B. subtilis*, *E. coli,* and *C. glutamicum* systems

Organism	Substrate	Enzyme	Product	Yield (g/L)	References
B. subtilis	Cellulose	Endoglucanase	Lactate	3.1	(Zhang et al., 2011)
E. coli	Benchwood xylan	Xylanase	FAEE	0.012	(Steen et al., 2010)
E. coli	Birchwood xylan	Xylanase, acetylxylan esterase, xyloside permease, b xylosidase	Ethanol	3.7	(Shin et al., 2010)
B. subtilis and *Clostridium butylicum*	Cassava starch	Amylase	ABE	7.4	
C. glutamicum	Xylan	Endoxylanase, xylosidase	Glycine	2	(Yim et al., 2016)

26

C. glutamicum	Xylan	Endoxylanase, xylosidase	Xylonic acid	6.23	(Yim et al., 2017)

The reason why consolidated bioprocesses were developed was to reduce the cost incurred by commercial enzymes in the bioprocess. As shown in Table 2.5, we can see a cost difference of approx. 13 million $. The comparison of the conventional process and CBP shows that the major difference in the cost comes from enzyme cost, which was zero in consolidated bioprocess, making CBP a promising bioprocess approach.

Table 2.6 Cost (in million $ per year) breakdown comparison of consolidated bioprocess (CBP) and separate hydrolysis followed by fermentation (conventional process) (Raftery and Karim, 2017)

	CBP	Conventional process
Annual capital cost	23.66	13.44
Fermentation cost	2.97	0.66
Enzyme cost	0.00	25.91
Total biomass cost	44.45	44.45
Total pre-treatment cost	1.98	1.98
Process water cost	6.67	9.82
Wastewater treatment cost	12.84	11.29
Utilities cost	2.48	0.07
Labour cost	34.47	39.77
Total annual cost	123.89	137.58

CHAPTER 3

CONSOLIDATED BIOPROCESSING OF HEMICELLULOSE USING *BACILLUS SUBTILIS*: *ESCHERICHIA COLI* CONSORTIA FOR PRODUCTION OF SUCCINIC ACID

Abstract

Lignocellulosic feedstock is an inexpensive and renewable carbon source for the sustainable production of fuels and chemicals. However, isolating sugars from plant biomass for bioconversion by microbial cell factories requires the use of expensive enzymes to break down the hemicellulosic components. In contrast, consolidated bioprocessing of plant biomass is efficient and cost-effective as it combines enzyme production, hemicellulose hydrolysis as well as fermentation in a single pot. In the present work, as a first step we have aimed to develop *Bacillus subtilis* strains for heterologous expression and secretion of endoxylanases for extracellular depolymerization of hemicellulose. Two xylanases from *Trichoderma resei (Tr)* and *Bacilus pumilis (Valero-Valdivieso et al.)*, were selected based on their pH and temperature compatibility to the optimal growth conditions of *Bacillus subtilis*. Different combinations of signal peptides YwmC, SacC, and AmyE with the two xylanases were explored for the selection of an optimal design. Engineered strain SSL26, harbouring YwmC-XynA(Valero-Valdivieso et al.), displayed a 2 fold increase in endoxylanase activity compared to strains engineered with SacC and AmyE signal peptides. *In situ* depolymerization of xylan with SSL26 produced a maximum xylose titre of 15 g/L, which is 4 folds higher than most effective titre reported previously in literature. As a final step, a *B. subtilis: E. coli* consortia was

28

developed to break down xylan and produce succinate in a single pot achieving a succinate yield of 3.7 g/L from 10 g/L xylan. This approach can be further explored for the consolidated bioprocessing of cellulose and hemicellulose obtained directly from plant biomass for the production of a wide variety of fermentation by-products.

3.1 Introduction

The advent of the 21st century has seen a surge in energy demands, depletion of fossil fuel reserves, and detrimental effects of the fossil fuel industry on the environment. Therefore, alternative energy sources have been extensively explored to reduce our dependence on non-renewable fuel resources. Lignocellulosic plant biomass has been considered a bountiful and cheap feedstock for the production of fuels and chemicals and extensive efforts are being invested worldwide to valorise it. Lignocellulosic plant biomass is made up of 3 major biopolymers viz. cellulose, hemicellulose, and lignin (Furkan H. Isikgora and Remzi Becer 2015).

Cellulose is a long chain biopolymer composed of glucan subunits, linearly linked via β- 1,4 glycosidic linkages, arranged in hierarchical conformations of microfibrils (Zaaba, Jaafar, and Ismail 2021). Unlike cellulose, lignin is an arbitrarily branched heteropolymer comprised of aromatic derivatives (Eudes et al. 2014; Wu et al. 2017). Similarly, hemicellulose is branched together into sheets, forming non cellulosic polysaccharide, which is mainly found in the form of xylan, glucuronoxylan, arabinoxylan, glucomannan, and xyloglucan. Lignocellulosic biomass can be coherently hydrolysed by thermochemical treatments, but its demerits include formation of non-benign chemicals (furfural, hydroxymethylfurfural etc), its energy intensiveness, and its requirement for

expensive catalysts (Li et al., 2010; Sun and Cheng, 2002; Taherzadeh and Karimi, 2008; Wan et al., 2011b; Stephanopoulos 2007). Enzymatic hydrolysis on other hand, has potential advantages over thermochemical hydrolysis, such as lower pollution generation, greater specificity, milder conditions, no loss of substrate due to modification, and higher yields (Isroi et al. 2011; Taherzadeh and Karimi 2008; Thomson 1993; Vasco-Correa, Ge, and Li 2016). Although, enzymatic hydrolysis has multiple merits, the slower rates and high cost make it industrially quixotic. A consolidated bioprocessing approach seeks at reducing process complexity and cost by amalgamating bioprocess operations.

Consolidated bioprocessing involves one-step enzyme secretion, hydrolysis, and fermentation; which has a lower operating and capital cost than dedicated enzyme production (Jiang et al. 2018; Olson et al. 2012; Stephanopoulos 2007; X. Z. Zhang et al. 2011). Selection of germane organism for consolidated bioprocess is extremely important, owing to wide range of functions accomplished concomitantly in the process. Lignocellulosic biomass components can be synergistically depolymerized by filamentous soil fungi and soil bacterium. However, these depolymerization reactions require dedicated effort from these organisms and are comparatively slower than thermochemical processes. These factors make utilization of these naturally capable organisms inefficacious for depolymerization and indicates pressing need to develop microbial consortia. Bacterial systems have been copiously utilized for production of chemicals owing to their well-developed genetic engineering tools. Hence, engineering bacterial consortia for efficient enzyme secretion and fermentation can help develop efficient, cost effective and industrially scalable consolidated bioprocess. While, enzyme secretion and export has been

extensively studied in gram negative bacteria like *Escherichia coli*, gram positive bacteria have shown better secretion system because of their single cellular membrane (Anné et al. 2014; Ng and Sarkar 2013; W. Wang et al. 2013). *Bacillus subtilis* is a gram positive bacterial host system explored in present work due to its enzyme secretion abilities.

B. subtilis WB800N is gram positive bacteria, which has its native signal peptide machinery and low protease activity. Secretion of proteins in gram positive bacteria takes place by signal peptide sequence tagged at the N terminus, which is responsible for exporting proteins via Sec and Tat pathways: these signal peptides can be used to facilitate protein export (Anné et al. 2014; Braun et al. 1999; Dozot et al. 2006; Freudl 2013; Maffei, Francetic, and Subtil 2017). An exhaustive study on signal peptides of *B. subtilis* has been reported by (Brockmeier et al. 2006a, 2006b), which shows that signal peptides can increase the extracellular enzyme export in *B subtilis*. *B. subtilis* has been extensively used in industries to produce enzymes, such as amylases and proteases, because of its efficient enzyme export system. It is anticipated that because of its wide industrial applications, *B. subtilis* will play an essential role in converting biomass to bioproducts (Nielsen et al. 2009; X. Z. Zhang et al. 2011). Xylose obtained after enzymatic hydrolysis of hemicellulose is arduous, or often impossible to metabolize in many bacterial species. Microbes which can metabolize xylose cannot assimilate xylose in presence of glucose, because of carbon catabolite repression (CCR). CCR is a regulatory mechanism which exhibits biphasic growth characteristic in which glucose is preferred over secondary carbon sources. Co-culture processes use microbial consortia which can be used to distribute metabolic load

31

based on inherent abilities of organisms. An *E. coli* production strain with no CCR will be co-cultured with the *B. subtilis* strain developed in this study

In this work, we demonstrate heterologous overexpression of endo-1,4-b-xylanase enzyme system in *B. subtilis* host and development of a sequential process for production of succinic acid from hemicellulose (Figure 3.1). Different enzyme and signal peptide combinations were used to select recombinant strains with the highest xylan degradation activity. Recombinant strains were able to successfully breakdown complex hemicellulosic polymer xylan to monomeric xylose sugar. A *B. subtilis* and *E. coli* consortia was used in sequential process for breakdown of xylan to xylose and utilization of xylose for production of succinic acid.
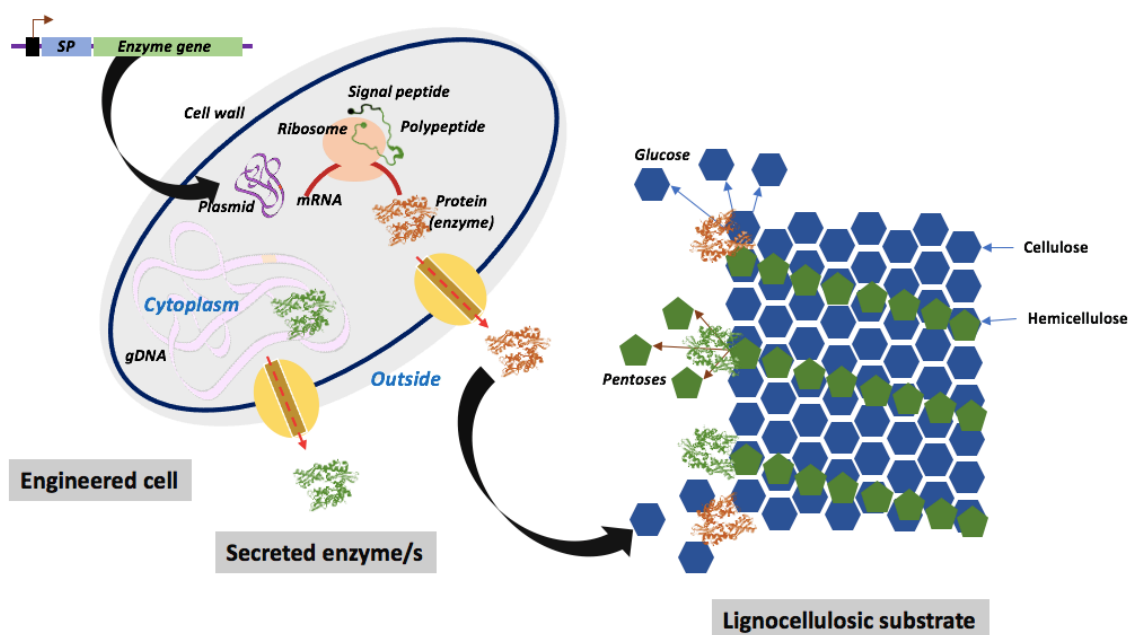
Figure 3.1: Demonstration of *in situ* depolymerization of biomass in a consolidated bioprocess. The figure shows signal peptide-enzyme constructs, transformed in *B. subtilis* WB800N strain in pHT254 vector system, having Pgrac100 promoter, Chloramphenicol, and Ampicillin markers. Furthermore, enzyme export in the *B. subtilis* strain and depolymerization of lignocellulosic biomass components is shown.

3.2 Materials and Methods

3.2.1 Chemicals and Materials

All the chemicals were reagent grade or higher, purchased from Sigma Aldrich (St. Louis, MO, USA), unless separately mentioned. Birchwood xylan was purchased from Megazyme Inc (Bray, Ireland). Oligonucleotides used in the present study were purchased from Milipore sigma (St. Louis, MO, USA). Details of the oligonucleotides are given in Table 3.1. All restriction enzymes were purchased from Thermo Fischer Scientific Inc (San Francisco bay area, CA, USA). Signal peptides and Gene sequences were synthesized by Genescript (Piscataway, NJ, USA).

3.2.2 Bacterial strains, media and plasmids

E. coli (*Escherichia coli*) Dh5α strains were used as a host for plasmid transformation. A protease deficient *Bacillus subtilis* WB800N strain was used as a host organism for xylan fermentations. Luria Bertani (Tryptone 10g; Yeast extract 5 g; Sodium chloride 10g) media was used for culturing *E. coli* cells at 37 °C at 250 rpm. 2xYT (Tryptone 16g; Yeast extract 10 g; Sodium chloride 5g) media was used to cultivate and transform *B. subtilis* cells. *In vitro* xylan breakdown was carried in modified media henceforth referred to as 3M media. Plasmids constructed and used in the present study and genotypes of bacterial strains, are given in table 3.2.

Table 3.1: Oligonucleotide sequences used in present study

Primer Name	Sequence	Description
AMYE FWD	gcggataacaattcccatataaaggaggaaggatccatgtttgcaaa acgattcaaaacctctttactgccg	Amy E signal peptide insert forward primer
AMYE 10 REV	cccgccaacagagacgtaaaagataccatcagcactcgcagccgc	Amy E signal peptide insert reverse primer for Pkb 10
XYN2 10 FWD	gcggctgcgagtgctgatggtatcttttacgtctctgttggcggg	Xy(Tr) gene overhang for Pkb 10 forward primer
XYN2 10 Rev	gatggtgatgagcgacgtcgactctagattaggacaccgtaatgctt gcggag	Xy(Tr) gene overhang for Pkb 10 reverse primer
SacC FWD	gagcggataacaattcccatataaaggaggaaggatccatgaaaaa gagactgattcaagtcatgatcatgttcaccc	SacC signal peptide insert forward primer
SacC 06 REV	cccgccaacagagacgtaaaagataccatctgcatctgccgaaaat gccatagtcaac	Amy E signal peptide insert reverse primer for Pkb 06
Xyn2 06 FWD	gttgactatggcattttcggcagatgcagatggtatcttttacgtctctgt tggcggg	Xy(Tr) gene overhang for Pkb 06 forward primer
Xyn2 06 REV	ggtgatgagcgacgtcgactctagattaggacaccgtaatgcttgcg gagc	Xy(Tr) gene overhang for Pkb 06 reverse primer

Table 3.2 Plasmids and strains

Plasmids/strains	Description	Source /reference
pHT254	Backbone plasmid for all the developed constructs with ColE1 Ori*	Mobitec, Inc
pKB01	Derived from pHT254 with *YwmC-XynA* and Pgrac100 promoter	This study
pKB02	Derived from pHT254 with *YwmC-Xyn2* and Pgrac100 promoter	This study
pKB06	Derived from pHT254 with AmyE-*Xyn2* and Pgrac100 promoter	This study
pKB10	Derived from pHT254 with *SacC-Xyn2* and Pgrac100 promoter	This study
Strains		
E. coli Dh5alpha	Cloning host strain	New England biolabs
AF30	LP001 *Δ*galP glk::Kan	Borrowed from Prof. Wang lab
B. subtilis	WB800N: *nprE aprE epr bpr mpr::ble nprB::bsr Δvpr wprA::hyg cm::neo*	Mobitec, Inc
SSL26	*B. subtilis* Pgrac100:: *YwmC-XynA::*Cm^r	This study
SSL27	*B. subtilis* Pgrac100:: *YwmC-Xyn2::*Cm^r	This study
SSL30	*B. subtilis* Pgrac100:: AmyE-*Xyn2::*Cm^r	This study
SSL33	*B. subtilis* Pgrac100:: *SacC-Xyn2::*Cm^r	This study

3.2.3 Plasmid construction and transformation

The vector pHT254, having Pgrac100 promoter, was used for the construction of pKB plasmids. Oligonucleotides were used to amplify the respective gene and signal peptide sequences. pKB 01 and pKB 02 constructs were developed by restriction digestion of plasmid and inserts at BamHI and XbaI restriction sites. Final constructs were developed using ligation of digested fragments. Plasmid pKB 06 and pKB 10 were constructed using the CPEC cloning method by joining fragments amplified with oligonucleotides (Table 3.1). *E. coli* transformation was performed using heat shock transformation method (JoVE Science Education Database 2017). *Bacillus subtilis* transformation method was modified from (Zhang et al. 2011)

3.2.4 Enzymatic Assays

Recombinant strains were grown in 5 mL 2xYT (Tryptone 16 g/L; Yeast Extract 10 g/L; Sodium Chloride 5 g/L) media till logarithmic growth phase (OD_{600}: 0.8) and induced (1mM Isopropyl β-D-1-thiogalactopyranoside (IPTG)) to enable enzyme secretion. Supernatant samples were collected after 24 hours and further used for enzyme reactions. The enzyme reaction was carried out in citrate phosphate buffer at 50 °C for 1 hour at pH 5. Reducing sugar content in enzyme reaction was estimated using DNS assay (Kim et al. 2014).

3.2.5 Xylan fermentation

Xylan fermentations were carried out at 37 °C for 5 days. The media used in xylan fermentation was 3M buffered media at pH 6 (Table 3.3). Recombinant strains were grown in 3M media at 250 rpm for 4 hours. The strains were induced with 0.2 mM IPTG to express

the xylanase enzyme. The fermentation batches were samples after 24, 48, 72, 96 hrs after IPTG induction. Fermentation batch samples were further analysed for OD_{600} and HPLC analysis.

Table. 3.3 M9 media in citric acid buffer (10x)

Sr no	Chemical name	Chemical formula	Amount (grams)
1	Sodium phosphate dibasic	Na_2HPO_4	3.21
2	Monopotassium phosphate	KH_2PO_4	0.6
3	Sodium chloride	Nacl	0.5
4	Citric acid	$C_6H_8O_7$	1.79

Table 3.4 Trace metal solution (1000x)

Sr no	Chemical name	Chemical formula	Concentration (mM)	Amount (grams)
1	Manganese sulphate	$MnSO_4$	100	0.169
2	Copper sulphate	$CuSO_4$	100	0.249
3	Ferrous sulphate	$FeSO_4$	100	0.278
4	Zinc sulphate	$ZnSO_4$	60	0.172

Table 3.5 3M media composition for 5 mL total volume

Name	Concentration	Volume
Magnesium sulphate ($MgSO_4$)	2M	10 µl
M9 media in citric acid buffer	10x	500 µl
Trace metal solution	1000x	5 µl
Calcium chloride ($Cacl_2$)	1M	0.5 µl
D- glucose ($C_6H_{12}O_6$)	20% (w/v)	500 µl
Chloramphenicol	50 mg/ml	0.5 µl
Birchwood xylan	10% (w/v)	500 µl
Deionized water		3484 µl

Note: concentration of xylan has been increased in some experiments.

3.2.6 Coculture fermentation

SSL26 (*B. subtilis*) strain were cultured in 1% xylan 3M media and IPTG (0.2 mM) induced at OD_{600} of 0.8. The fermentation was carried out in aerobic conditions for 24 hours after induction. *E. coli* strains were added in different (0.5:1; 1:1; 1.5:1; 2:1) *E. coli: B. subtilis* ratio.

3.2.7 Analytical methods

High-performance liquid chromatography (HPLC) (Agilent technologies 1100 series; G1311A, Santa Clara, CA) was used to quantitate metabolites formed in fermentation media. The compounds were separated using Rezex ROA-organic acid H^+ column (300 * 7.8 mm) at a temperature of 70 $^{\circ}$C with 5mM H_2SO_4 as mobile phase at a flow rate of 0.6 ml/min and detected with a refractive index detector (Agilent technologies 1200 series; G1362A, Santa Clara, CA). The samples were quantified using comparison with D-Xylose, Birchwood xylan and succinic acid calibration curves (2 to 20 g/L).

3.3 Results

3.3.1 Development of signal peptide- endoxylanase constructs

Host organism selected for present study was *Bacillus subtilis* WB800N strain because of its secretion efficiency and protease deficient nature. Unlike other components of lignocellulosic biomass like cellulose and lignin which require synergistic application of multiple enzymes hemicellulose can be depolymerized to xylose using endoxylanases (Shin et al. 2010). The endoxylanases cleave the β-1,4-linked backbone of polysaccharide xylan to D-xylose. The genomic studies show that *B. subtilis* has secretory endoxylanases, but wild-type strain does not have xylan to xylose breakdown ability (Kunst et al. 1997;

Harold Tjalsma et al. 2000; Wolf et al. 1995). Endo-1,4-b-xylanase that initiates xylan's degradation into xylooligosaccharides, is the most critical enzyme in xylan breakdown (Jeong et al. 1998). Endoxylanases used in the present study were derived from *T. resei* (Xyn2) and *B. pumilis* (XynA). Enzymes were selected based on their reported activity, optimal temperature and pH. The enzymes were used in a consolidated bioprocess, hence we wanted them to show optimal performance at favorable temperature and pH and were selected based on that criterion. Heterologous Endoxylanase (Xyn2) from *T. resei* expressed in *S. cerevisiae* showed 1,577 nkat/ml of xylanase activity (La Grange et al. 2001). XynA isolated from *B. pumilis* conveyed efficient degradation of xylanases (Qu and Shao 2011).

A
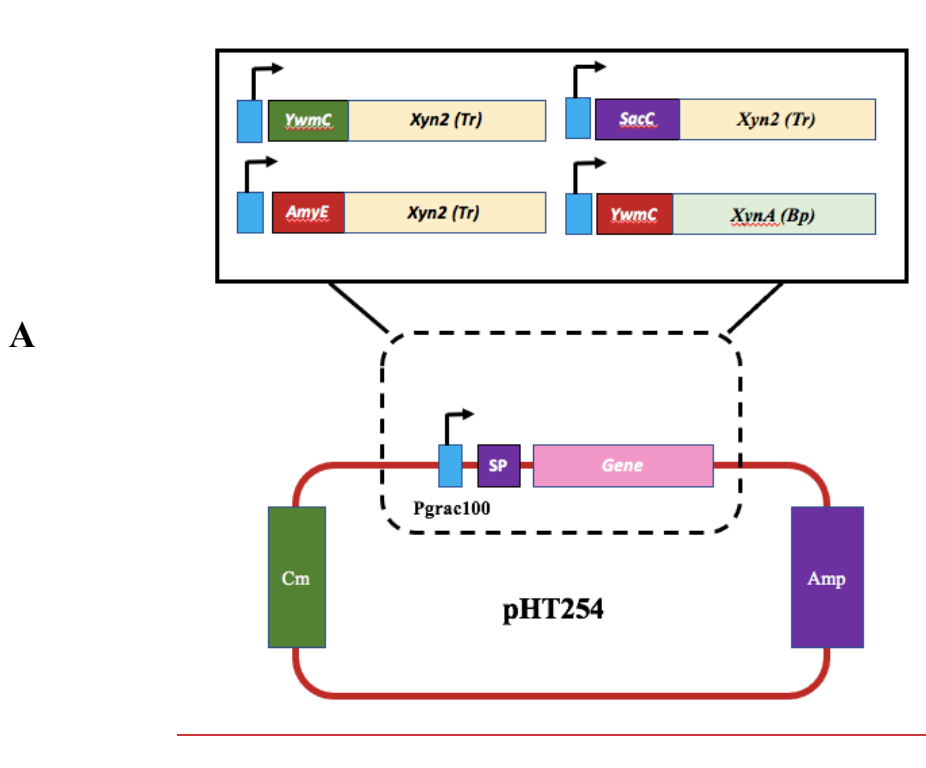
B
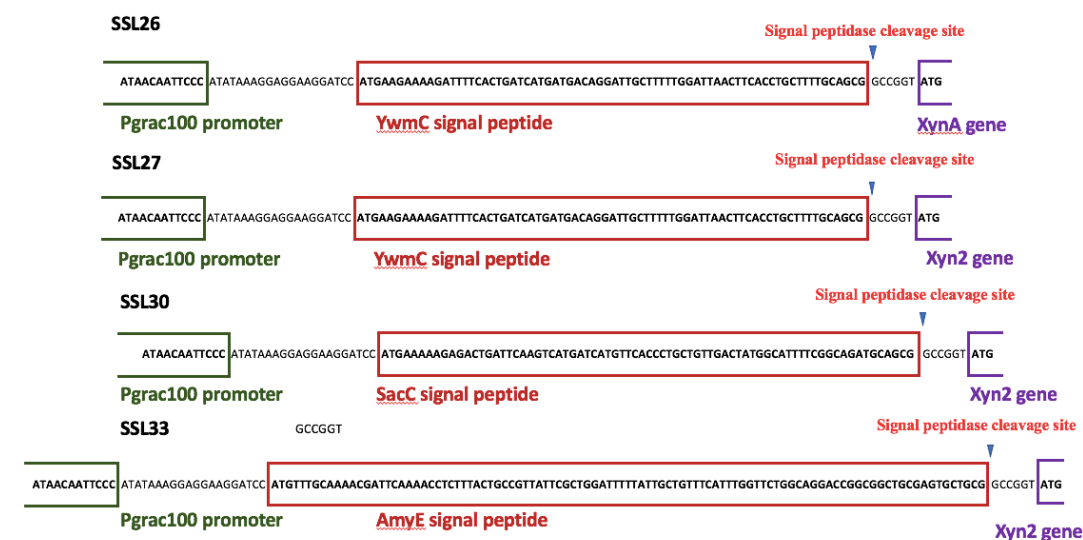
Figure 3.2: Detailed overview of plasmid constructs developed in present work: A) Overview of plasmid constructs developed in work and its transformation in WB800N *B. subtili*s strain. All four constructs developed in present study having Endoxylanases XynA from *B. pumilis (Valero-Valdivieso et al.)* and Xyn2 from *T. resei (Tr)* were linked to AmyE, SacC and YwmC native signal peptide, to constrict SSL26, SSL27, SSL30, SSL33 strains. B) Sequences of Pgrac100 promoter, signal peptide, signal peptidase cleavage site and gene for SSL26 (*YwmC – XynA*), SSL27 (*YwmC – Xyn2)*, SSL30 (*SacC – Xyn2*) and SSL33 (*AmyE – Xyn2*) strains

Signal peptides are short-chain peptides that assist in protein secretion in bacterial cells, and play a vital role in protein export, specifically in the Sec pathway. There are 173 known signal peptides involved in the export of proteins via the Sec pathway in *Bacillus subtilis* (Brockmeier et al. 2006b). Signal peptide and protein combinations are precise; appropriate signal peptide and protein combinations can show a drastic increase in protein secretion levels (Brockmeier et al. 2006b; H. Tjalsma et al. 2000).We engineered secretion of the two endoxylanases discussed above using three signal peptide sequences native to *Bacillus subtilis*. Signal peptide libraries used in present study were AmyE, YwmC and

40

SacC. Although signal peptide-enzyme combinations are highly specific, comprehensively studied signal peptides were used in present work. AmyE is native *B. subtilis* signal peptide which facilitates secretion of amylases. Around 70% of industrially produced amylases are produced by *Bacillus subtili*s, hence AmyE is thoroughly studied for secretion of different types of heterologous proteins (Brockmeier et al. 2006b; Hemilä et al. 1992; Kakeshita et al. 2011; H. Tjalsma et al. 2000). Similarly, YwmC signal peptide showed two-fold higher extracellular cutinase activity in a *B. subtilis* sec signal peptide library (Hemmerich et al. 2016). Also, SacC signal peptide has demonstrated coherent secretion of heterologous expression of proteins like PETase, levanase, pectate lyase etc. (Martin et al. 1987; Scotti et al. 1996; N. Wang et al. 2020) Signal peptide sequences were linked to endoxylanases at N terminal with signal peptidase cleavage site between signal peptide and endoxylanase (Figure 2.2b). Signal peptide linked to endoglucanase constructs were further transformed in *Bacillus subtilis* WB800N strain.

3.3.2 Engineering of *B. subtilis* strain for endoxylanase secretion and hemicellulose depolymerization

Supernatant samples of *Bacillus subtilis* WB800N strain transformed with pKB 01, 02, 06, and 10 constructs, induced with 1mM IPTG, were used in enzyme reaction. DNS assay was performed at the end of the reaction to determine reducing sugars (g/L) in enzyme reaction. Figure 3.3 shows reducing sugar produced (g/L) in an enzyme reaction. Significant difference in color change was visible in SSL 26 strain compared to all the other strains after DNS assay reaction (Figure 3.3). As shown in Figure 3.3A, instantaneous increase in reducing sugar formation was observed in first 15 minutes of enzyme reaction

in SSL26 strain. DNS assay studies showed 3-fold increase in the reducing sugar at 0.5% birchwood xylan substrate concentrations, in SSL26 strain compared to other constructs developed in the present study (SSL 27, SSL32, SSL33). Furthermore, enzyme reaction was performed for increasing substrate concentrations and SSL26 consistently showed 3-fold increase in reducing sugar (g/L) in 1%, 2% and 5% xylan. As discussed previously *B. subtilis* has native endoxylanase which can contribute to background noise. Wild type strains similar to SSL27, SSL30 and SSL 33 strains showed minimal color change and reducing sugar production compared to SSL26. The reducing sugar produced in enzyme reactions was 12.25 ± 2.06 % of the added substrate. These results indicate pKB 01 strain showing significant degradation (3-fold) compared to wild-type and commercial xylanase.
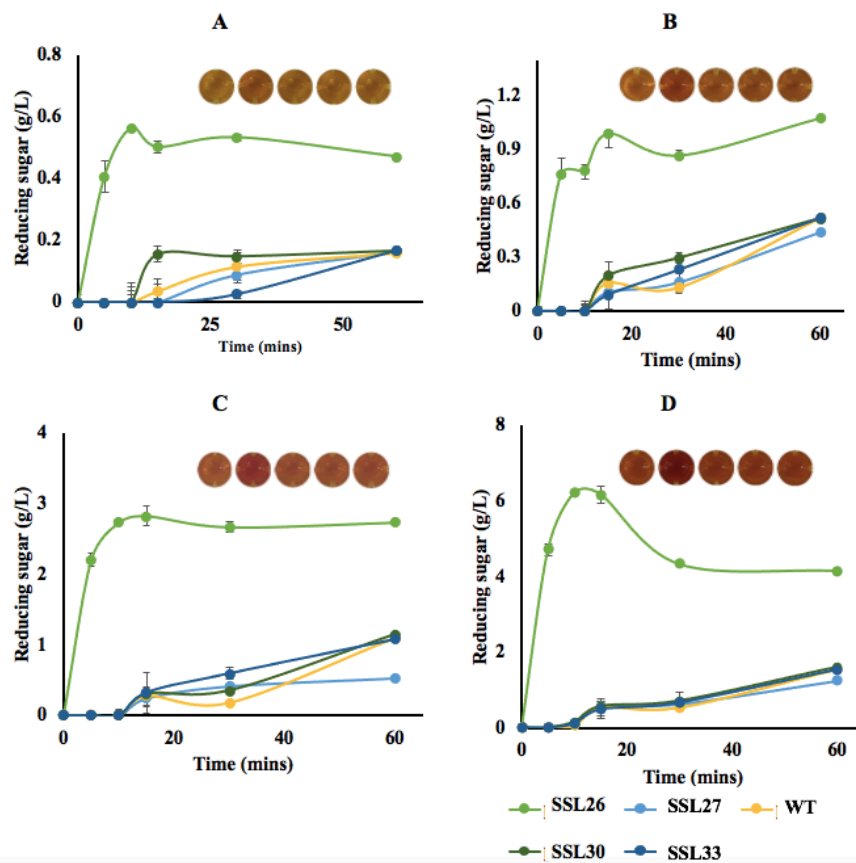
Figure 3.3: Comparison of reducing sugar (g/L; means ± SD; n=3) kinetics between developed recombinants and wild type strain: Different strains used in the present work were as follows: SS26 (pKB01 construct): pHT254 vector harbouring *YwmC – XynA (B. pumilis;* SS27 (pKB02 construct): pHT254 vector harbouring *YwmC – Xyn2 (T. Resei);* SS30 (pKB06 construct): pHT254 vector harbouring *SacC – Xyn2;*

SS33 (pKB10 construct): pHT254 vector harbouring *AmyE – Xyn2* and WT: *Bacillus subtilis* strain WB800N. A) Reducing sugar (g/L; means ± SD; n=3) kinetics for 0.5% birch wood xylan with colored wells representing WT, SSL26, SSL27, SSL30, SSL33 (left to right direction)
B) Reducing sugar (g/L; means ± SD; n=3) kinetics for 1% birch wood xylan with colored wells representing WT, SSL26, SSL27, SSL30, SSL33 (left to right direction)
C) Reducing sugar (g/L; means ± SD; n=3) kinetics for 2% birch wood xylan with colored wells representing WT, SSL26, SSL27, SSL30, SSL33 (left to right direction); D) Reducing sugar (g/L; means ± SD; n=3) kinetics for 5% birch wood xylan with colored wells representing WT, SSL26, SSL27, SSL30, SSL33 (left to right direction). All the mentioned strains were cultured in 2xYT media and IPTG (1mM) induced at logarithmic growth phase. The supernatant after 24 hrs fermentation was added in 1:1 ratio (V/V) with 1% birchwood xylan in an enzyme

3.3.3 Demonstration of Xylan depolymerization in *in situ* fermentations

In situ fermentations involve one-pot degradation of xylan in *B. subtilis* fermentations. Many previous works have shown that one pot hydrolysis process can efficiently process biomass (Lynd et al. 2005; Shin et al. 2010; X. Z. Zhang et al. 2011). In the present study, the fermentation batches had 3M media added with 1% xylan as substrate. The 3M media was developed after modification in M9 media mainly for media compatible with *in situ* enzyme reactions (Supplementary data). Xylan (obtained from Megazyme Inc.) constituted 85.6 % xylose, 8.7 % glucuronic acid and 5.7 % other sugars. A significant increase in xylose peak was observed in HPLC spectra of SSL 26 strain

43

compared to wildtype control in 5% birchwood xylan substrate 3M media *In situ* fermentation batches as shown in figure 3.4A. Different IPTG concentrations (0, 0.1, 0.2, 0.5, 1 and 2 mM) were used to optimize enzyme secretion in fermentation batches. Substantial xylan breakdown was observed in 5 days of xylan fermentation batches with highest reduction in 1 mM IPTG batches (74.88% DW) followed by 2mM (70.15% DW) and 0.2 mM batches (66.09 % DW) (Figure 3.4).

A)
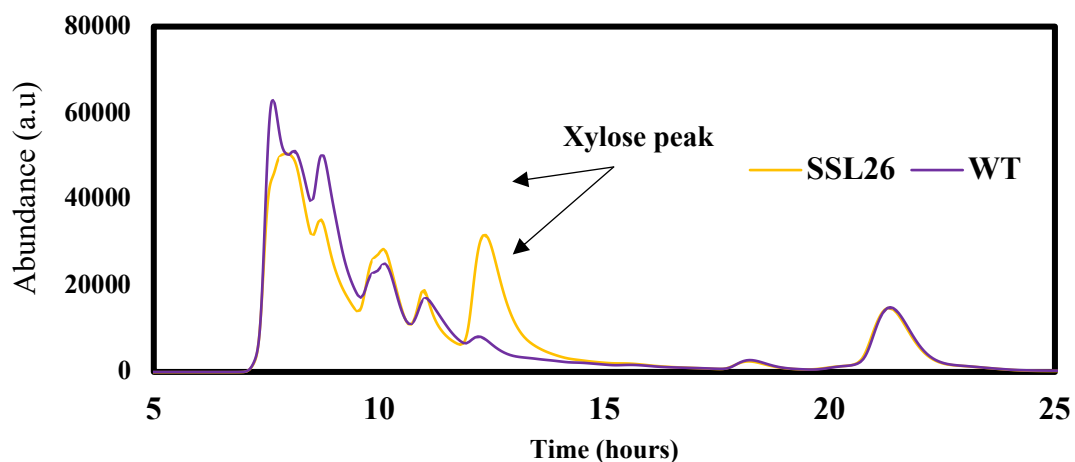
B)
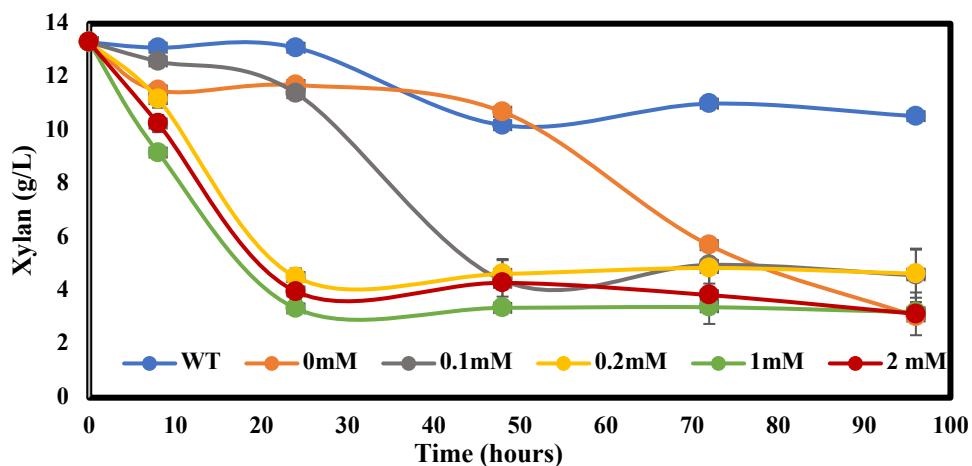
C)
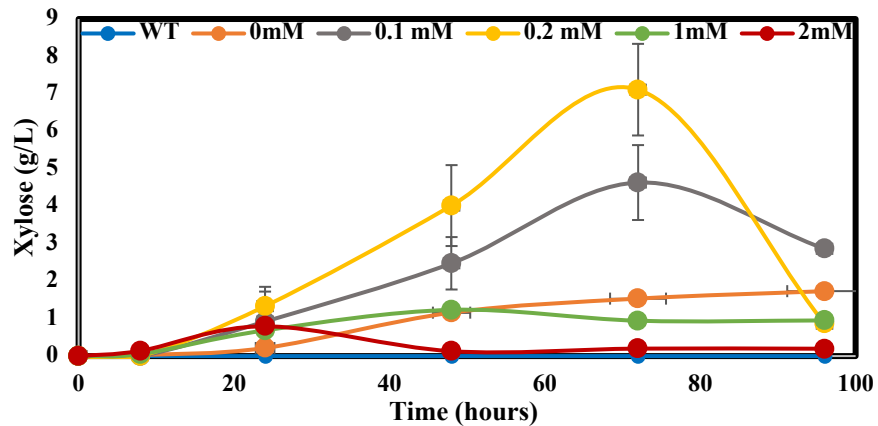
Figure 3.4: *In situ* depolymerization of xylan in monoculture batches: A) Comparison of HPLC spectra of fermentation media obtained after 4 day Xylan (5% W/V) fermentation of *Bacillus subtilis* WB800N (Sands et al.) strain and *B. subtilis* recombinant (SSL26) ; B) Effect of IPTG concentrations (0; 0.1; 0.2; 0.5; 1; 2 mM) on xylan (1% W/V) reduction (g/L; means ± SD; n=3); C) Effect of IPTG concentrations on Xylose (g/L; means ± SD; n=3) titers: SSL26 *B. subtilis* transformant cultured and induced at different IPTG concentrations (0; 0.1; 0.2; 0.5; 1; 2 mM) compared with WB800N wild type *B. subtilis* strain.

Reduction in xylan indicates that endoxylanases exported in extracellular supernatant could carry out xylan breakdown in fermentation media. Minimal reduction in birchwood xylan was observed in wildtype control followed by 0 and 0.1 mM IPTG batches (Figure 3.4B). However, transient reduction in birchwood xylan in 0.2, 1 and 2 mM IPTG batches indicate higher xylan reduction in high IPTG concentrations. Xylan reduction observed in 1mM and 2mM IPTG batches did not translate into increase in xylose production. As shown in the Figure 3.4, the highest xylose production obtained was 7.1 g/L titer after the culture was induced at 0.2 mM IPTG concentration. Theoretical xylose content in biomass was 85.5 %, 0.2 mM batch produced 7.1 g/L of xylan which is 89% of

theoretical xylose yield. 1mM IPTG batches showed highest reduction in xylan but did not lead to highest xylose yield. Highest xylose yield was observed in 0.2 mM IPTG batches. Figure 3.4 shows variation in xylose production after culture was induced at different IPTG concentrations (0.1; 0.2; 0.5; 1; 2 mM of IPTG). Although higher IPTG concentrations signify higher intracellular expression levels, present results indicate high IPTG concentrations do not necessarily lead to high enzyme export outside cell membrane. Increase in substrate (xylan) concentration led to higher xylose titers wherein 5% xylan fermentations demonstrated 15 g/L of xylose titers.

In comparison to literature, as shown in the table 3 present study showed two folds higher xylose production. We were able to demonstrate the efficient breakdown of xylan and produce high yields of xylose.
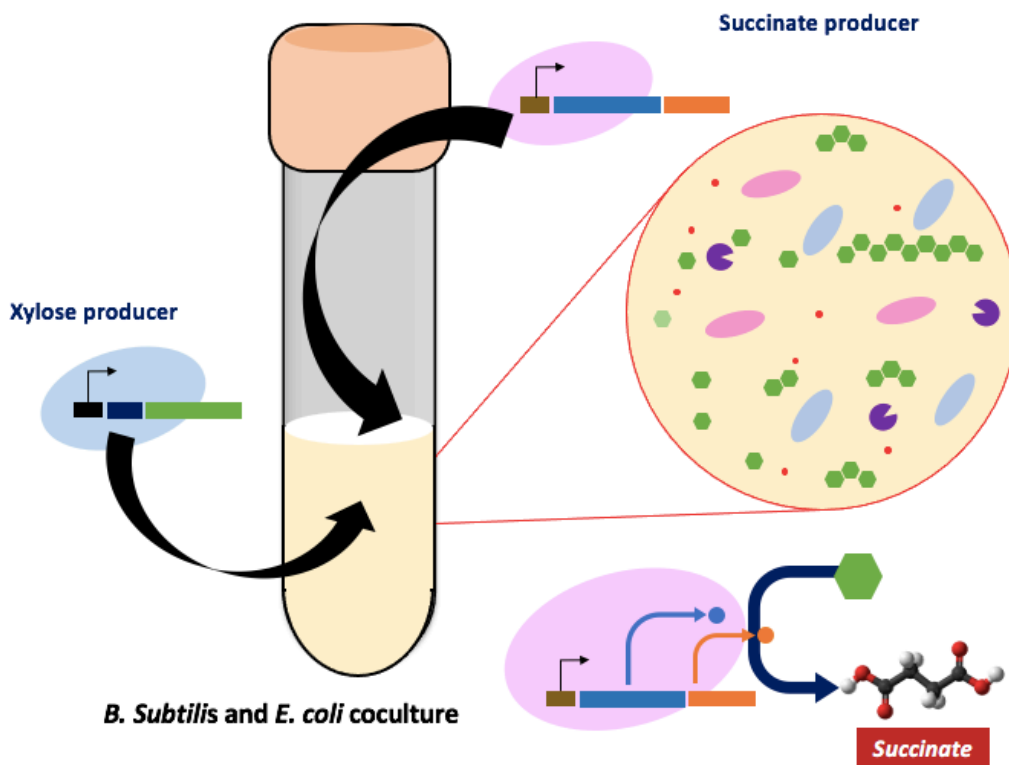
Figure 3.5: Overview of co-culture study xylose producer strain (SSL26) cultured in 1% xylan 3M media to breakdown xylan into xylose and succinate producer strain assimilates xylose to produce succinate in a single tube co-culture process.

3.3.4 Production of succinic acid in a co-culture system

In situ xylan breakdown system showed an efficient breakdown of xylan to xylose sugars. A co-culture system was developed to utilize xylose produced in fermentation. The coculture system proposed in the present study involves xylose producer (SSL26) breaking down xylan to xylose and succinate producer (AF30) using xylose to produce succinate (Figure 3.5). Xylose producer is *Bacillus subtilis* SSL26 strain containing pKB01 vector system tested in *in situ* xylan degradation experiments and showed efficient degradation of xylan. Succinate producer is *E. coli* mutant engineered to metabolize xylose as the primary carbon source and produce succinate as the product. The coculture process began with culturing of xylose specialists in 3M media in the presence of 1% xylan substrate. Samples were cultured for 24 hours in aerobic conditions to ensure rapid growth and sufficient secretion of extracellular endoxylanases. Succinate producer was then added in the xylose producer fermentation culture, and fermentation was continued in anaerobic conditions. Different ratios of xylose producer to succinate producer were used to optimizing the correct co-culture conditions. Overall OD_{600} increased in recombinant batches compared to control batches having wildtype *B. subtilis* strains. Highest increase (1.6-fold) in OD600 was observed in 0.25 E: 1B (0.25 E: 1B : 0.25 OD_{600} of *E. coli* recombinant/ 1 OD_{600} of *B. subtilis* recombinant added in coculture batch) coculture ratio. The higher overall growth

of the coculture consortia does not rectify higher product formation. But in this work highest growth data was in agreement with the highest succinate production of 3.9 g/L observed in 0.2 E: 1B batches (Figure 3.6b). Increase in *E. coli* ratio led to decrease in succinate production. One possible reason to this trend can be that the seed added at higher OD has already reached stationary phase of growth because of which the product formation was less. Genetic engineering of secretion and production in a single system can hinder other metabolic processes and bacterial growth. Hence, the present study aimed at utilizing the natural attributes of bacterial species like the ability to export proteins in *bacillus subtilis* and adaptive evolution in *E. coli* to develop a co-culture process to convert hemi cellulosic xylan to succinic acid.

A)

Wildtype B. subtilis: E. coli   Recombinant B. subtilis: E. coli
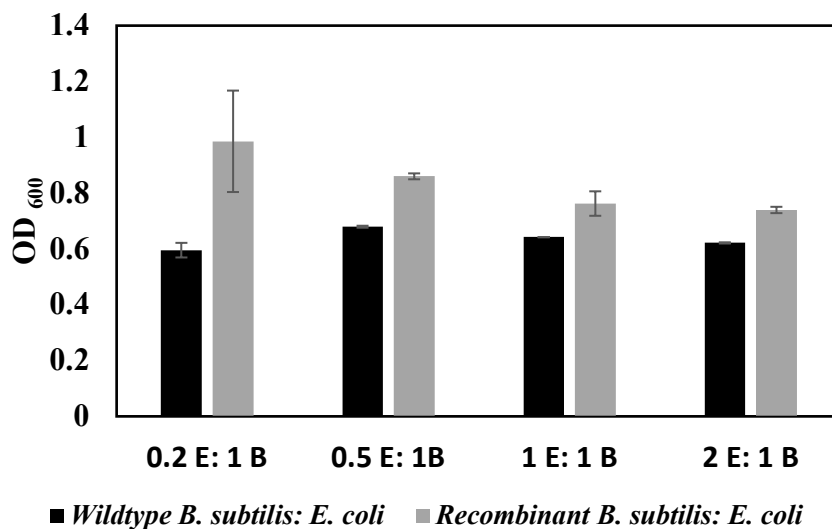
B)
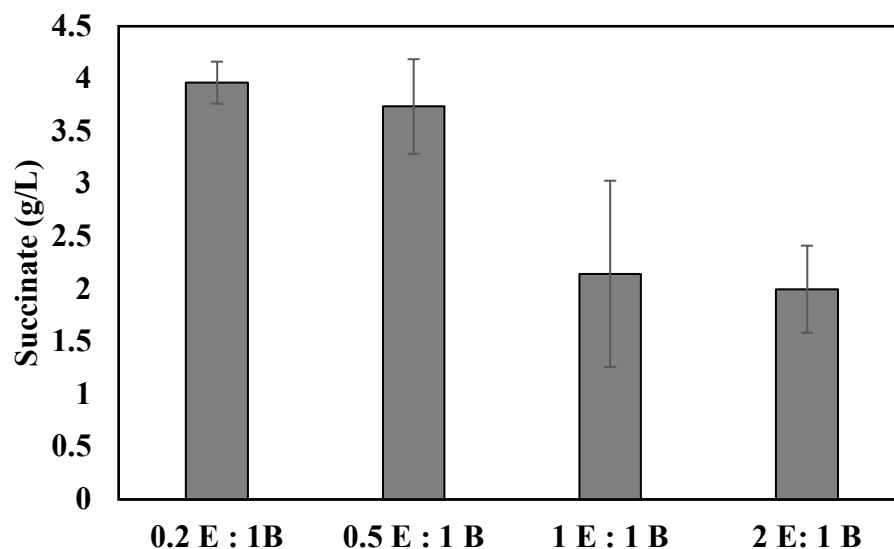
Figure 3.6: A) Comparison of OD$_{600}$ in wild type *B. subtilis*: *E. coli* coculture batches and recombinant *B. subtilis*: *E. coli* coculture. 0.25 E: 1B : 0.25 OD$_{600}$ of *E. coli* recombinant/ 1 OD$_{600}$ of *B. subtilis* recombinant added in coculture batch; 0.5 E: 1B : 0.5 OD$_{600}$ of *E. coli* recombinant/ 1 OD$_{600}$ of *B. subtilis* recombinant added in coculture batch; 1 E: 1B : 1 OD$_{600}$ of *E. coli* recombinant/ 1 OD$_{600}$ of *B. subtilis* recombinant added in coculture batch; 2 E: 1B : 2 OD$_{600}$ of *E. coli* recombinant/ 1 OD$_{600}$ of *B. subtilis* recombinant added in coculture batch. **B) Variation in succinate titer** (g/L; means ± SD; n=3) observed in different *B. subtilis*/*E. coli* ratios; 0.25 E: 1B : 0.25 OD$_{600}$ of *E. coli* recombinant/ 1 OD$_{600}$ of *B. subtilis* recombinant added in coculture batch; 0.5 E: 1B : 0.5 OD$_{600}$ of *E. coli* recombinant/ 1 OD$_{600}$ of *B. subtilis* recombinant added in coculture batch;

1 E: 1B : 1 OD$_{600}$ of *E. coli* recombinant/ 1 OD$_{600}$ of *B. subtilis* recombinant added in coculture batch; 2 E: 1B : 2 OD$_{600}$ of *E. coli* recombinant/ 1 OD$_{600}$ of *B. subtilis* recombinant added in coculture batch. The coculture batches included xylan fermentation (1% xylan in 3M media) for 24 hours and then addition of *E. coli* cells in different ratios, mentioned above, for 96-hour fermentation cycle.

3.3.5. Expanding coculture consortium for production of lactate and ethanol

Comprehending the results obtained during cross species coculture for succinate production, the optimized initial co-culture ratio of 0.2:1 was further exploited to

demonstrate the production profiles from *E. coli* cells distinctly engineered for producing lactate (lactate producer: X2L) and ethanol (strain name). Detailed study was performed to estimate ethanol and lactate production for cocultures on daily basis. Our results indicated significant ethanol and lactate titers, where both the strains showed around 1.64 g/L of ethanol and lactate within 24 hours. The amount improved to around 2 g/L after 72 hours. Production of ethanol and lactate was concurrent with the decrease in the xylose concentration.

To understand the coculture dynamics, along with estimating metabolite concentrations in the medium, corresponding total number of cells were calculated based on their individual antibiotic selectivity (for example chloramphenicol for *E. coli* cells). The results exhibited that the number of CFUs were maintained over the period of 72 hours (Figure 3.7). As the focus of the current work is to establish a coculture platform, a separate detailed investigation could be carried out to optimize the fermentation conditions, thereby sustaining the effective cell viability.
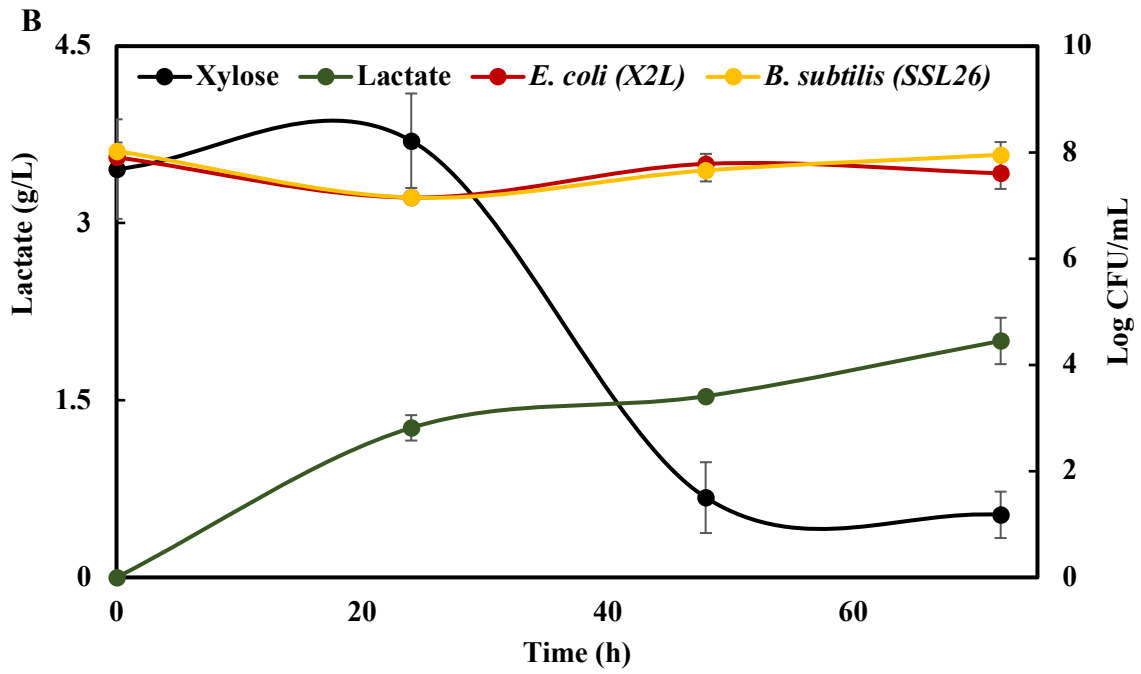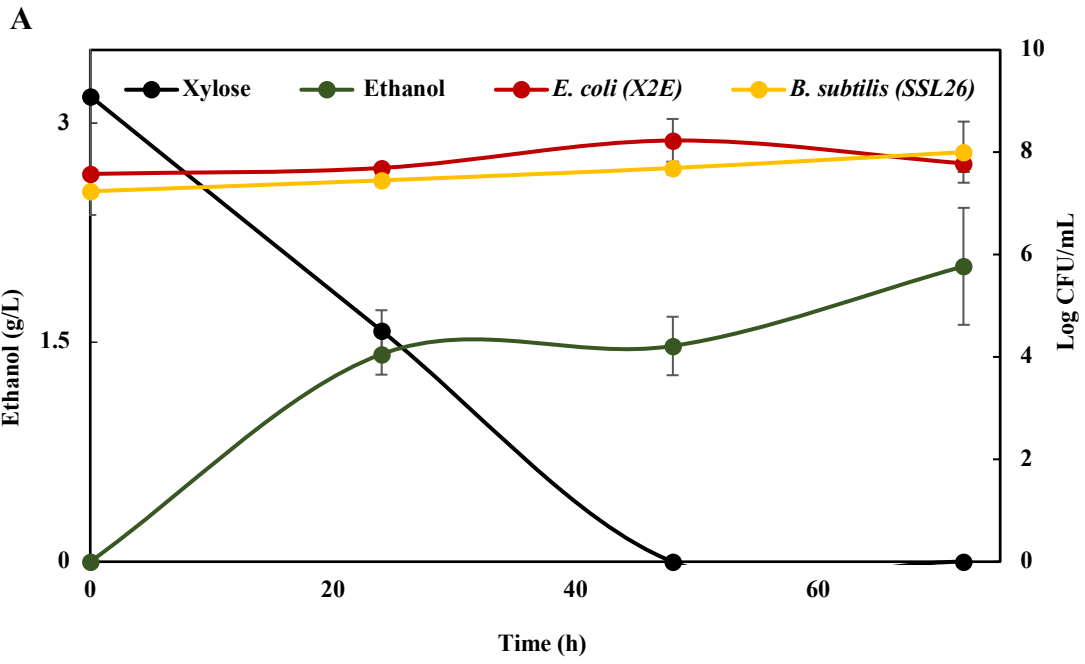
Figure 3.7: CCBP of xylan to D-lactate and ethanol. A) Comparison between xylose consumption, population dynamics of X2E (ethanol to xylose), SSL26 (xylose producer) and ethanol production kinetics. B) Comparison between xylose consumption, population dynamics of X2L (ethanol to D-lactate), SSL26 (xylose producer) and D-lactate production kinetics. All the titers are represented in g/L; mean ± SD; n = 3 and colony forming units data is represented in CFU/mL; mean ± SD; n = 3.

3.4   Discussion

Bacillus Subtilis has been a model organism for producing different types of enzymes mainly due to their ability to secrete different enzymes like α-amylase, xylanase, lichenase, lipase, cellulase, or pectinase, etc. (Su et al. 2020). Signal peptides have been demonstrated to improve extracellular enzymes' secretion levels (Brockmeier et al. 2006b; Hemmerich et al. 2016; H. Tjalsma et al. 2000). *B. Subtilis* has 173 different signal peptides that facilitate protein secretion via sec pathway. Systemic screening of signal peptide sequences in *Bacillus subtilis* was conducted by Brockmeier et al., 2006 wherein different signal peptides were fused with cutinases and esterases. It was observed that different signal peptides showed optimal performance in the case of cutinases and esterases. As it is evident from Brockmeier et al., 2006 work, it is impossible to predict suitable signal peptides to be fused with heterologous protein. Hence, combinations of signal peptides and endoxylanases were selected in the present study. The performance of developed constructs was analyzed using DNS assay. *B. Subtilis* strain harboring pKB01 construct showed three folds higher, reducing sugar production compared to wild Type strain. SSL 01 strain contained YwmC signal peptide fused with endoxylanase enzyme. YwmC-endoxylanase combination of signal peptides showed better enzyme secretion compared to AmyE and SacC signal peptides. As discussed previously, appropriate signal peptide and enzyme

combinations are unique, and it is still unknown how specific signal peptides improve the secretion of certain heterologous proteins. SSL 01 strain performed at par with commercial xylanase and three folds better than other recombinants. Hence, it can be concluded that YwmC signal peptide showed better secretion of endoxylanases compared to other signal peptides considered in present study (Figure 3.3).

After the selection of optimal strain using DNS assay, its potential was explored in *in situ* experiments. The endoxylanase enzyme used in the present study cleaves β-1,4 linkage backbone of hemicellulosic xylan polymer. Meticulous folding and appropriate export of enzymes are essential for the proficient breakdown of xylan structure to xylose. Accumulation of recombinant enzymes due to overexpression can lead to disturbance in protein folding and secretion. Hence, it is essential to develop optimal secretory machinery for recombinant enzymes. Different expression levels were investigated using varying IPTG concentrations to optimize the endoxylanase secretion. IPTG concentration of 0.2 mM was optimal with the highest xylose production compared to higher IPTG concentrations. One reason why higher IPTG concentration did not show improved secretion can be that higher expression levels do not guarantee accurate protein folding and export. Higher intracellular expression levels can lead to the formation of inclusion bodies due to the accumulation of intracellular proteins because of which better secretion was observed in lower IPTG concentrations (Peng et al. 2019). *In situ* breakdown of xylan showed two-times higher xylose production compared to literature (Table 3.6).

After the demonstration of successful *In situ* breakdown of birchwood xylan for xylose production, a co-culture consortium was explored to produce succinic acid.

Different co-culture systems have been explored for solving multiple metabolic engineering bottlenecks. Co-culture systems are fascinating because it is bio-energetically costly to perform various tasks by the mono culture system (Fang Liu 2016). Carbon catabolite repression is a phenomenon wherein bacteria cannot consume two sugar sources at the same time. *E. coli* co-culture system has been reported by Flores et al., 2020 wherein division of carbon source assimilation (glucose and xylose) in *E. coli* co-cultures showed substantial coproduction of lactic acid (88 g/L) and succinic acid (84 g/L). The *B. subtilis* recombinant, used in *in situ* experiments, utilizes glucose as the preferred carbon source. On the other hand, recombinant the *E. coli* strain was engineered to assimilate xylose as a sole carbon source to produce the succinic acid product. Tuning of co-cultures lead to a yield of 3.9 g/L of succinate, which is 61% utilization of the xylose produced by *B. subtilis* recombinant. *B. subtilis* and *E. coli* co-culture was one of its kind demonstrations of gram-positive and gram-negative microbial consortia working mutually for conversion of birchwood xylan to succinic acid. Inherent ability of enzyme secretion of *B. Subtilis* and comprehensively studied *E. coli* can be further explored to produce wide variety of essential products from biomass components.

Via this co-consortia process, we were able to successfully develop endoxylanase secretion machinery in *B. subtilis* system. *In situ* breakdown of birchwood xylan showed a xylose titer of 7.1 g/L with 74% reduction in xylan. *B. subtilis* - *E. coli* Coculture system was successfully developed to demonstrate conversion of xylan to succinic acid. To confirm the feasibility of our approach, the study was extended to other *E. coli* cells engineered to produce ethanol and lactate using the optimised culture ratios of 0.2:1.

Similar to X2S: SSL26 coculture system, even these two systems exhibited 2 g/L of ethanol and lactate with corresponding decrease in the amount of xylose. This *B. subtilis*: *E. coli* coculture was the first demonstration of cross species coculture system. Hereby, we successfully demonstrated Gram-positive and Gram-negative microbial consortia working mutually for one pot conversion of beechwood xylan and further metabolism to various commercially valuable biochemicals. The inherent ability of *B. Subtilis* for enzyme secretion and comprehensively studied *E. coli* can be further explored to produce a wide variety of value added chemicals from biomass components.

Table 3.6. Comparison of present work with literature

References	Reducing sugar / Xylose yield (g/L)	Xylose production Rate (g/L/H)	Hydrolysis yield %	Substrate concentration (g/L)	Organism	Product	Titer (g/L)
Shin et al. 2010	3.92	0.1	39	10	*E. coli*	Ethanol	3.22
Zheng et al. 2012	3.7			10	*E. coli*	Succinate	4.84
Liu et al. 2019	3			50	*Clostridium beijierinckii*	Isopropanol	3.5
Zin et al., 2018	2.89			60	*Thermoanaerobacterium sp.*	Butanol	8.34
Present study	6.8±1.09	0.1	68	10	*Bacillus subtilis*	Succinate	3.7
Present study	15	0.2	30	50	*Bacillus subtilis*		
Zheng et al., 2010	0.18				*E. coli*	Succinate	
Tsai et al., 2010	3.12	0.03	31	10	*Saccharomyces cerevisiae*	Ethanol	0.95
Cunha et al. 2020	1.8				*Saccharomyces cerevisiae*	Ethanol	
Jiang et al. 2018	17.6	0.2	29.3	60	*Thermoanaerobacterium sp.*	Butanol	8.34

CHAPTER 4

DEVELOPMENT OF A MUTUALISTIC BACTERIAL PLATFORM FOR

CELLULOSE DEPOLYMERIZATION TO GLUCOSE

4.1 Introduction

Plant biomass is the most abundant source of carbon on earth. Plant biomass waste is often burned which contributes to air pollution and utilizing this widely available resource will help mitigate these environmental effects. This abundantly available untapped resource is in form of cellulose, hemicellulose and lignin. Cellulose is a long chain biopolymer formed from a linear chain of D- glucose linked together by β-(1,4)-glycosidic bonds (Haghighi Mood et al., 2013). It is the major component of plant biomass and the most abundant biopolymer found on earth, making it a promising renewable resource. Cellulose is not edible, and hence use for cellulose for the production of fuel and utility chemicals does not create food vs fuel competition which makes it a suitable energy source. Cellulose can be broken down into glucose monomers, primary carbon sources in central metabolic pathways in bacterial platforms. Hence, cellulose can be used to feed bacteria which can be engineered to produce utility chemicals and fuels. Cellulose cannot be directly assimilated in all the bacterial platforms. Most commonly, cellulose is hydrolyzed into glucose by a process called hydrolysis to produce glucose which bacteria can further consume. Hydrolysis reaction can be either carried out using the thermochemical method or enzymatic method. Thermochemical hydrolysis is energy-intensive, can produce corrosive byproducts, and its products can be toxic to bacteria.

On the other hand, Enzymatic hydrolysis is highly specific, environmentally friendly, operates at milder conditions, and has a high atom economy. Hence enzymatic

hydrolysis was widely explored for cellulose depolymerization into glucose monomers (Haghighi Mood et al., 2013; Lynd et al., 2005; Trivedi et al., 2013; Zhang et al., 2011). Although enzymatic hydrolysis has many merits, it makes bioprocess extremely expensive due to high enzyme purification costs. Hence bacterial platforms were engineered to secrete hydrolytic enzymes to reduce the process. Fungi like white-rot fungi, *T. resei*, *A niger*, *N fischeri*, etc are sources of hydrolytic enzymes and were considered for enzyme secretion and hydrolysis. Still, due to lack of genetic engineering machinery in these organisms, *E. coli*, *B. subtilis*, *C. glutamicum*, etc were studied to develop a consolidated bioprocess (Brijwani et al., 2010; Inui et al., 2005; Kalyani et al., 2012; Shin et al., 2010; Zhang et al., 2011).

Consolidated bioprocess is when enzymatic hydrolysis of the biomass components and fermentation steps are carried out in one single reactor. Consolidated bioprocess helps improve process economics and volumetric productivity by removing enzyme costs and reducing the number of steps in a bioprocess. Cellulose has been considered an ideal substrate for consolidated bioprocessing processes, and several works have tried to utilize cellulose as a carbon source in fermentation processes (Kumar et al., 2013; Trivedi et al., 2013; Zhang et al., 2011). The present work aims to develop efficient enzyme secretion machinery in *bacillus subtilis* for efficient breakdown and cellulose biopolymer utilization. As shown in figure 4.1, two significant enzymes essential for cellulose depolymerization are *β* glucosidase, and endoglucanase. The present work aims to develop a secretion system in *B. subtilis* for these two enzymes.
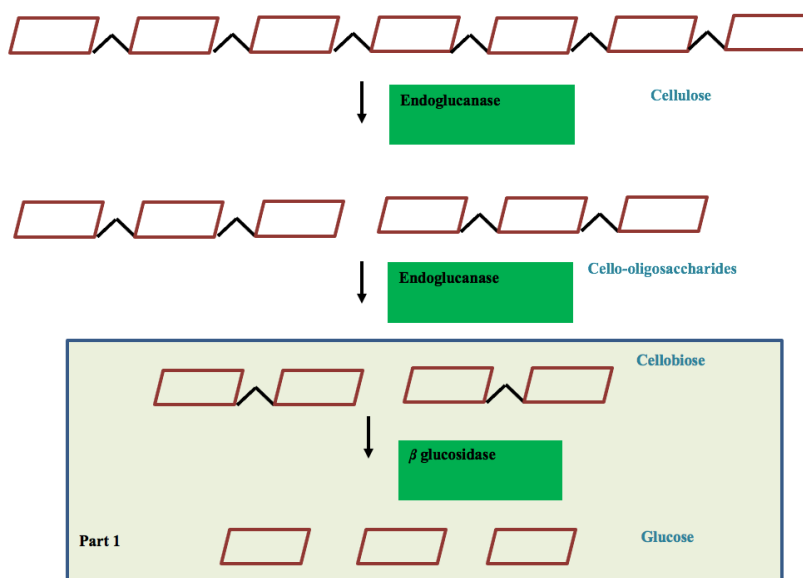
Figure 4.1: Overview of cellulose depolymerization reaction: Endoglucanase enzyme cleaves β-(1,4)- glycosidic bonds in cellulose backbone and depolymerizes cellulose to cello-oligosaccharides like cellobiose and glucose. Further β glucosidase enzyme cleaves cellobiose dimer into monomeric D-glucose subunits.

4.2 Materials and Methods

4.2.1 Media, growth conditions

2xYt media containing yeast extract and tryptone was used to cultivate *Bacillus subtilis* cells at 37 °C, 250 rpm shaking conditions. Luria Bertani (L.B) media was used to cultivate *Escherichia coli* cells at 37 °C, 250 rpm shaking conditions. Solid media plates used for colony screening were prepared by adding 1.5% agar in L.B. and 2xYT media.

4.2.2 Bacterial strains and plasmid

Bacillus subtilis (WB800N: WB800N: *nprE aprE epr bpr mpr::ble nprB::bsr Δvpr wprA::hyg cm::neo*) strain was used in the present study as a non-model organism for enzyme secretion. *Escherichia coli* Dh5a strain was used for transforming developed

constructs and storing freezer stocks. PHT254 plasmid was used as a vector in construct development.

Table 4.1 Plasmid constructs developed in present work for *b glucosidase* expression and secretion

Plasmids	Description	Source /reference
pHT254	Backbone plasmid for all the developed constructs with ColE1 Ori*	Mobitec, Inc
pKB03	Derived from pHT254 with *YwmC- β glucosidase (N. fisheri)* and Pgrac100 promoter	This study
pKB04	Derived from pHT254 with *YwmC- β glucosidase (T. resei)* and Pgrac100 promoter	This study
pKB07	Derived from pHT254 with SacC- *β glucosidase (N. fisheri)* and Pgrac100 promoter	This study
pKB8	Derived from pHT254 with Sac*C- β glucosidase (T. resei)* and Pgrac100 promoter	This study
pKB11	Derived from pHT254 with AmyE- *β glucosidase (N. fisheri)* and Pgrac100 promoter	This study
pKB12	Derived from pHT254 with AmyE- *β glucosidase (T. resei)* and Pgrac100 promoter	This study

Table 4.2 Plasmid constructs developed in present work for *Endoglucanase* expression and secretion

Plasmids	Description	Source /reference
pHT254	Backbone plasmid for all the developed constructs with ColE1 Ori*	Mobitec, Inc
pAMR01	Derived from pHT254 with BglC- *endoglucanase (B. subtilis)* and Pgrac100 promoter	This study
pAMR02	Derived from pHT254 with BglC- *endoglucanase (T. resei)* and Pgrac100 promoter	This study
pAMR03	Derived from pHT254 with SpybdN- *endoglucanase (N. fisheri)* and Pgrac100 promoter	This study
pAMR04	Derived from pHT254 with YwmC- *endoglucanase (T. resei)* and Pgrac100 promoter	This study

| pAMR05 | Derived from pHT254 with NprE- *endoglucanase (T. resei)* and Pgrac100 promoter | This study |

4.2.3 Gene Amplification, cloning using classical cloning and CPEC method

Amplification of the desired gene was done by Polymerase chain reaction (PCR) using Q5 DNA polymerase obtained from NEB at standard PCR conditions. Signal peptides were isolated by colony PCR at standard PCR conditions, preceded by a lysis cycle having the following thermocycler method: 95 ºC; 2 minutes, 4 ºC 1 minute, the number of cycles: 10. The oligonucleotide sequences used in the present work are given in Table 4.1. The PCR product was purified by Wizard S.V. gel and PCR purification kit. The concentration of the purified construct was determined by Thermo fischer nanodrop equipment. PCR product was passed through polyacrylamide gel electrophoresis set up with 1% gel, 100V, for 60 minutes. Sample volume varied based on reaction volume.

The amplified gene inserts (1 ug) and vector samples (1ug) were restriction digested (R.D.) in 20ul reaction with the help of fast digest Thermo scientific buffer (2ul) and enzyme (1ul) at 37 ºC for 1 hr. The R.D. product was further gel purified and stored at -20 ºC for further cloning. The R.D. product was used in ligation reaction (Vector: Insert Molar ratio = 1:3) using 2ul buffer and 1 ul ligase in 20ul reaction with thermocycler conditions as follows: 16 ºC for 1 hr.

4.2.4 Circular polymerase extension cloning (CPEC)

CPEC was performed according to the protocol published by Quan and Tian, 2011. The CPEC inserts were prepared by PCR reaction with standard PCR conditions. All the constructs designed in the present study are given in Table 4.2.

4.2.5 Transformation of developed constructs

E. coli transformation

Competent *E. coli* cells (50ul) were incubated in ice and 100 ng of the plasmid/ cloning product (10ul) for 30 mins. The samples were added to the water bath at 42 °C for 45 seconds. The samples were immediately kept in ice for 5 mins. Lb medium (1ml) was added in samples and were incubated for 45 mins in an incubator shaker at 37 °C, 250 rpm shaking. The sample was later plated on resistance plates for 24 hrs. Colonies obtained after 24 hrs were confirmed with colony PCR.

B. subtilis transformation

Competent *E. coli* cells (50ul) were incubated in ice and 100 ng of the plasmid/ cloning product (10ul) for 10 mins. The samples were electroporated in a micro electroporator setup in 0.1 mm cuvettes at 2.4 KV for 4 ms. 2xYT medium (1ml) was added in samples and were incubated for 3 hrs in an incubator shaker at 37 °C, 250 rpm shaking. The sample was later plated on resistance plates for 24 hrs. Colonies obtained after 24 hrs were confirmed with colony PCR.

4.2.6 Extracellular enzymatic reactions

Recombinant strains were grown in 5 mL 2xYT (Tryptone 16 g/L; Yeast Extract 10 g/L; Sodium Chloride 5 g/L) media till logarithmic growth phase (OD_{600}: 0.8) and induced (1mM Isopropyl β-D-1-thiogalactopyranoside (IPTG)) to enable enzyme secretion. Supernatant samples were collected after 24 hours and further used for enzyme reactions. The enzyme reaction was carried out in citrate phosphate buffer at 50 °C for 1 hour at pH 5. Reducing sugar content in enzyme reaction was estimated using DNS assay (Kim et al. 2014). Similarly, the enzyme reaction was set up in citrate phosphate (pH 5.5)

for glucosidases 100 ul of *p* NPG (1%) added in 100 ul of supernatant, and the reaction was conducted at 40 $^{\circ}$C 1 hr. At the end of enzymatic reaction absorbance readings were taken at 420 nm to quantify mM of pNP produced. pNP standards were used to develop a calibration curve.

4.2.7 Cellulose fermentations

Cellulose fermentations were carried out at 37 $^{\circ}$C for 5 days. The media used in cellulose fermentation was 3M buffered media with 1% cellulose at pH 7 (Table 3.3, 3.4 and 3.5). Recombinant strains were grown in 3M media at 250 rpm for 4 hours. The starting OD_{600} of the strains was 0.02. The strains were induced in a two-step process with 0.2 mM IPTG at OD_{600} of 0.8 and then topped with 0.5 mM of IPTG at OD_{600} of 1.5 to express the enzyme. The fermentation batches were samples after 24, 48, 72, 96 hrs after IPTG induction. Fermentation batch samples were further analysed for OD_{600} and HPLC analysis. For Whatman filter paper, the filter paper was cut into 2cm * 2cm squares, UV treated in a laminar air flow and added in the induced cultures. For insoluble cellulose fermentations like Avicel cellulose and Whatman filter paper the residual cellulose was washed with DI water in three cycles and once with 70% ethanol. The washed residual cellulose was then dried at 105°C for 16h to get dried product for weight measurements.

4.2.8 U-^{13}C fingerprinting studies

The seed cultures were set up in minimal medium, as described previously. Cells were centrifuged and washed with minimal media to avoid any carryover of carbon substrates and media nutrients. For the labelling study, 50 µL of washed cells were inoculated into 5 mL of media tubes containing 5 g/L [U-^{13}C] glucose + 10 g/L carboxymethyl cellulose

(CMC); 5 g/L [U-^{13}C] glucose control. Bacterial cells were harvested after 24 hours, and the biomass was hydrolyzed to obtain proteinogenic amino acids.

The amino acids were derivatized with TBDMS (N-(tert-butyldimethylsilyl)-N-methyl-trifluoroacetamide, Sigma-Aldrich) by following previously reported protocols (Varman et al., 2014; You et al., 2012). The derivatized amino acids were analyzed for their mass isotopomer abundance by GC-MS, as described elsewhere (Xiao et al., 2012; You et al., 2012). The m/z ion [M-57]$^{+}$ that corresponds to the entire amino acid was used to calculate the ^{13}C abundance in amino acids [m0 m1…. mn]. The m/z of [M-15]$^{+}$ was used for leucine and isoleucine alone since their [M-57]$^{+}$ overlaps with other mass peaks (Wahl et al., 2004). The natural abundance of isotopes, including ^{13}C (1.13%), ^{18}O (0.20%), ^{29}Si (4.70%), and ^{30}Si (3.09%) contributes noise to the mass isotopomer spectrum. This background noise was rectified in the calculation of ^{13}C fractions for amino acids using a published algorithm, and the detailed correction protocol can be found elsewhere (Tang et al., 2009).

4.2.9 Analytical methods

GC MS (Gas Chromatography Mass spectrometry) analysis was carried out to study amino acid profiles of derivatized biomass fraction. The sample (1ul) was injected in a GC system, having an oven temperature of 250 C passed through the column using a mass spectrometer detector.

4.3. Results

4.3.1 Development of signal peptide enzyme construct to develop strain library

Deconstruction of cellulose has been conducted with the help of cocktail of hydrolases like endoglucanase, glucosidase and cellobiohydrolase. To imitate this cocktail mixture commonly used for cellulose hydrolysis in *in situ* conditions a endoglucanase and glucosidase secretion system was developed. To have advantage of regulating the enzyme levels in supernatant two *B. subtilis* WB800N strains were engineered to secrete each hydrolase for optimal breakdown of cellulose in one pot bioprocess. β glucosidase is the hydrolytic enzyme which cleaves the 1,4 glycosidic linkages. Cellobiose is a dimeric reducing intermediate which is hydrolysed by β glucosidase into D- glucose. β glucosidase enzymes from fungi and bacteria are extensively explored for their structure and activity studies (Sternberg et al., 1977; Tiwari et al., 2013). For present study two β glucosidase were selected based on their operability and applicability. β glucosidase from *N. fishcheri* was selected because its optimal activity at 40 C and pH 6 which is close to the *in situ* bioprocess conditions (Ramachandran et al., 2012). Similarly, β glucosidase from *T. reesei* is one of the most explored glucosidase with highest reported activities (Tiwari et al., 2013). To efficiently secrete glucosidase enzyme it was linked with a signal peptide. SEC pathway signal peptides YwmC, Amye and SacC were chosen to prepare a signal peptide library. Total 6 strains were developed from combinations of 3 signal peptides and 2 enzymes. Similarly second enzyme selected for this work was endoglucanase which cleaves long chain cellulose structure into intermediary quadmers, trimers and dimers. *B subtilis* has native endoglucanase enzyme which was selected as one of the endoglucanase for this work as it having a native export machinery which can be tapped for optimal export.

Second endoglucanase selected was a mutant which was obtained from (Zhang et al., 2011) which has shown promising cellulose deconstruction compared to native endoglucanase. Third endoglucanase was from *T. resei* which had highest native endoglucanase activity at milder conditions suitable for *in situ* bioprocess. Signal peptide library was only developed for endoglucanase from *T. resei* as other *B. subtilis* endoglucanase has native signal peptide to export it. Also, mutant endoglucanase had a signal peptide screened for its optimal export. Total 5 strains were developed for efficiently exporting endoglucanase. After developing total 11 strains, 6 for glucosidase export and 5 for endoglucanase export, enzymatic assays were used to select best performing glucosidase and endoglucanase exporter.

4.3.2 Selection and optimising of best performing strain from the strain library

Enzymatic assays are a efficient method of screening large number of strains for their activity and selecting best performing strain based on their activity (Mhatre et al., 2022; Zhang et al., 2016). In present study, DNSA and *p*-NPG assay was used to select the best performing strains from the developed 11 strains. The enzymes secreted for 24 hours in the medium were used in the enzymatic assays to check their activities. SSL35 strain showed highest pNP production in pNPG assay (Figure 4.2 B). SSL35 strain had AmyE signal peptide natively used to export amylases in *B. subtilis* strains. More than 5 folds increase in pNP production was observed in the SSL35 strain and his it was further considered for *in situ* studies. Similarly, DNS assay was used to estimate reducing sugar formed after the enzymatic reaction CMC in this case. Highest reducing sugar titer was observed in SSL118

strain. More than two folds in the reducing sugars titers lead to selection of SSL118 strain for further DNS study. SSL118 strain is SpydN signal peptide linked with Bsce5a mutant. Based on the assays we were able to conclude that SSL118 and SSL35 strain had appropriately folded and higher concentration of endoglucanase and glucosidase in the culture medium compared to other variants. These selected strains were further optimised for higher secretion levels. IPTG inducible promoter Pgrac100 was used for expression of enzymes linked with signal peptides. Different IPTG concentrations were used to see the effect of expression levels on the invitro enzyme reactions. As seen in figure 4.3 higher IPTG concentration of 1mM did not show high enzyme activity and this can be correlated to flooding of export gates due to high intracellular expression levels (Mhatre et al., 2022). Optimal performance was observed in case of 0.2 mM IPTG concentration for endoglucanase and 0.5 mM for beta glucosidase. Selected strains were further studied in in situ one pot bioprocesses to deconstruct different types of cellulose and cellulose derivatives.
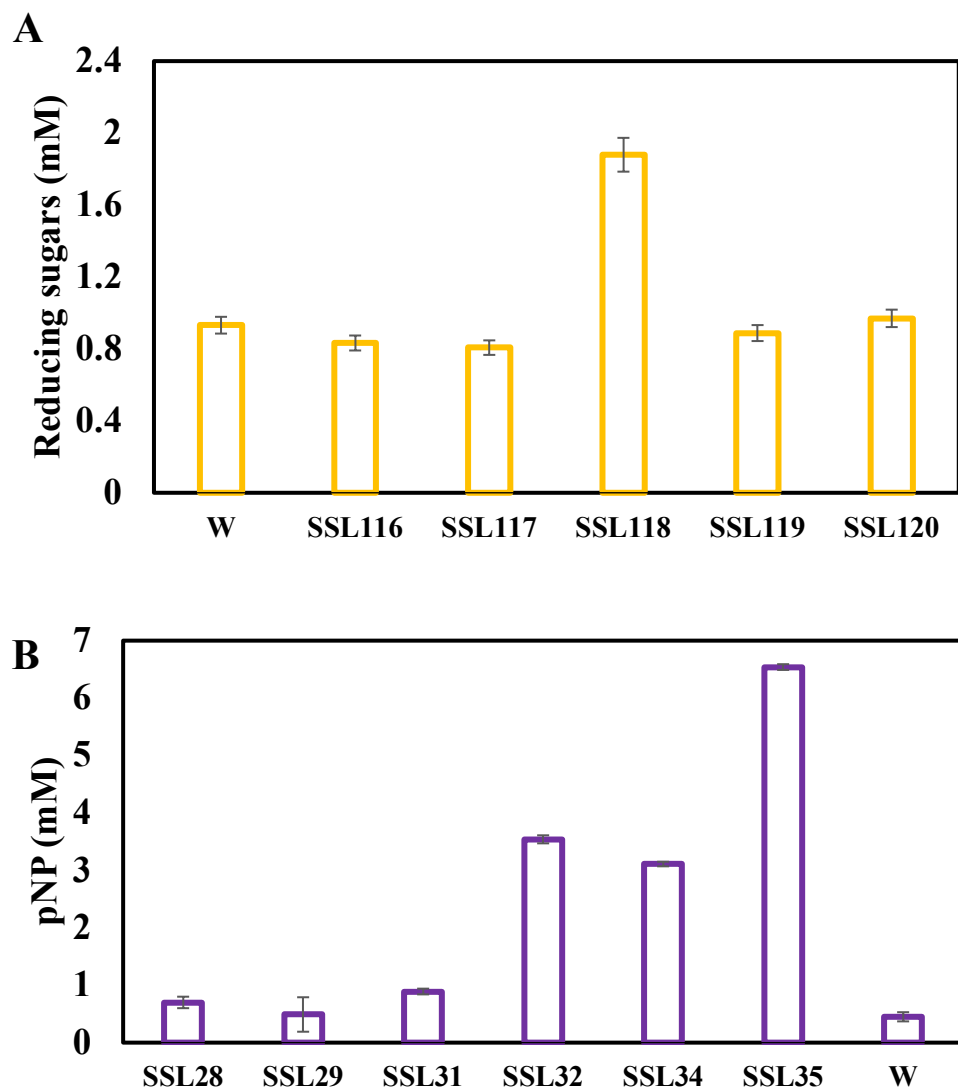
Figure 4.2: Selection of best performing strains, A) **Endoglucanase secreting strain comparison with respect to reducing sugar produced (mM; means ±SD; n=3):** SSL116 (pAMR01 construct): pHT254 vector harbouring *BglC – Egls (B. subtilis;* SSL117 (pAMR02 construct): pHT254 vector harbouring *BglC – Cel5a (T. Resei);* SSL118 (pAMR03 construct): pHT254 vector harbouring *SPybdN – Bscel5;* SSL119 (pAMR04 construct): pHT254 vector harbouring *YwmC – Cel5a;* SSL120 (pAMR05 construct): pHT254 vector harbouring *NprE – Cel5a;* W: negative control WB800N *strain* containing pHT254 vector B) β **glucosidase secreting strain comparison with respect to pNP produced (mM; means ±SD; n=3):** SSL28 (pKB03 construct): pHT254 vector harbouring *YwmC – Bglu (N. fischeri;* SSL29 (pKB04 construct): pHT254 vector harbouring *YwmC – Bglu (T. Resei);* SSL31 (pKB07 construct): pHT254 vector harbouring *SacC – Bglu (N. fischeri);* SSL32 (pKB08 construct): pHT254 vector harbouring *SacC – Bglu (T. Resei);* SSL34 (pKB11 construct): pHT254 vector harbouring *AmyE – Bglu (N. fischeri);* SSL35 (pKB12 construct): pHT254 vector harbouring *AmyE – Bglu (T. Resei);* W: negative control WB800N *strain* containing pHT254 vector.
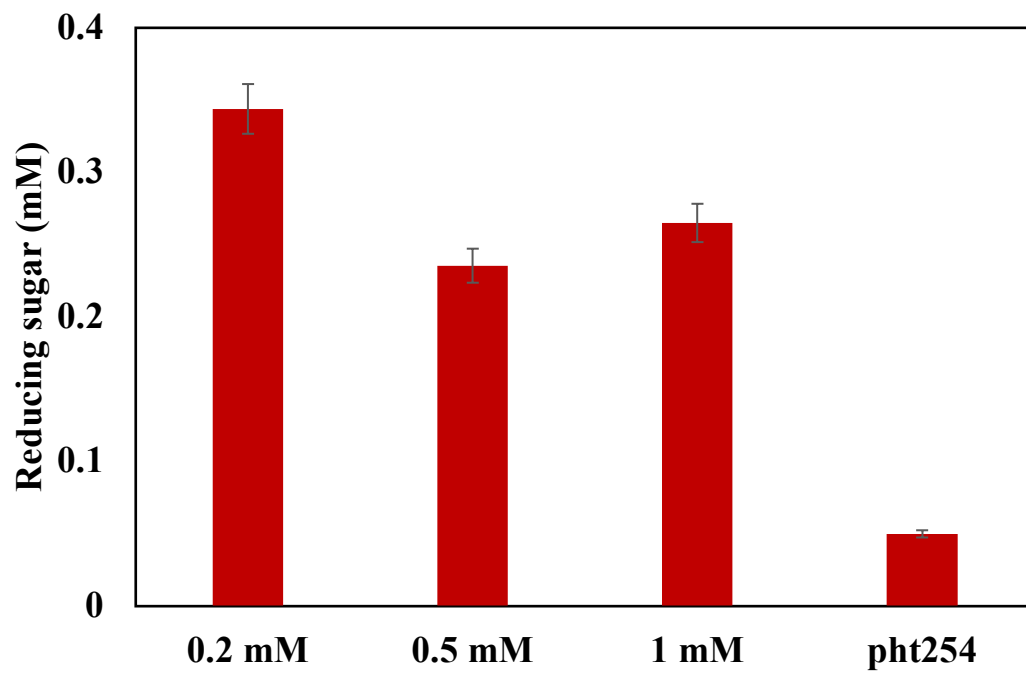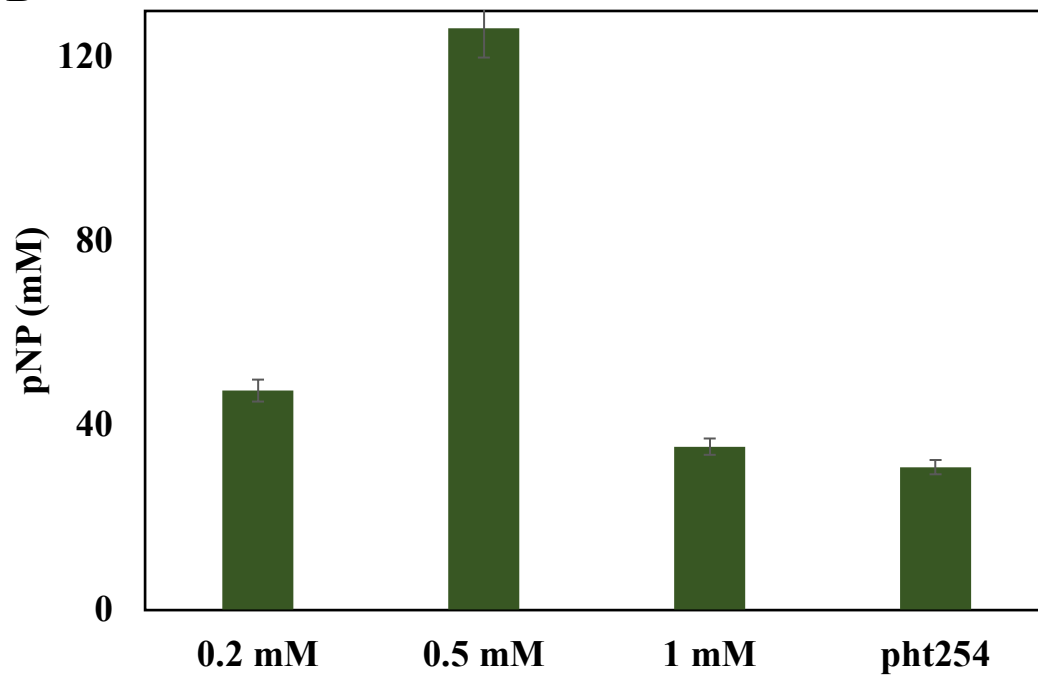
Figure 4.3: Optimisation of secretion levels in endoglucanase and glucosidase exporters, A) Endoglucanase secreting strain reducing sugar produced (mM; means ±SD; n=3): B) with respect to increasing IPTG concentrations (0.2 mM, 0.5 mM, 1 mM) compared to pHT254 empty vector strain. B) β glucosidase secreting strain pNP produced (mM; means ±SD; n=3) with respect to increasing IPTG concentrations (0.2 mM, 0.5 mM, 1 mM) compared to pHT254 empty vector strain.

4.3.3 One pot consolidated bioprocess for CMC and Whatman filter paper
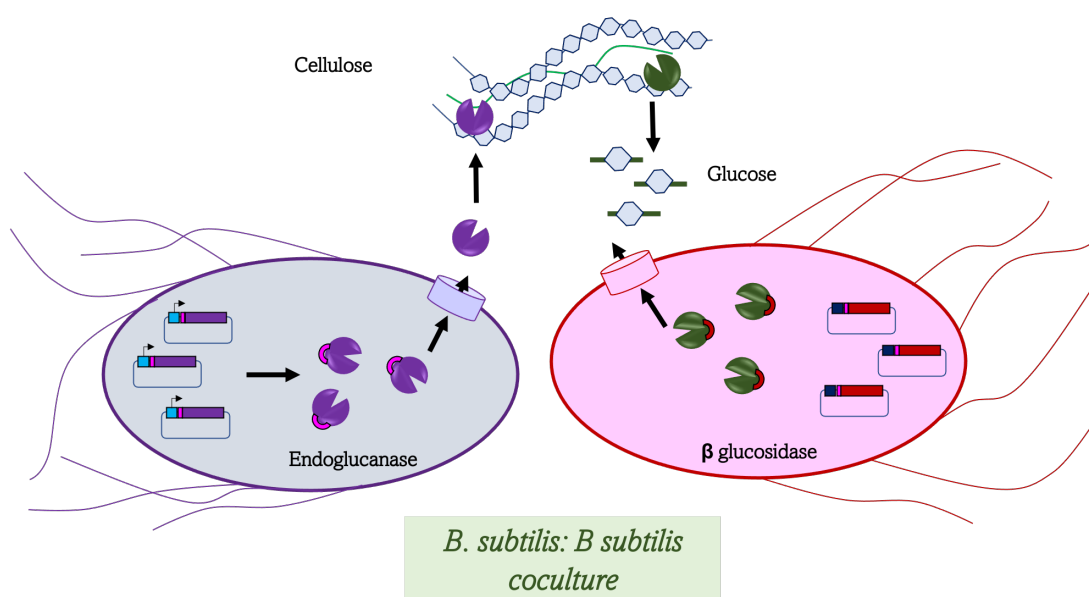
Figure 4.4: Overview of *B. subtilis* (endoglucanase exporter): *B. subtilis* (β glucosidase exporter) coculture processes for deconstruction of cellulose and further assimilation and utilisation of monomeric glucose formed after hydrolysis of substrate.

two

strain to avoid metabolic load (Flores et al., 2020(Zhang, 2015 #1038; Kalbarczyk et al., 2018; Mhatre et al., 2022)). Consolidated process is used to combine two steps in a process to reduce number or steps and avoid losses. In this work a consolidated coculture process was developed to deconstruct cellulose in one pot. Two strains as shown in figure 4.4 were

used in this work with one strain exporting endoglucanse enzyme and other strain exporting glucosidase enzyme and synergistically working to deconstruct cellulose to glucose. Endoglucanase exporter strain will breakdown cellulose to cellobiose and glucosidase exporter strain will further breakdown cellobiose to glucose. This glucose will be used as carbon source by the strains. Different substrates like CMC, Whatman paper and avicel cellulose were explored to quantify performance of this coculture consolidated bioprocess.

Carboxymethy cellulose (CMC) is anionic, water soluble derivative of cellulose. Similar to other cellulose derivatives CMC has repeating units linked by glycosidic bonds. Only difference in CMC and cellulose structure is CMC has carboxymethyl groups replacing hydrogen atoms in cellulose structure and CMC has shorter chain length than cellulose (Rahman et al.). CMC was added as substrate in 3M media along with the coculture strains. Monocultures of the individual SSL118 and SSL35 strains were setup as control to understand the collective effect of the cocultures. Significant difference in growth was observed in the monocultures and cocultures as shown in figure 4.5 A. Dual growth was observed in different coculture ratios unlike the monocultures. Dual growth is correlated to possible utilisation of carbon available from CMC along with the carbon added for growth. Dual growth was not observed on the monocultures or in the empty vector control. To further verify the effectiveness of the cocultures ^{13}C labelling studies were conducted to study carbon enrichment from glucose obtained from CMC. As shown in figure 4.5 B, two column denote cofeeding of labelled U-^{13}C glucose and CMC in a minimal media cultures. Higher enrichment of carbons from CMC will lead to reduction in labelled fraction as labelled fraction comes from labelled glucose. IGCP24 is a empty vector control and as seen in the heatmap the column is predominantly red which means

carbon contribution is mainly from the labelled glucose. Alanine, glycine, serine have almost all their carbons coming from labelled glucose which shows no significant enrichment from CMC which also shows not significant hydrolysis of CMC to glucose which can be consumed by the bacterial cells. On the other hand in case of IGCAK24 cocultures 25-30% reduction in labelled fraction was observed in central metabolic pathway amino acids like alanine, phenylalanine and serine and TCA cycle amino acids like methionine, isoleucine. This can be attributed to successful hydrolysis of CMC to glucose and further assimilation of its carbons in the recombinant cocultures.

A

B

		IGCP24	IGCAK24	% Reduction
All carbons from cellulose	ALANINE	0.92	0.63	31.54
	GLYCINE	0.91	0.71	21.76
	VALINE	0.86	0.67	22.67
	LEUCINE	0.71	0.64	9.96
Partial carbon contribution	ISOLEUCINE	0.68	0.46	32.59
	METHIONINE	0.72	0.53	25.87
	SERINE	0.96	0.66	31.17
All carbons from glucose	PHENYLALANINE	0.85	0.78	8.31
	TYROSINE	0.86	0.62	28.28
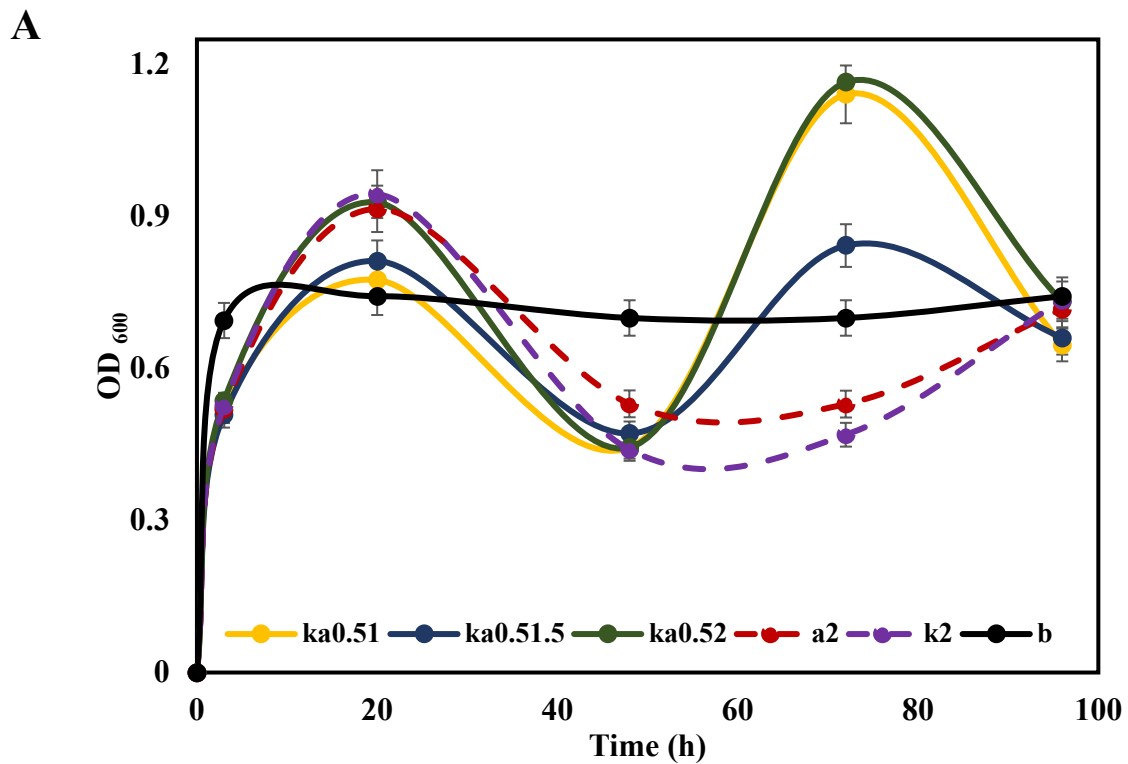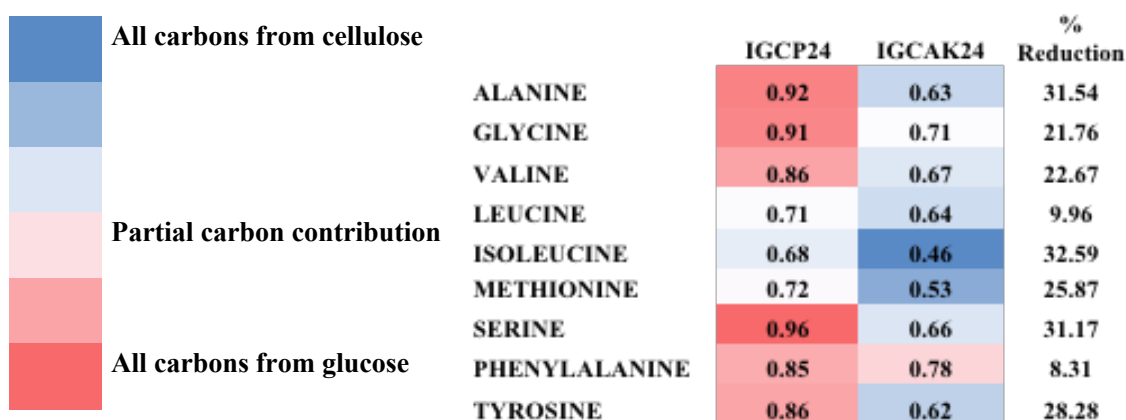
Figure 4.5: Coculture fermentation studies containing endoglucanase exporter and glucosidase exporter for CMC as a substrate. A) Growth kinetics (mM; means ±SD; n=3)
study for the coculture fermentations studied over course of 96 hours.

B) Heat map depicting labelled fraction in minimal media culture containing 5g/L U-13C glucose and 10 g/L CMC in IGCP24 (WB800N *B. subtilis* strain containing pHT254 empty vector control) and IGCAK24 (endoglucanase and glucosidase exporter coculture).

To further effectiveness of cocultures Whatman filter paper was used as a substrate. Whatman filter paper contains 99% cellulose having both amorphous and crystalline regions. As shown in figure 4.6 A, significant difference in the appearance of the filter paper was observed after 24 hours of fermentation in empty vector negative control and engineered cocultures. Significant size reduction in the added sheet was observed compared to the negative control. Endoglucanase exporter-empty vector coculture and endoglucanase-glucosidase cocultures showed 20-30% reduction in the total weight of the added Whatman filter paper. The weight reduction was 2-4 folds higher than the empty vector negative control. Minimal reduction in the empty vector control can be because of the nature endoglucanase exported by *B. subtilis*. Although better breakdown of Whatman

filter paper was observed in engineered strains compared to the empty vector. Similarly, SEM images confirmed difference in the images of negative control and engineered cocultures. Negative control image has more closely packed fibres (Figure 4.7). In case of comparing cocultures and monocultures, SEM images of monoculture had microfibrils on fibril tubes and cocultures had cleaner surface with higher orientation (Figure 4.7). To further confirm synergistic activity of enzymes consolidated cocultures avicel cellulose substrate was studied. Avicel cellulose is solely microcrystalline cellulose with lower amount of amorphous regions which makes it comparatively difficult to breakdown substate compared to Whatman filter paper which has both amorphous and crystalline regions. Avicel cellulose substrate was used in an *in situ* consolidated coculture process.

A

Empty vector strain monoculture

Endoglucanase exporter and empty vector strain coculture

Endoglucanase exporter and empty vector strain coculture
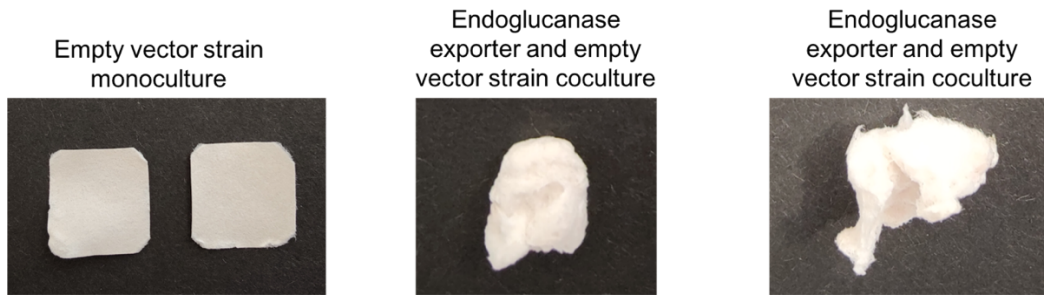
B
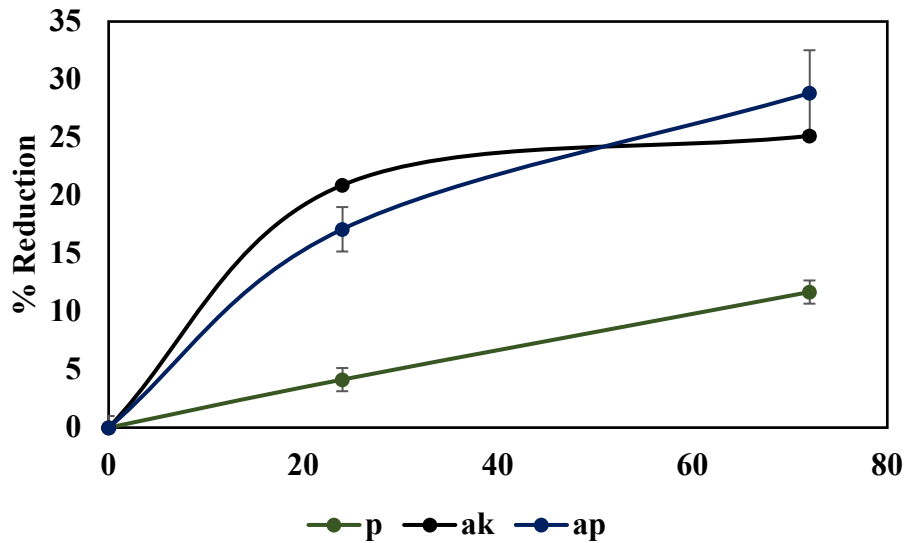
Figure 4.6: Coculture fermentation studies containing endoglucanase exporter and glucosidase exporter for Whatman filter paper as a substrate. A) Filter paper images harvested after 24 hours. From left to right image of filter paper added in empty vector pHT254 strain, filter paper image added in endoglucanase exporter-empty vector pHT254 strain, filter paper image added in endoglucanase exporter-glucosidase exporter coculture B) Weight reduction in filter paper substrate in course of 72 hours of fermentation cycle in empty vector control (p), endoglucanase exporter-glucosidase exporter (ak) and endoglucanase exporter-empty vector control (ap)
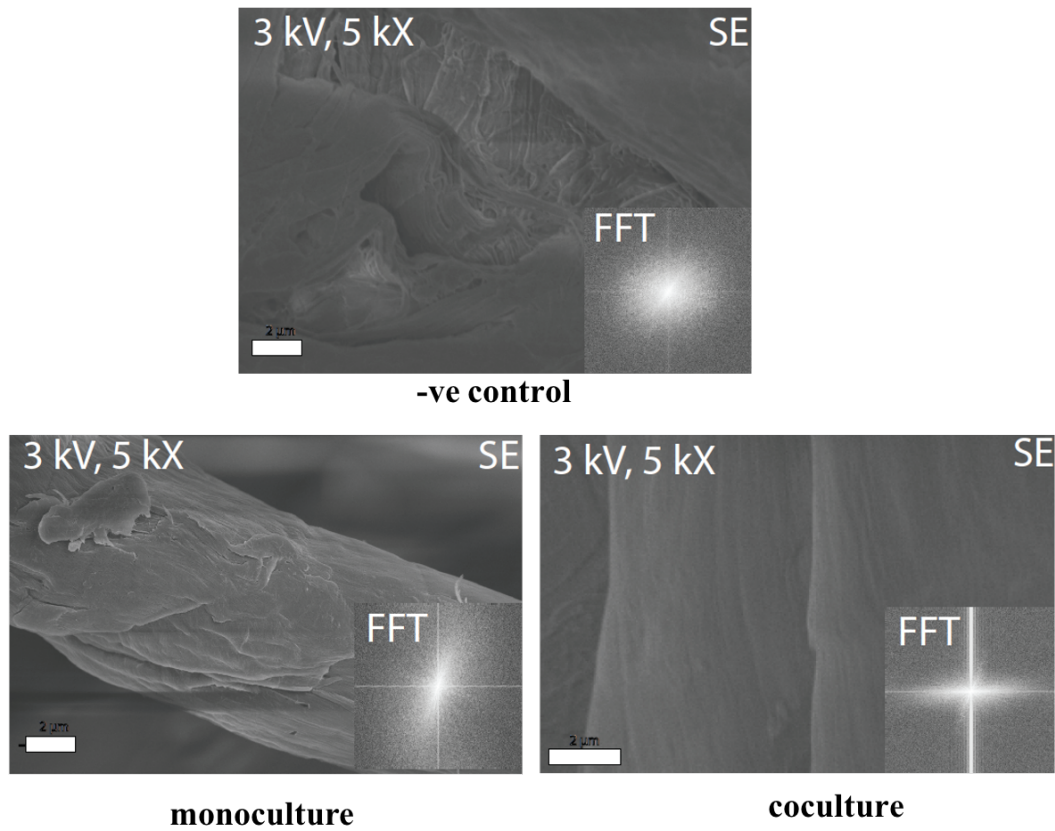
Figure 4.7: Scanning electron microscopic images of Whatman filter paper residues left in negative control (pHT254 empty vector in WB800N *B. subtilis* strain), monoculture (Endoglucanase exporter grown with negative control strain to see impact of single enzyme) and coculture (Coculture system harbouring endoglucanase and glucosidase exporters). Fast fourier transform conducted to find overall orientation of the images.

One pot consolidated bioprocess for avicel cellulose substrate

A
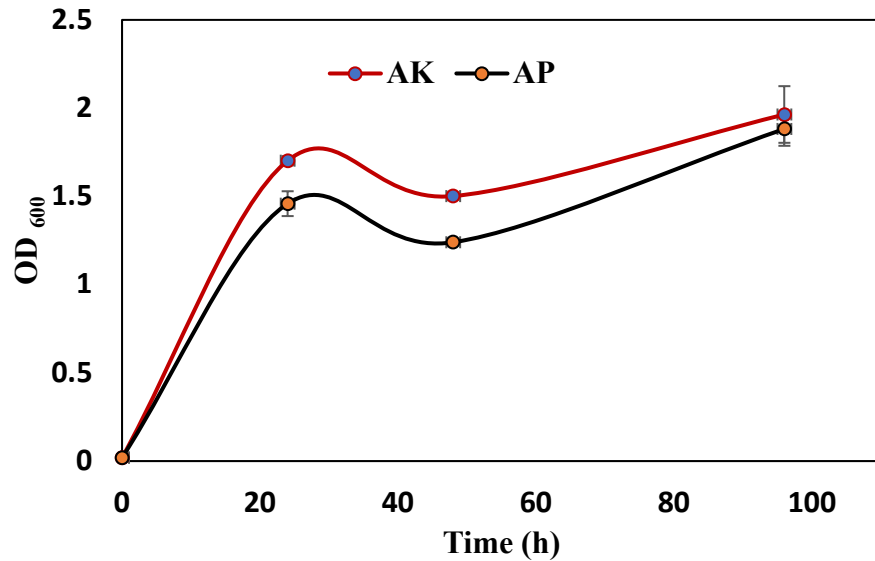
B
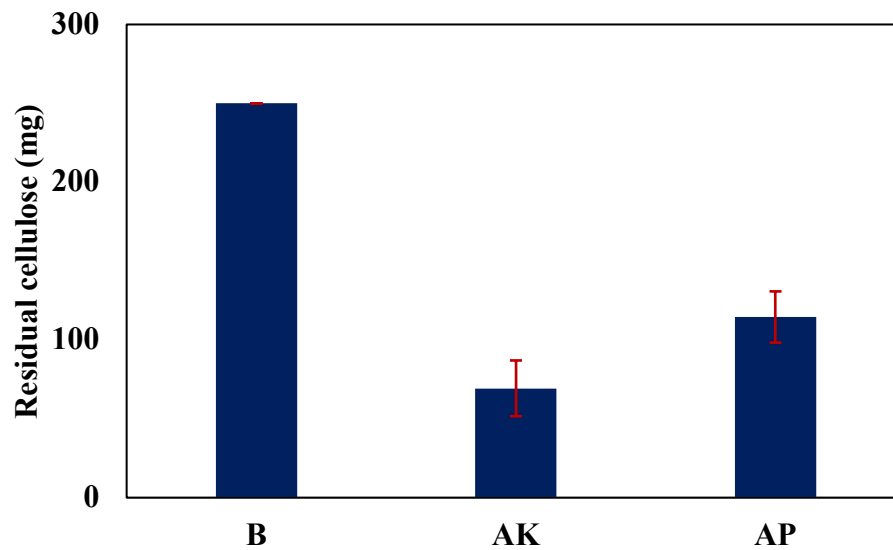
Figure 4.8: Coculture fermentation studies containing endoglucanase exporter and glucosidase exporter for avicel cellulose as a substrate. A) Growth kinetics (mM; means ±SD; n=3) study for the coculture fermentations studied over course of 96 hours B) Residual cellulose in avicel cellulose substrate in course of 96 hours of fermentation cycle in blank media (B), endoglucanase exporter-glucosidase exporter (AK) and endoglucanase exporter-empty vector control (AP)
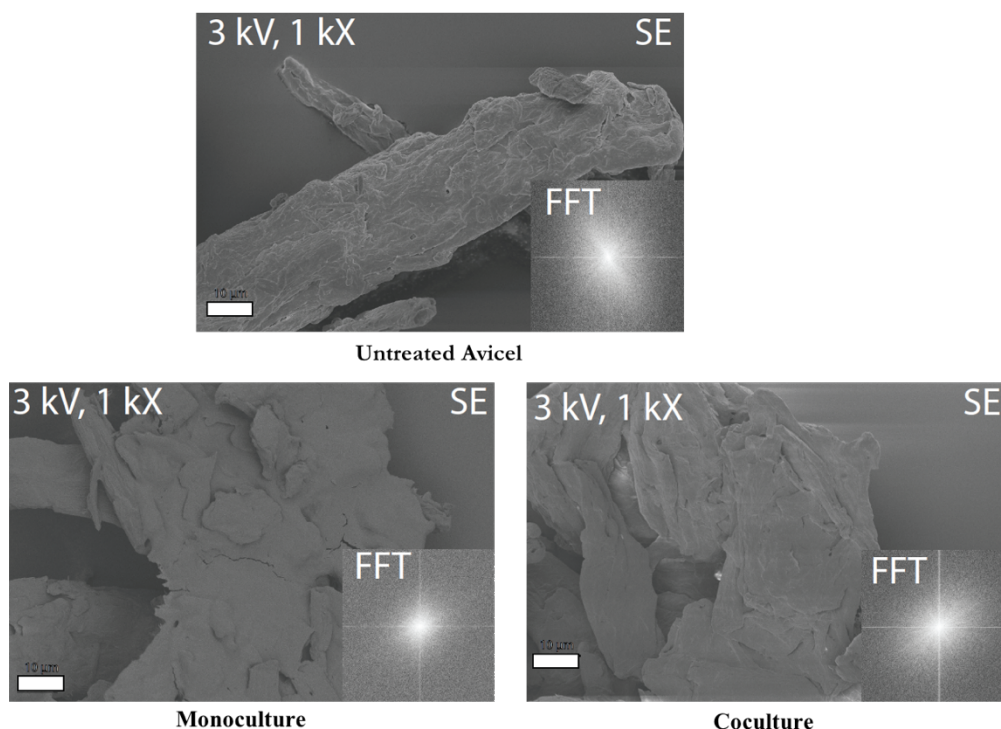
Figure 4.9: Scanning electron microscopic images of avicel cellulose residues left in negative control (untreated microcrystalline avicel cellulose), monoculture (Endoglucanase exporter grown with negative control strain to see impact of single enzyme) and coculture (Coculture system harbouring endoglucanase and glucosidase exporters). Fast fourier transform conducted to find overall orientation of the images.

Higher reduction in overall weight was observed in endoglucanase-glucosidase exporters coculture compared to endoglucanase-empty vector coculture (Figure 4.8 B). SEM images of avicel cellulose showed agglomeration of particles in case of monocultures and cocultures which was not observed in untreated avicel cellulose. Surface difference was observed in coculture and monoculture SEM images wherein monoculture agglomerates had smother surface but coculture had crevices and valleys. This was also translated in the growth kinetics of the fermentation with higher growth was observed in the engineered cocultures compared to just endoglucanase-empty vector strain coculture.

Hence synergistic activity of the coculture strains can be an effective strategy in breaking down cellulose substrate.

4.4 Discussion

Cellulose, the most abundant component of the plant biomass can be a rich source of carbon in biochemical processes. Enzymatic hydrolysis of cellulose is a catchy alternative to explore this tapped potential of cellulose. To conduct enzymatic hydrolysis in one pot enzymes were secreted in the *B. subtilis* WB800N strain. To obtain optimal secretion of these hydrolase SEC pathway signal peptide library was developed to efficiently export enzymes. Optimal secretion levels were observed at lower IPTG concentrations mainly due to flooding of export gates at higher intracellular expression of the enzymes (Mhatre et al., 2022; Peng et al., 2019). *In situ* breakdown of CMC confirmed deconstruction of cellulose and its utilization in 13C fingerprinting studies. CMC is soluble in water and a shorter chain cellulose derivative. Hydrophilicity of CMC makes it easier candidate for accessibility of enzymes and cleavage of glycosidic linkages compared to recalcitrant substrates. Whatman filter paper is mainly cellulose containing both amorphous and crystalline regions. Cellulose microfibril is formed by cellulose polymer bundles stacked together to for high crystalline regions. Microfibrils are linked together by amorphous regions and Whatman filter paper has both these regions (Mboowa et al., 2020). Hence good breakdown was observed in Whatman filter paper by endoglucanase. Although Whatman filter paper showed weight reduction, significant evidence of synergistic effect of enzymes was observed in avicel cellulose which is mainly crystalline cellulose and comparatively difficult to hydrolyze than filter paper. Glucosidase is half the size of endoglucanase and

its higher motility and accessibility in highly stacked crystalline structure must have helped in high breakdown of avicel cellulose in presence of both the enzymes.

4.5 Conclusion

Efficient export of endoglucanase and glucosidase enzyme was optimized in *B. subtilis* strains. Higher intracellular expression does not necessarily be connected to higher export of enzymes. Signal peptide library facilitate proper export of the enzyme. Around 25-30% reduction in labelled fraction confirmed assimilation and metabolism of CMC carbons in the coculture strains. *In situ* fermentation showed efficient reduction of Whatman filter paper weight and appearance. Around 72% reduction in weight was observed in avicel cellulose and synergistic effect of enzyme was essential for breakdown of cellulose.

CHAPTER 5

ENGINEERING BACILLUS SUBTILIS FOR THE ENZYMATIC BREAKDOWN OF

POLYETHYLENE TEREPHTHALATE (PET)

5.1 Introduction

According to the U.S. Environmental Protection Agency, the plastics industry contributed 14 million tons of waste out of a total of 26. 8 million tons, a significant portion of which comes from Polyethylene Terephthalate. More commonly referred to as PET, it is lightweight plastic and primarily used for packaging. While the U.S. currently recycles 31% of the consumed PET, it is not biodegradable through traditional methods, thus precipitating the need for an alternative recycling method. Accumulation of PET has an ecological and environmental impact, especially on aquatic life. It is vital to develop strategies to utilize this abundant source of carbon for making valuable products. PET can be depolymerized into terephthalic acid and ethylene glycol, ethylene glycol has applications in refrigeration, air conditioner industry etc. PET depolymerization can be carried out by several thermochemical treatments, as discussed in chapter 1. Thermochemical treatments are energy-intensive and use of corrosive chemicals (catalysts) can lead to contamination of water bodies. Enzymatic depolymerization is a precise, milder, and benign method of PET depolymerization. In 2016, *I. sakaiensis* strain was discovered by Japanese researchers which had ability to breakdown and metabolise PET plastic bottles (Yoshida et al., 2016). At present, there are at least 200 known strains which have been reported to have PET hydrolysis ability. Several enzymes have been reported to breakdown PET into terephthalate and ethylene glycol (de Castro et al., 2017a; Ronkvist et al., 2009; Shosuke Yoshida, Kazumi Hiraga, Toshihiko Takehana et al., 2016; Silva et

al., 2011; Sulaiman et al., 2012). PET plastic was first introduced in market around 1940, s so in less than 80 years we know strains which have ability to metabolise PET strains.

Early discovered strains although had ability to breakdown PET plastic, their hydrolytic enzymes were slow. Early PET hydrolase from *I. sakaienis* took 60-70 days for compete breakdown of PET substrate. Further developments in enzyme enzyme engineering and machine learning lead to development of PET hydrolases which can deconstruct plastic in 24-48 hours (Lu et al., 2022)). PET hydrolase enzyme deconstructs PET structure into intermediates like BHET and MHET (Figure 5.1). BHET further breaks into ethylene glycol and MHET. MHET breaks into terephthalic acid and ethylene glycol. These monomeric units can be used as utility chemicals in other industries; for example, ethylene glycol is used in freezing units and air conditioners and has a market value of 33 billion dollars in 2020. Some of the major differences in PET substrate compared to previously explored substrates like cellulose and hemicellulose is PET is highly crystalline and level of crystallinity varies in different PET sources. Even PET plastic bottles have high crystallinity at the neck and bottom compared to the centre part. Higher level of crystallinity limits the accessibility of the enzyme. Also, PET surface is highly hydrophobic in nature and enzymatic reactions mainly use water as a solvent especially in consolidated bioprocesses. To circumvent highly hydrophobic nature of enzyme surface UV treatment can be conducted. UV treatment has shown to improve the hydrophilicity of plastic surface and facilitate biodegradation (Lee & Li; Zhao et al., 2007). This project aims at using PET depolymerizing enzymes for synergistic *in situ* depolymerization of PET by *B. subtilis* bacterial platform. Three PET hydrolase enzymes were chosen to develop PET

deconstruction one pot process. Consolidated bioprocess was combined with UV pre-treatment to explore its impact on deconstruction.
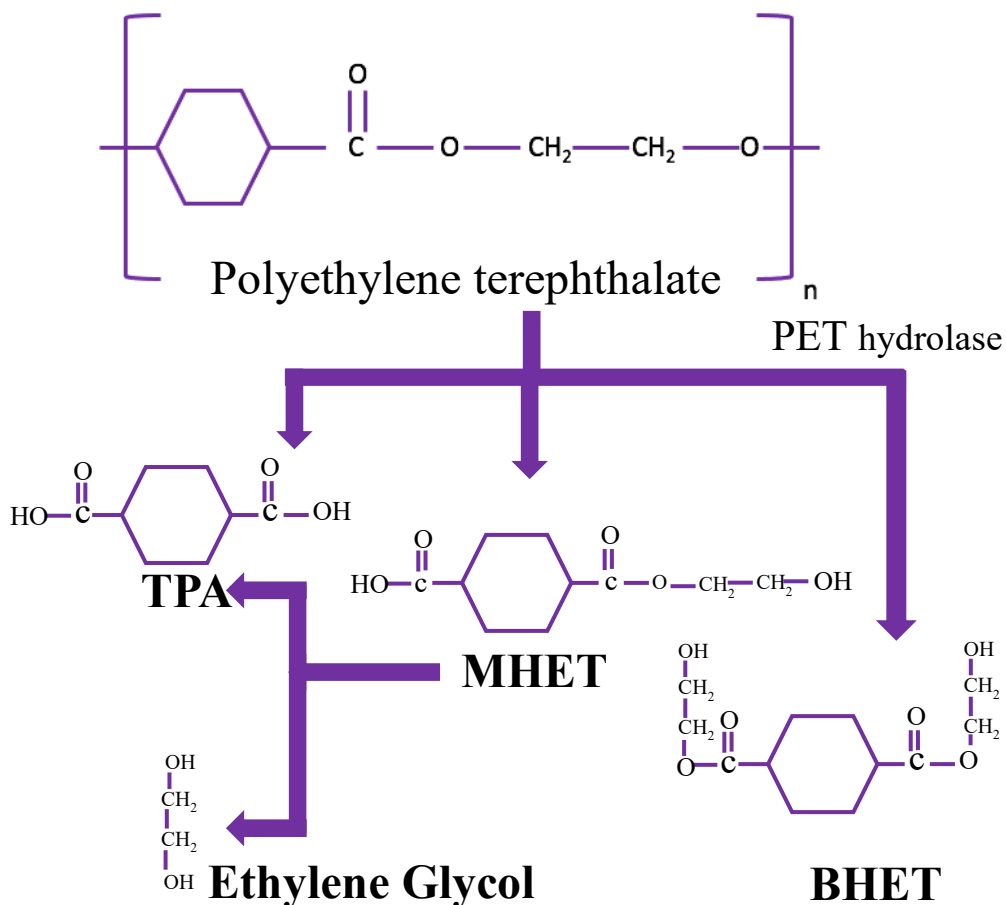
Figure 5.1: PET deconstruction schematic showing PET structure deconstructed into intermediates of BHET and MHET. BHET further deconstructs into MHET and ethylene glycol and MHET breaks into terephthalic acid and ethylene glycol.

5.2   Materials and methods

5.2.1 Chemicals and Materials

All the chemicals were reagent grade or higher, purchased from Sigma Aldrich (St. Louis, MO, USA), unless separately mentioned. PET plastic was purchased from Amazon

Inc (San diego, USA). Oligonucleotides used in the present study were purchased from Milipore sigma (St. Louis, MO, USA). All restriction enzymes were purchased from Thermo Fischer Scientific Inc (San Francisco bay area, CA, USA). Signal peptides and Gene sequences were synthesized by Genescript (Piscataway, NJ, USA).

5.2.2 Media, growth conditions

2xYt media containing yeast extract and tryptone was used to cultivate *Bacillus subtilis* cells at 37 °C, 250 rpm shaking conditions. Luria Bertani (L.B) media was used to cultivate *Escherichia coli* cells at 37 °C, 250 rpm shaking conditions. Solid media plates used for colony screening were prepared by adding 1.5% agar in L.B. and 2xYT media.

5.2.3 Bacterial strains and plasmid

Bacillus subtilis (WB800N: WB800N: *nprE aprE epr bpr mpr::ble nprB::bsr Δvpr wprA::hyg cm::neo*) strain was used in the present study as a non-model organism for enzyme secretion. *Escherichia coli* Dh5a strain was used for transforming developed constructs and storing freezer stocks. PHT254 plasmid was used as a vector in construct development.

Table 5.1 List of plasmids developed in the present study

Plasmids	Description	Source /reference
pHT254	Backbone plasmid for all the developed constructs with ColE1 Ori*	Mobitec, Inc
pBK01	Derived from pHT254 with *NprE- Leaf branch compost cutinase (Leaf branch compost)* and Pgrac100 promoter	This study
pBK 02	Derived from pHT254 with *YwmC- Leaf branch compost cutinase (Leaf branch compost)* and Pgrac100 promoter	This study
pBK 03	Derived from pHT254 with *AmyE- PET hydrolase (Ideonella sakaiensis)* and Pgrac100 promoter	This study
pBK 04	Derived from pHT254 with *YwmC- PET hydrolase (Ideonella sakaiensis)* and Pgrac100 promoter	This study

pBK 05	Derived from pHT254 with *AmyE- p nitrobenzyl esterase (Bacillus subtilis)* and Pgrac100 promoter	This study
pBK 06	Derived from pHT254 with NprE- *p nitrobenzyl esterase (Bacillus subtilis)* and Pgrac100 promoter	This study
pBK 07	Derived from pHT254 with *YwmC- p nitrobenzyl esterase (Bacillus subtilis)* and Pgrac100 promoter	This study
pBK 08	Derived from pHT254 with *AmyE- Leaf branch compost cutinase (Leaf branch compost)* and Pgrac100 promoter	This study
pBK 09	Derived from pHT254 with *NprE- PET hydrolase (Ideonella sakaiensis)* and Pgrac100 promoter	This study

5.2.4 Plasmid construction and transformation

The vector pHT254, having Pgrac100 promoter, was used for the construction of pKB plasmids. Oligonucleotides were used to amplify the respective gene and signal peptide sequences. pKB 08 and pKB 09 constructs were developed by restriction digestion of plasmid and inserts at BamHI and XbaI restriction sites. Final constructs were developed using ligation of digested fragments. Plasmid pKB 01, pKB 02, pKB 03, pKB 04, pKB 05, pKB06 and pKB07 were constructed using the CPEC cloning method by joining fragments amplified with oligonucleotides (Table 5.1). *E. coli* transformation was performed using heat shock transformation method (JoVE Science Education Database 2017). *Bacillus subtilis* transformation method was modified from (Zhang et al. 2011).

5.2.5 Extracellular enzymatic reactions

Recombinant strains were grown in 5 mL 2xYT (Tryptone 16 g/L; Yeast Extract 10 g/L; Sodium Chloride 5 g/L) media till logarithmic growth phase (OD_{600}: 0.8) and induced (1mM Isopropyl β-D-1-thiogalactopyranoside (IPTG)) to enable enzyme secretion. Supernatant samples were collected after 24 hours and further used for enzyme reactions. The enzyme reaction was carried out in citrate phosphate buffer at 40 °C for 1

hour at pH 5.5. Similarly, the enzyme reaction was set up in citrate phosphate buffer 100 ul of p NPA (1%) added in 100 ul of supernatant, and the reaction was conducted at 40 °C 1 hr. At the end of enzymatic reaction absorbance readings were taken at 420 nm to quantify mM of pNP produced. pNP standards were used to develop a calibration curve.

5.2.6 BHET coculture fermentations

The cell culture seed were grown in 5 mL 2YT media overnight. 3M media as described in table 3.1, 3.2 and 3.3 was used along with 1% BHET. The fermentation cultures were conducted in 50 mL if BHET-3M media. Cultures were induced at OD_{600} of 0.8 with IPTG. The samples were studied for growth and HPLC. UV crosslinker was used to expose BHET to UV treatment of 1 or 2h. After UV treatment BHET beads were added in the fermentation media.

5.2.7 *In vitro* PET breakdown

Recombinant strains were grown in 5 mL 2xYT (Tryptone 16 g/L; Yeast Extract 10 g/L; Sodium Chloride 5 g/L) media till logarithmic growth phase (OD_{600}: 0.8) and induced (1mM Isopropyl β-D-1-thiogalactopyranoside (IPTG)) to enable enzyme secretion. Supernatant samples were collected after 24 hours and further used for enzyme reactions. 1% PET plastic sheets in collected supernatant in 1mL total volume were incubated at 55 °C for 24 hours to 120 hours as stated in results. The supernatant samples were studied in HPLC for terephthalic acid production.

5.2.8 Analytical methods

High-performance liquid chromatography (HPLC) (Agilent technologies 1100 series; G1311A, Santa Clara, CA) was used to quantitate metabolites formed in fermentation media. The compounds were separated using C18 column (300 * 7.8 mm) at a temperature

of 40 °C with ACN as mobile phase at a flow rate of 1 ml/min and detected with a UV detector at 420 nm (Agilent technologies 1200 series; G1362A, Santa Clara, CA). The samples were quantified using comparison with terephthalic acid calibration curves (2 to 20 g/L).

5.2.9 PET plastic processing
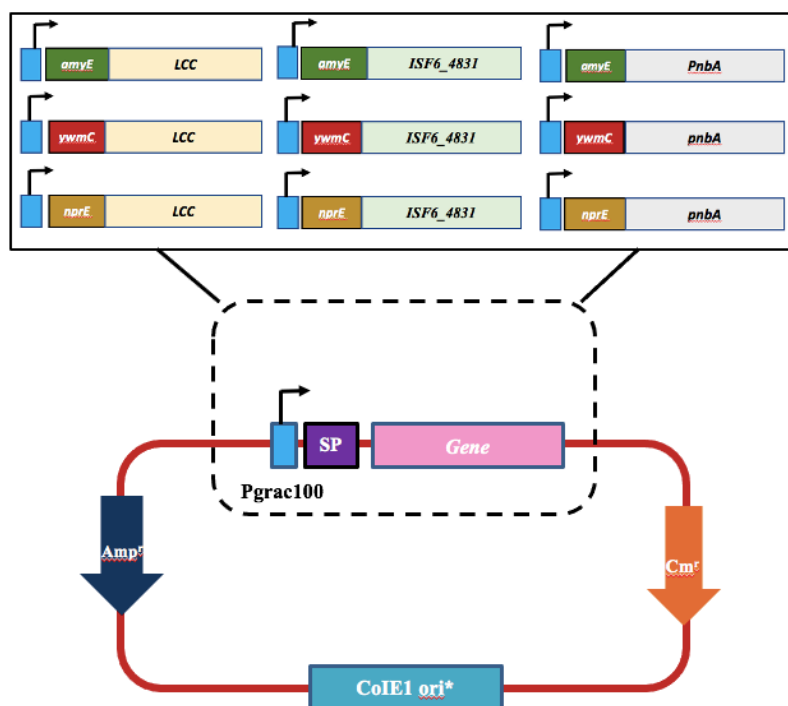
Figure 5.2: Overview of plasmid construction: figure gives a brief overview of the signal peptide enzyme selected for the present work. Three signal peptide libraries to be constructed in the current work contains *amyE*, *ywmC*, and *nprE*. Three enzymes shown in the figure are LCC (leaf branch compost cutinase) from Leaf branch compost, *pnbA* (*p* nitrobenzylesterase) from *bacillus subtilis*, and ISF6_4831 from *Ideonella sakaiensis*. Nine combinations of signal peptides and enzymes will be cloned into pHT254 vector harbouring ampicillin and carbenicillin marker and Pgrac100 promoter.

5.3 Results

5.3.1 Plasmid construction and enzyme- signal peptide library development

Due to surging research in field of PET deconstruction, lot of enzyme candidates have been engineered which can efficiently break down PET plastics. During construct designing for this work, *B. subtilis* was selected as a host organism due to its ability to efficiently secrete enzymes and available information about its export machinery. *B. subtilis* WB800N strain was used as its proteases are deleted which ensures our exported enzymes are not cleaved. PET deconstruction enzymes isolated from nature are mainly different types of esterases and cutinases which have evolved with time to act on PET plastic surface. Cutinases and esterases are known to cleave hydrophobic surfaces and hence with time they have evolved to breakdown plastic. Three enzyme candidates selected for this work were different cutinases and esterases like leaf branch compost cutinase, nitrobenzyl esterase native to *B. subtilis* and PET hydrolase enzyme from *I. sakaiensis.* The thought process in selecting these enzymes was to select candidates which have good performance based to published literature of that time. Esterase from B. subtilis had reported PET breakdown activity and as it was native to host organism it will be compatible with the enzyme export machinery of the bacterium (Ribitsch et al., 2011). PET hydrolase from *I. sakaiensis* was first known PET hydrolase which has PET plastic as its substrate natively and hence possibility of overexpression and export of this enzyme was studied in this work. LCC enzyme was improved using directed evolution and enzyme engineering methods to make it one of the fastest PET deconstruction enzymes known during the project designing (Wei et al., 2016). Similar to previous work, three native signal peptides were selected to improve the enzyme export in the host organism. SEC pathway is known

to export most of the signal peptides in *B. subtilis* and hence SEC pathway signal peptides were used in this work YwmC, NprE and AmyE were the three selected signal peptides linked with three enzyme candidates of LCC, PET hydrolase and nitrobenzyl esterase to form 9 construct library as shown in figure 5.2. Enzymatic assays were used to quantify the strain supernatant activities to select the best performing strains.

5.3.2 Selection of best performing constructs

Enzymatic assays are extensively used for selection of strains from a library of strains mainly because a bigger sample size can be analysed by using a simple absorbance readings in a 96 well plates. In present work as discussed previously a library of 9 constructs was developed using native signal peptides linked using a linker with the enzyme candidates. The developed *B. subtilis* candidates were cultured in rich media and induced with IPTG as Pgrac100 IPTG inducible promoter was in the upstream region of the enzyme signal peptide assembly. The strains were induced in late log phase of growth and were allowed to grow overnight. After allowing enzyme secretion in strains the cultures were centrifuged and the supernatant was separated. This supernatant was used in pNPA assay commonly used for esterase and cutinase activity (Brockmeier et al., 2006; Ribitsch et al., 2011). In pNPA assay the added enzyme cleaves pNP which shows color change from colorless to yellow. This color is studied for absorbance to quantify pNP concentration based on pNP calibration curve. More pNP production indicates higher enzyme activity. Firstly pNPA assay was conducted for all 9 strains for a span of 1hr. Based on the results of this assay 6 strains were selected harbouring LCC and PET hydrolase showed good activity which were used for kinetics study shown in figure 5.3. LCC enzyme has been reported to show better performance compared to other enzymes and this was also

observed in present work where all the LCC constructs showed higher pNP production from PET hydrolase and nitrobenzyl esterase. As shown in figure 5.3A YwmC signal peptide linked to LCC enzyme showed 6-7 folds higher pNP production than other strains in first 10 mins of the enzyme reaction. All the engineered strains showed better activity than pHT254 negative control. Overall LCC constructs of all 3 signal peptides were better than PET hydrolase constructs. Compared to three signal peptide candidates used in this work mainly YwmC, NprE and AmyE; YwmC signal peptides showed highest secretion of enzyme which got translated into high pNP production in pNPA assay. pH is an essential parameter in enzyme reactions. At an non optimal pH enzyme reaction are either low or are hindered. To understand the optimal pH of the present developed constructs, an *in vitro* enzyme reactions was conducted at varying pH of 6, 7, 8 and 9. No activity was observed at pH of 6 and 9 which confirmed either denaturation or change in enzyme conformation which hindered proper breakdown. pH of 8 was seen to be optimal with highest activity preceded by pH 7 (Figure 5.3B). pH studies were important with respect to consolidated bioprocess because optimal pH should be in the range of the growth of the host strains. B. subtilis is able to grow in the pH range of 7-8 and hence further *in situ* studies were conducted at that pH.
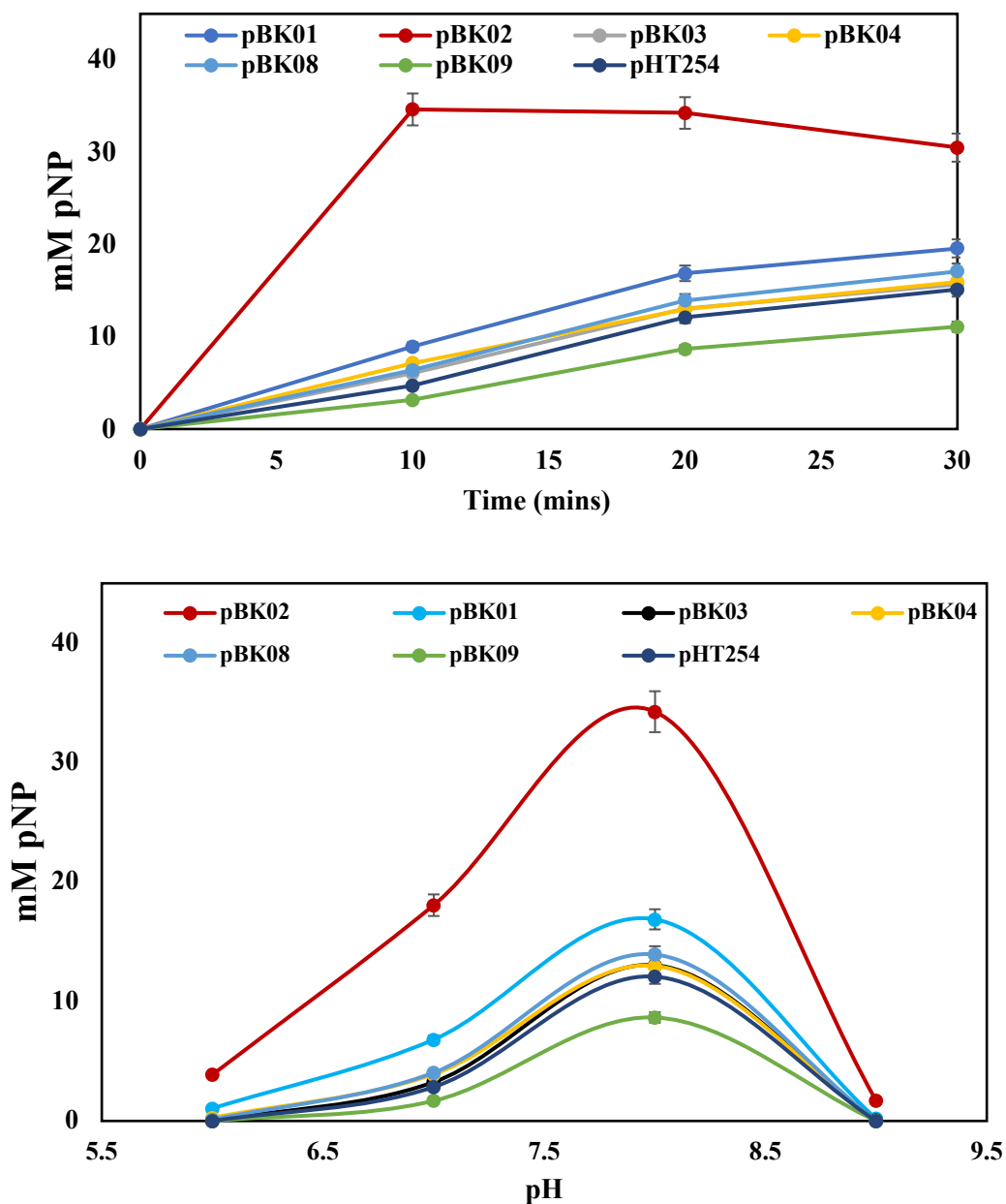
Figure 5.3: pNPA enzymatic assay results for 1mg/ml protein load from induced supernatants of the developed constructs. A) pNP production (mM; means ±SD; n=3) kinetics with respect to time in minutes for different constructs (pHT254: empty vector negative control; pBK01: NprE-LCC; pBK02: YwmC-LCC; pBK03: AmyE-ISF6; pBK04: YwmC-ISF6; pBK08: AmyE-LCC and pBK09: NprE-ISF6 p) B) Effect of pH (6, 7, 8 and 9) on the pNP (mM; means ±SD; n=3) production.

PET hydrolysing enzymes have been extensively used in in vitro conditions mainly due to their high optimal temperatures. Higher optimal temperatures help PET hydrolysis reaction mainly because higher temperatures reduce the level of crystallinity of highly crystalline PET surface. One of the major demerits of high operating temperatures of these PET enzymes is that most of the host systems are not compatible with these temperatures and is essential to develop lower temperature *in situ* processes which will help translating this technology in outer world. One of the roadblock in deconstruction of PET surface at room temperature is its highly hydrophobic nature. To improve hydrophobicity of the PET surface UV treatment was conducted. Figure 5.4 A shows confirmation of increase in hydrophilicity of PET surface using UV treatment. Significant reduction in contact angle of untreated surface to UV treated surface was observed which confirmed increasing hydrophilicity using UV treatment. Effect of UV treatment was also studied on *in situ* BHET consolidated process. BHET is a PET intermediate which can be deconstructed into MHET and MHET can further breakdown into monomeric terephthalic acid and ethylene glycol. BHET beads were UV treated for 1h and 2h initially. These pellets were then added in pBK02 strain harbouring YwmC-LCC culture. The strains were induced in later log phase with IPTG concentration of 0.2 and 0.5 mM. In BHET *in situ* consolidated bioprocess around 4-5 folds increase in terephthalic acid production was observed compared to pHT254 empty vector negative control strain. UV treatment significantly showed favourable impact on the process with all the UV treated batches showed 3-4 folds higher terephthalic acid production compared to untreated batches. IPTG concentrations of 0.2 and 0.5 mM both showed fair increase in terephthalic acid production. Higher UV treatment time showed higher product titres.

A

UV treated surface
(Contact angle: 43º)

Untreated surface (Contact
angle: 60º)
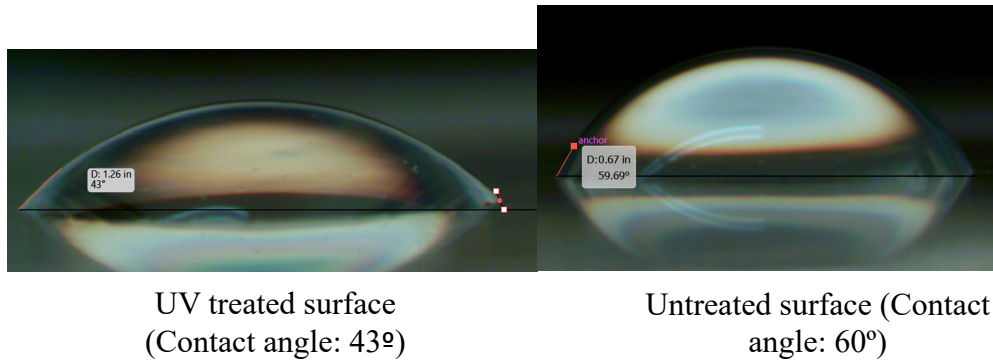
B
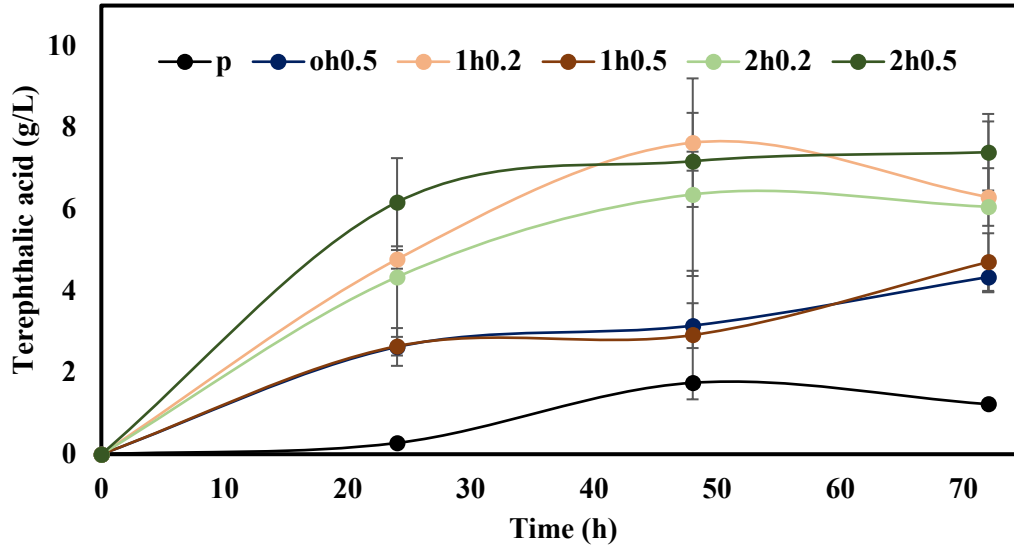
Figure 5.4: BHET *in situ* consolidated bioprocess. A) Images of drop test on PET plastic surface to study the effect of UV treatment on hydrophilicity of the surface, image on right is a untreated surface with higher contact angle and picture on left is treated surface with lower contact angle. B) Terephthalic acid production (g/L; means ±SD; n=3) kinetics in *in situ* BHET consolidated process with respect to time in minutes for different variants in pBK02 strain; p is empty vector control; 0h0.5 is no UV treatment with 0.5 mM IPTG induction; 1h0.2 is 1h UV treatment with 0.2 mM IPTG induction; 1h 0.5 is 1h UV treatment with 0.5 mM IPTG induction, 2h0.2 is 2h UV treatment with 0.2 mM IPTG induction; 2h0.5 is 2h UV treatment with 0.5 mM IPTG induction

Table 5.2: BHET in situ deconstruction batches data

Name	Details	Terephthalic acid (g/L)	% reduction
P	Negative control	1.22	17.06
0h0.5	No treatment	4.34	60.95
1h0.2	1h UV treatment batch; 0.2 mM IPTG induction	6.3	95.05
1h0.5	1h UV treatment batch; 0.5 mM IPTG induction	4.7	66.29
2h0.2	2h UV treatment batch; 0.2 mM IPTG induction	6.0	88.62
2h0.5	2h UV treatment batch; 0.5 mM IPTG induction	7.4	100

As shown in table 5.2 comprehensive list of all the variations attempted in *in situ* BHET process confirm UV treatment facilitates PET intermediate breakdown. Complete reduction in BHET was observed in 2h UV treated sample induced at 0.5 mM of IPTG. This is a first consolidated PET intermediate bioprocess developed till now.

5.3.4 *In vitro* PET to terephthalic acid production process

After developing first *in situ* BHET deconstruction process and observing helpful effects of UV treatment on deconstruction process, effect of UV was studied on PET sheet. PET sheets were cut into squares and exposed to UV for a span of 1hr. pBK02 strain was

cultured in 2YT media and induced at late log phase, after induction culture was allowed to grow to secrete hydrolysing enzyme for 24 hours. PET sheets and the supernatant were added and enzyme reaction was conducted for 24 hours in optimal conditions. Around 0.2 g/L of terephthalic acid was produced in the *in vitro* process. Empty vector control was used as a negative control in this work and as shown in figure 5.5 significant terephthalic acid peak was observed compared to the control strain.
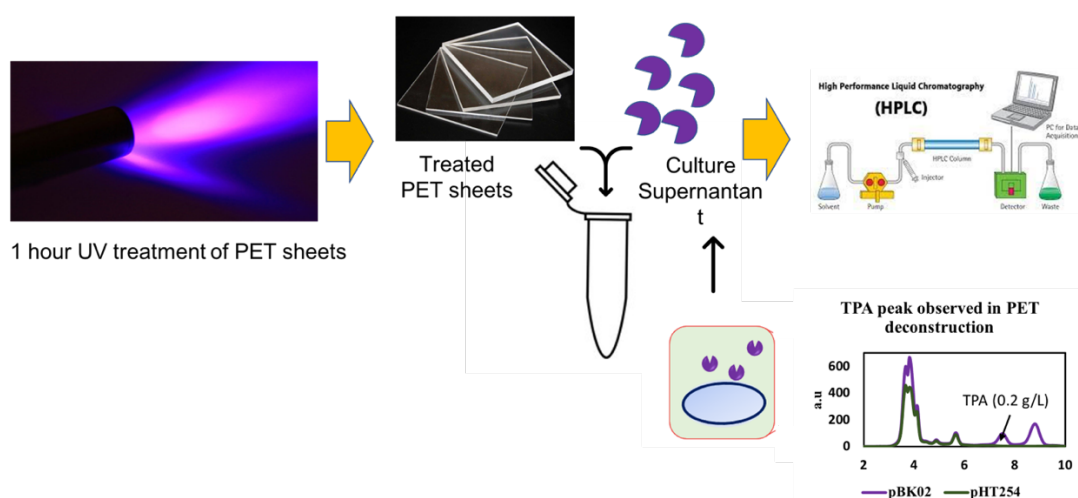
Figure 5.5: Schematic showing PET plastic *in vitro* reaction setup and terephthalic acid titre observed at the end of the reaction

After preliminary studies on PET sheets in invitro conditions, effects of the LCC on particle size was studied by conducting invitro enzyme reaction of PET sheet and PET powder. Reduction in particle size showed 3 folds improvement in TPA production (Figure 5.6 A). Effect of UV treatment was further studied by conducting in vitro reactions for 2h, 5h and 10h of UV treatment and UV treatment more than 5h was enough to exponentially improve

TPA production to 3-4 g/L (Figure 5.6 B). *In vitro* enzyme reaction was conducted at 55 and 37 C and higher temperature was more favorable for PET breakdown (Figure 5.6 C).

A
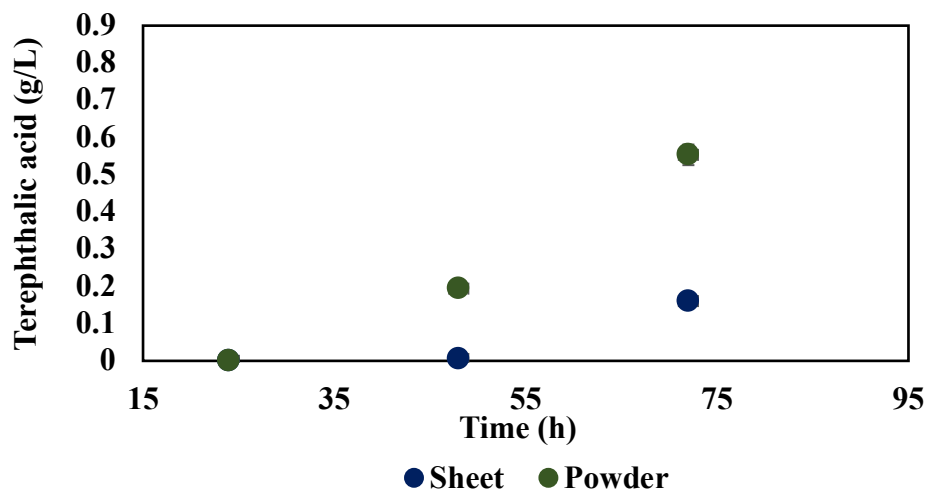
B
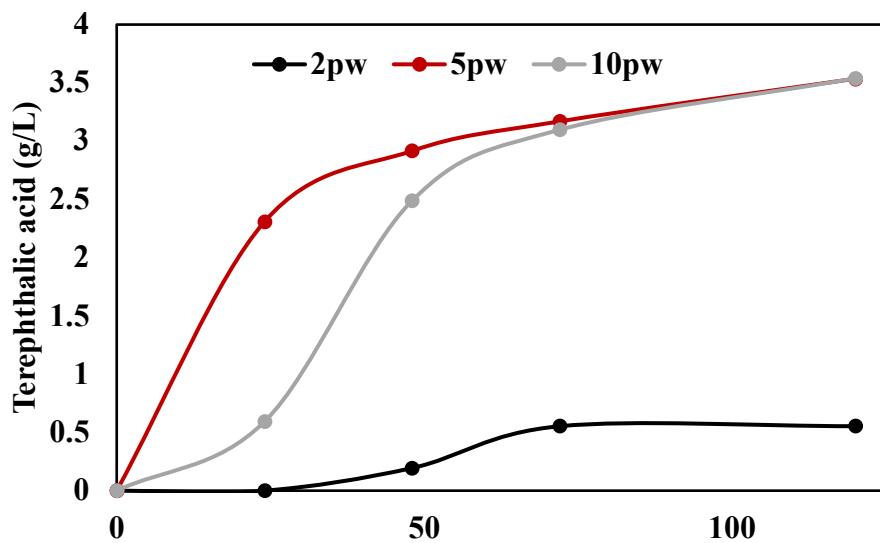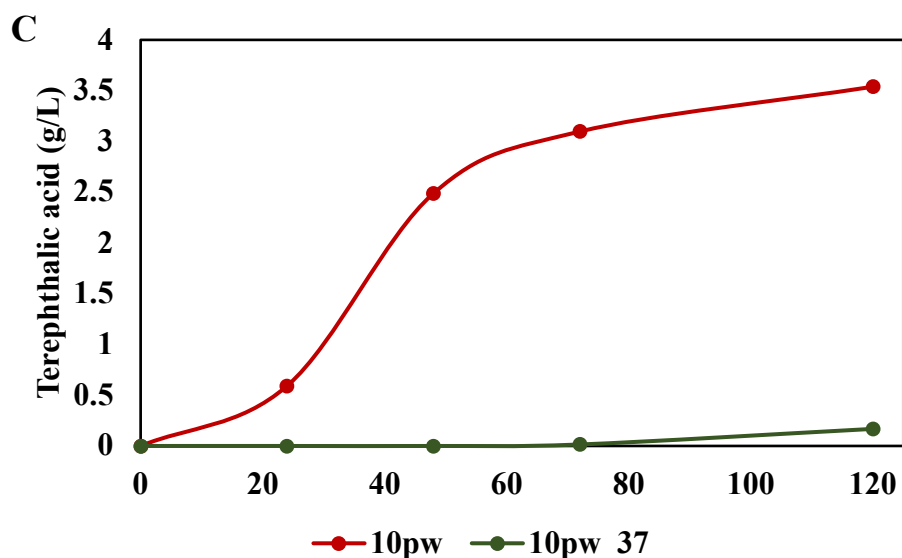
Figure 5.6: *In vitro* reaction results: *B. subtilis* strain harbouring pBK02 plasmid was induced and supernatant obtained after 24 hours was used in *in vitro* enzymatic reaction. A) Effect of terephthalic acid (TPA) production in PET plastic sheet and PET plastic powder B) Effect of UV treatment time on TPA production where 2pw, 5pw, 10pw are PET powder treated for 2, 5 and 10 hours. C) Effect of temperature on TPA production

5.4 Discussion

PET plastic is a major source of ocean pollution and enzymatic hydrolysis can be a interesting alternative in future. To circumvent expensive enzyme cost, enzymes can be exported in host organisms and signal peptides can be used to hack this enzyme export mechanism. Enzymes used in this work mainly LCC, PET hydrolase and benzyl esterase. Three SEC pathway signal peptides used in this work NprE, YwmC and AmyE. Signal peptide enzyme combinations are highly specific and one universal signal peptides cannot be used to export all the enzymes (Mhatre et al., 2022; Sulaiman et al., 2012). In present work YwmC signal peptide showed best performance for LCC enzyme, AmyE and YwmC signal peptide linked with PET hydrolase enzyme showed better performance than NprE

signal peptide. Although mechanism is not completely known YwmC signal peptide seemed to facilitate the LCC export in *B. subtilis* system. PET plastic surface is highly hydrophobic in nature compared to other types of biopolymers explored previously. Enzymatic reactions mainly use water as a solvent to conduct the reaction and hence it is difficult to access sites on the substrate for enzymes to successfully conduct the enzymatic reactions. Among the three enzyme candidates LCC enzyme showed best performance in enzymatic assays conducted. One major reason to this can be the fact that esterase from *b subtilis* and PET hydrolase were mainly native enzymes and LCC was evolved for plastic surface and hence after achieving successful folding and export of this enzyme it proved to be a better candidate than other enzymes. UV treatment is known to improve the hydrophilicity of the plastic surface and improve its water contact. UV light mainly gets absorbed by the plastic surface and excites photons which leads to formation of free radicals, presence of oxygen species leads to degradation of plastic surface which makes it more hydrophilic (Eberl et al., 2009; Zhao et al., 2007). UV degradation was seen to be of significant help in deconstruction of BHET in situ process which seemed to improve hydrophilicity of the surface and in turn improve enzyme substrate contact and hence better deconstruction of plastic intermediate. Along with UV treatment which improves surface contact of enzyme and PET plastic, temperature also plays a vital role as observed in our studies. Higher temperature favors movement of particles and better contacting of enzyme and substrate and also reduces level of crystallinity of PET surface making it easier substrate to breakdown. Developing one pot PET plastic deconstruction process is a promising step towards mitigation of plastic waste in future.

CHAPTER 6

CONCLUSIONS AND FUTURE WORK

6.1 Hemicellulose deconstruction

the endo-1,4-β-xylanase enzyme was meticulously exported via sec pathway in *B. subtillis* by screening multiple signal peptide enzyme combinations wherein YwmC$_{sp}$-XynA signal peptide enzyme combination showed 3-fold higher reducing sugar production compared to wild type WB800N strain. Furthermore, *in situ* depolymerization of xylan was successfully demonstrated wherein the engineered strain SSL26 achieved a maximum xylose yield of 0.66 g of xylose produced/g of xylose present in xylan. This is one of the first studies where a cross genus coculture system was developed and demonstrated for the consolidated bioprocessing of hemicellulosic biomass into value-added chemicals and fuel. The study demonstrates that through careful selection of a microbial host which has a natural ability for protein secretion, a robust CBP system can be developed as demonstrated by the highest sugar yield obtained in this study. Furthermore, employing a *B. subtilis - E. coli* coculture system allowed for the synergistic division of labor, thereby enabling the production of succinate directly from xylan. Signal peptide optimization can be performed to further improve the hydrolysis rate of xylan. On the other hand, by employing well-controlled bioreactor, fuels and chemicals can be obtained at a higher titer, rate, and yield as it will allow both the strains to function under optimal conditions throughout the study.

Aims and objectives successfully completed

a) Developing endoxylanase secretion strain

b) One pot hemicellulose breakdown into C5 sugar xylose

c) Assimilation and metabolism of xylose to produce industrially viable products

6.2 Cellulose deconstruction

Endoglucanase exporter strain was developed and optimized for the suitable signal peptide from the signal peptide library. Similarly, glucosidase exporter was developed for proper folding and export of glucosidase enzyme. Among the library of signal peptides SpybN signal peptide linked to Bscel5 endoglucanase showed two folds higher reducing sugar production than other strains and AmyE signal peptide linked with glucosidase enzyme 4-5 folds increase compared to other candidates. Furthermore, a cellulose derivative CMC based *in situ* consolidated process was developed. Growth kinetics indirectly confirmed availability of carbon source after 48 hours of fermentation only in engineered coculture and not in negative control. U-^{13}C fingerprinting studies were conducted to further confirm breakdown and carbon utilization in engineered coculture batches. Compared to negative control engineered coculture showed 25-30% reduction in labelled fraction in alanine, glycine, isoleucine, methionine and tyrosine. Then, Whatman filter paper squares were added in fermentation media which showed complete disappearance of sheet in engineered cocultures compared to the negative control. Avicel cellulose or microcrystalline cellulose confirmed 70% reduction in cocultures. Developed cocultures have been used to study different types of cellulose like Avicel, Whatman filter paper and CMC. Furthermore, this process can be next used for product formation to develop cellulose to product consolidated bioprocess. Aims and objectives completed:

a) Developing endoglucanase and glucosidase secreting strains

b) Selection of best exporters using enzymatic assays

c) Developing one pot cellulose breakdown process

6.2.1 Future plans
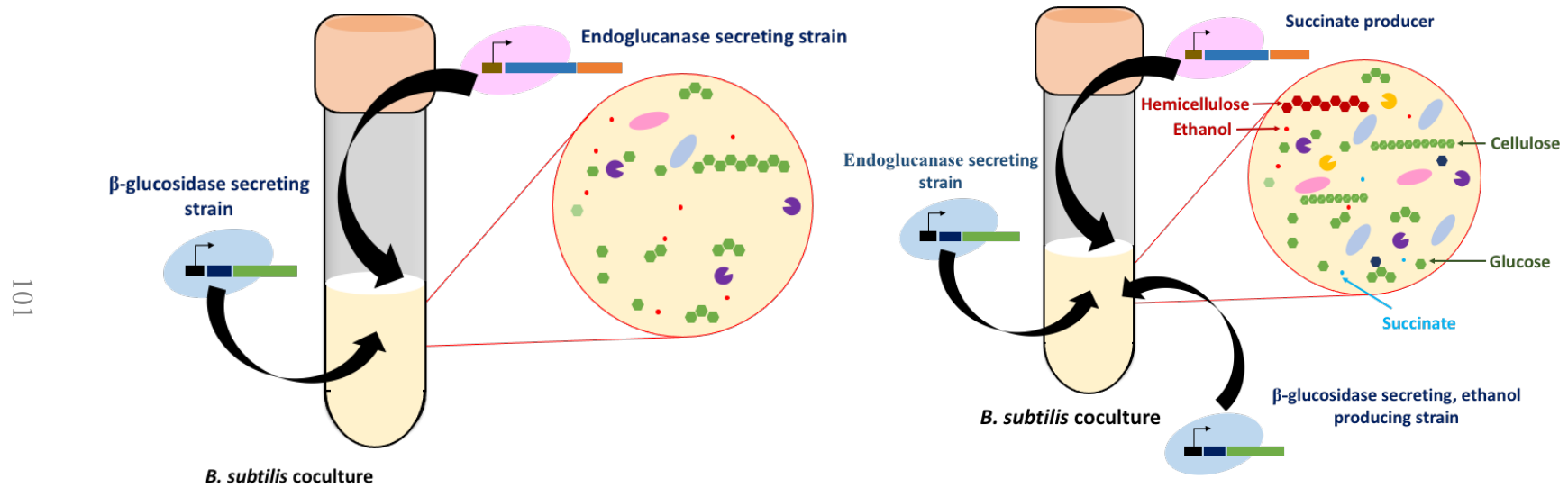
Figure 6.1: Future plans and possible developments in cellulose consolidated bioprocess; A) Development of lactate production process by engineering glucosidase strain. B) Development of plant biomass component coculture process with three strains, two *B. subtilis* and one *E. coli*

6.3 PET deconstruction

PET deconstruction enzyme secretion was optimized by development of signal peptide enzyme library. Among three signal peptides studied for this work AmyE, YwmC and NprE; YwmC signal peptide showed appropriate folding and export of the enzyme. Among combinations developed in library YwmC signal peptide linked with LCC enzyme showed best performance among all the screened candidates. YwmC signal peptide showed 2-3 folds higher pNP concentrations compared to other developed strains. UV treatment was used to improve bioavailability of the PET surface. Contact angle of the UV treated surface calculated by drop method showed contact angle reduction from 60° to 43°. UV treatment also showed improvement in BHET *in situ* bioprocess process. Approximately 5-6 folds increase in terephthalic acid titers was observed in UV treated BHET compared to untreated BHET. This was first in situ BHET deconstruction process developed. All the added BHET was converted to products. Highest terephthalic acid titers observed was 7.1 g/L. Furthermore, *in vitro* studies were conducted to for the supernatant containing exported enzyme. Highest *in vitro* titers for PET sheets were observed as 0.2 g/L. Further improvements in this technology can lead to higher deconstruction of PET sheets.

The project aims completed

a) Developing PET hydrolytic enzyme secreting strain

b) Develop strategy to increase bioavailability of PET surface

c) Demonstrating one pot deconstruction of PET derivative

6.3.1 Future plans

a)   Photocatalytic degradation of PET sheets

Photocatalytic degradation uses a catalyst which can facilitate the degradation of plastic surface using UV light. Most commonly used catalyst in this work is TiO_2 which absorbs light and helps in creating free radicals which further make the surface more bioavailable (Figure 2)
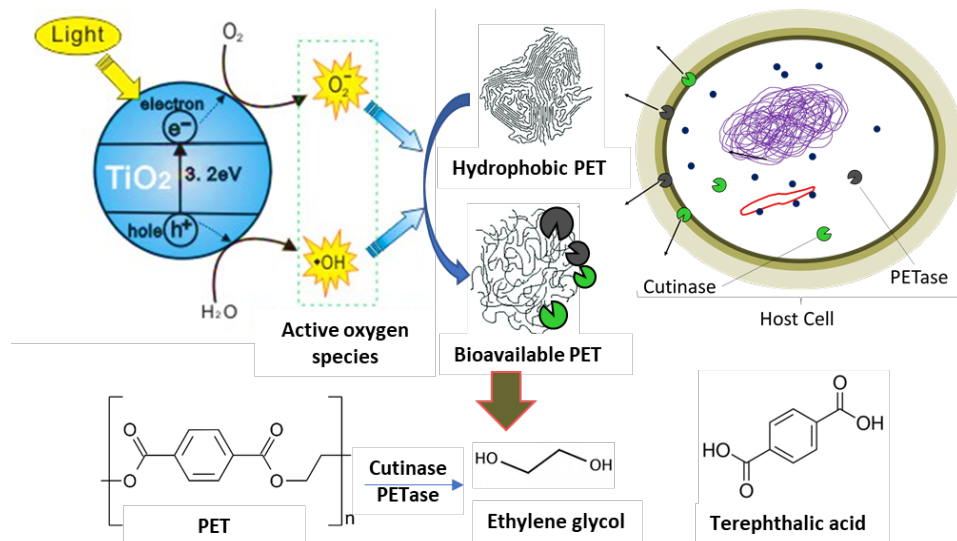
Figure 6.2. TiO_2 catalyzed valorization of plastics via a microbial secretion machinery engineered for secretion of PETase and cutinase in the presence of UV light.

Increase bioavailability of the PET surface using photocatalytic degradation will improve the PET deconstruction in an *in situ* fermentation conditions.

b)   Development of BHET to vinly phenol coculture system

BHET deconstruction to terephthalic acid process is already developed in *in situ* conditions. In this process the terephthalic acid developed by BHET process will be used

as carbon source by *C. glutamicum* strain. *C glutamicum* strain as TPA transporter which facilitates TPA assimilation in *C. glutamicum*. *C. glutamicum* will use terephthalic acid and produce vinyl phenol as a product.

BHET

Terephthalic acid producer

Vinyl phenol producer

Vinyl phenol
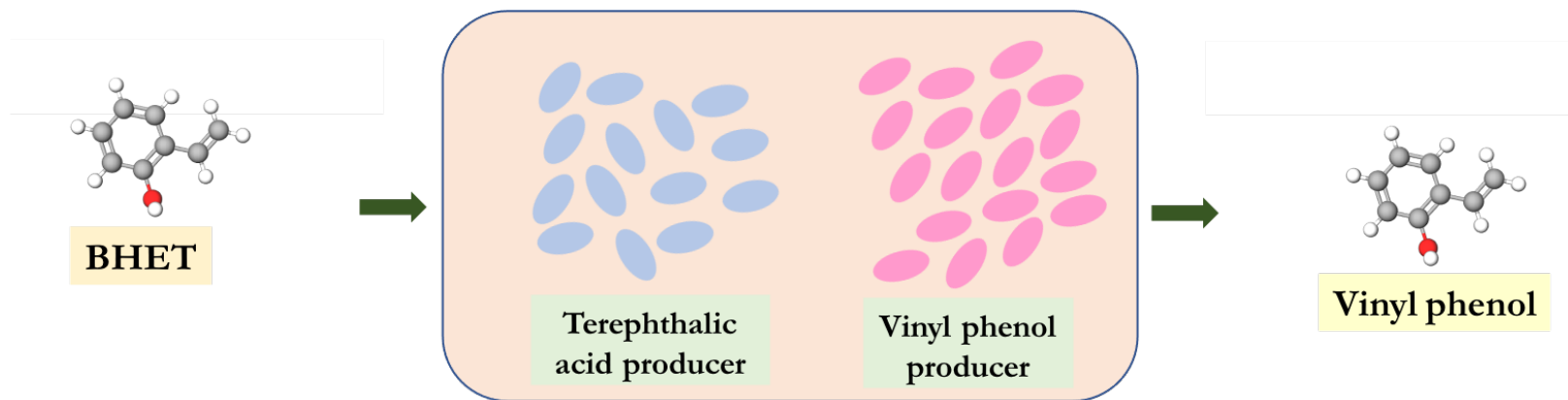
Figure 6.3: Proposed coculture process schematic

REFERENCES

Araújo, R., Silva, C., O'Neill, A., Micaelo, N., Guebitz, G., Soares, C.M., Casal, M., Cavaco-Paulo, A., 2007. Tailoring cutinase activity towards polyethylene terephthalate and polyamide 6,6 fibers. J. Biotechnol. 128, 849–857. https://doi.org/10.1016/j.jbiotec.2006.12.028

Aravinthan, A., Arkatkar, A., Juwarkar, A.A., Doble, M. 2016. Synergistic growth of Bacillus and Pseudomonas and its degradation potential on pretreated polypropylene. *Preparative Biochemistry & Biotechnology*, **46**(2), 109-115.

Arkatkar, A., Juwarkar, A.A., Bhaduri, S., Uppara, P.V., Doble, M. 2010. Growth of Pseudomonas and Bacillus biofilms on pretreated polypropylene surface. *International Biodeterioration & Biodegradation*, **64**(6), 530-536.

Ahn, Jung Ho, Yu Sin Jang, and Sang Yup Lee. 2016. "Production of Succinic Acid by Metabolically Engineered Microorganisms." *Current Opinion in Biotechnology*.

Banerjee, A., Chatterjee, K., Madras, G., 2014. Enzymatic degradation of polymers: A brief review. Mater. Sci. Technol. (United Kingdom). https://doi.org/10.1179/1743284713Y.0000000503

Bayer, E.A., Lamed, R., Himmel, M.E., 2007. The potential of cellulases and cellulosomes for cellulosic waste management. Curr. Opin. Biotechnol. https://doi.org/10.1016/j.copbio.2007.04.004

Bendtsen, J.D., Nielsen, H., Von Heijne, G., Brunak, S., 2004. Improved prediction of signal peptides: SignalP 3.0. J. Mol. Biol. https://doi.org/10.1016/j.jmb.2004.05.028

Brockmeier, U., Caspers, M., Freudl, R., Jockwer, A., Noll, T., Eggert, T., 2006. Systematic Screening of All Signal Peptides from Bacillus subtilis: A Powerful Strategy in Optimizing Heterologous Protein Secretion in Gram-positive Bacteria. J. Mol. Biol. 362, 393–402. https://doi.org/10.1016/j.jmb.2006.07.034

Brown, Alan, Israel S. Fernández, Yuliya Gordiyenko, and V. Ramakrishnan. 2016. "Ribosome-Dependent Activation of Stringent Control." *Nature*.

Bendtsen, J.D., Nielsen, H., Von Heijne, G., Brunak, S. 2004. Improved prediction of signal peptides: SignalP 3.0. *Journal of Molecular Biology*.

Brockmeier, U., Caspers, M., Freudl, R., Jockwer, A., Noll, T., Eggert, T. 2006. Systematic Screening of All Signal Peptides from Bacillus subtilis: A Powerful Strategy in Optimizing Heterologous Protein Secretion in Gram-positive Bacteria. *Journal of Molecular Biology*. Calvo-Flores, F.G., Dobado, J.A., 2010. Lignin as renewable raw material. ChemSusChem 3, 1227–1235. https://doi.org/10.1002/cssc.201000157

Chatterji, Dipankar, and Anil Kumar Ojha. 2001. "Revisiting the Stringent Response, PpGpp, and Starvation Signaling." *Current Opinion in Microbiology*.

Carniel, A., Valoni, É., Nicomedes, J., Gomes, A. da C., Castro, A.M. de, 2017. Lipase from Candida Antarctica (CALB) and cutinase from Humicola insolens act synergistically for PET hydrolysis to terephthalic acid. Process Biochem. https://doi.org/10.1016/j.procbio.2016.07.023

Chinn, M., Mbaneme, V., 2015. Consolidated bioprocessing for biofuel production: recent advances. Energy Emiss. Control Technol. https://doi.org/10.2147/eect.s63000

de Castro, A.M., Carniel, A., Nicomedes Junior, J., da Conceição Gomes, A., Valoni, É., 2017. Screening of commercial enzymes for poly(ethylene terephthalate) (PET) hydrolysis and synergy studies on different substrate sources. J. Ind. Microbiol. Biotechnol. 44, 835–844. https://doi.org/10.1007/s10295-017-1942-z

Degering, C., Eggert, T., Puls, M., Bongaerts, J., Evers, S., Maurer, K.H., Jaeger, K.E., 2010. Optimization of protease secretion in bacillus subtilis and bacillus licheniformis by screening of homologousand heterologous signal peptides. Appl. Environ. Microbiol. 76, 6370–6376. https://doi.org/10.1128/AEM.01146-10

Eberl, A., Heumann, S., Brückner, T., Araujo, R., Cavaco-Paulo, A., Kaufmann, F., Kroutil, W., Guebitz, G.M. 2009. Enzymatic surface hydrolysis of poly(ethylene terephthalate) and bis(benzoyloxyethyl) terephthalate by lipase and cutinase in the presence of surface active molecules. *Journal of Biotechnology*.

Feng, Xueyang et al. 2009. "Characterization of the Central Metabolic Pathways in Thermoanaerobacter Sp. Strain X514 via Isotopomer-Assisted Metabolite Analysis." *Applied and Environmental Microbiology* 75(15): 5001–8.

Fechine, G.J.M., Souto-Maior, R.M., Rabello, M.S., 2002. Structural changes during photodegradation of poly(ethylene terephthalate). J. Mater. Sci. https://doi.org/10.1023/A:1021067027612

Flores, I., Etxeberria, A., Irusta, L., Calafel, I., Vega, J.F., Martínez-Salazar, J., Sardon, H., Müller, A.J., 2019. PET- ran-PLA Partially Degradable Random Copolymers Prepared by Organocatalysis: Effect of Poly(l -lactic acid) Incorporation on Crystallization and Morphology. ACS Sustain. Chem. Eng. https://doi.org/10.1021/acssuschemeng.9b00443

Flores, Andrew D. et al. 2020. "Catabolic Division of Labor Enhances Production of D-Lactate and Succinate From Glucose-Xylose Mixtures in Engineered Escherichia Coli Co-Culture Systems." *Frontiers in Bioengineering and Biotechnology*.

Francisco, J.A., Stathopoulos, C., Warren, R.J.A., Kilburn, D.G., Georgiou, G., 1993. Specific adhesion and hydrolysis of cellulose by intact escherichia coli expressing surface anchored cellulase or cellulose binding domains. Bio/Technology. https://doi.org/10.1038/nbt0493-491

Freudl, R., 2013. Leaving home ain't easy: Protein export systems in Gram-positive bacteria. Res. Microbiol. https://doi.org/10.1016/j.resmic.2013.03.014

Fu, G., Liu, J., Li, J., Zhu, B., Zhang, D., 2018. Systematic Screening of Optimal Signal Peptides for Secretory Production of Heterologous Proteins in Bacillus subtilis. J. Agric. Food Chem. 66, 13141–13151. https://doi.org/10.1021/acs.jafc.8b04183

Flores, A.D., Choi, H.G., Martinez, R., Onyeabor, M., Ayla, E.Z., Godar, A., Machas, M., Nielsen, D.R., Wang, X. 2020. Catabolic Division of Labor Enhances Production of D-Lactate and Succinate From Glucose-Xylose Mixtures in Engineered Escherichia coli Co-culture Systems. *Frontiers in Bioengineering and Biotechnology*.

Hemmerich, J., Rohe, P., Kleine, B., Jurischka, S., Wiechert, W., Freudl, R., Oldiges, M. 2016. Use of a Sec signal peptide library from Bacillus subtilis for the optimization of cutinase secretion in Corynebacterium glutamicum. *Microbial Cell Factories*, **15**(1), 1-11.

Han, X., Liu, W., Huang, J.W., Ma, J., Zheng, Y., Ko, T.P., Xu, L., Cheng, Y.S., Chen, C.C., Guo, R.T., 2017. Structural insight into catalytic mechanism of PET hydrolase. Nat. Commun. 8. https://doi.org/10.1038/s41467-017-02255-z

Hasunuma, T., Okazaki, F., Okai, N., Hara, K.Y., Ishii, J., Kondo, A., 2013. A review of enzymes and microbes for lignocellulosic biorefinery and the possibility of their application to consolidated bioprocessing technology. Bioresour. Technol. https://doi.org/10.1016/j.biortech.2012.10.047

Hegde, K., Veeranki, V.D., 2013. Production optimization and characterization of recombinant cutinases from thermobifida fusca sp. NRRL B-8184. Appl. Biochem. Biotechnol. https://doi.org/10.1007/s12010-013-0219-x

Hemmerich, J., Rohe, P., Kleine, B., Jurischka, S., Wiechert, W., Freudl, R., Oldiges, M., 2016. Use of a Sec signal peptide library from Bacillus subtilis for the optimization of cutinase secretion in Corynebacterium glutamicum. Microb. Cell Fact. 15, 1–11. https://doi.org/10.1186/s12934-016-0604-6

Herrero Acero, E., Ribitsch, D., Steinkellner, G., Gruber, K., Greimel, K., Eiteljoerg, I.,

Trotscha, E., Wei, R., Zimmermann, W., Zinn, M., Cavaco-Paulo, A., Freddi, G., Schwab, H., Guebitz, G., 2011. Enzymatic surface hydrolysis of PET: Effect of structural diversity on kinetic properties of cutinases from Thermobifida. Macromolecules. https://doi.org/10.1021/ma200949p

Hong, S.J., Kim, H.J., Kim, J.W., Lee, D.H., Seo, J.H., 2015. Optimizing promoters and secretory signal sequences for producing ethanol from inulin by recombinant Saccharomyces cerevisiae carrying Kluyveromyces marxianus inulinase. Bioprocess Biosyst. Eng. 38, 263–272. https://doi.org/10.1007/s00449-014-1265-7

Hosseini Koupaie, E., Dahadha, S., Bazyar Lakeh, A.A., Azizi, A., Elbeshbishy, E., 2019. Enzymatic pretreatment of lignocellulosic biomass for enhanced biomethane production-A review. J. Environ. Manage. https://doi.org/10.1016/j.jenvman.2018.09.106

Hyeon, J.E., Jeon, W.J., Whang, S.Y., Han, S.O., 2011. Production of minicellulosomes for the enhanced hydrolysis of cellulosic substrates by recombinant Corynebacterium glutamicum. Enzyme Microb. Technol. https://doi.org/10.1016/j.enzmictec.2010.12.014

Inui, Masayuki et al. 2005. "Metabolic Engineering of Corynebacterium Glutamicum for Fuel Ethanol Production under Oxygen-Deprivation Conditions." *Journal of Molecular Microbiology and Biotechnology*.

Jain, Vikas, Manish Kumar, and Dipankar Chatterji. 2006. "PpGpp: Stringent Response and Survival." *Journal of Microbiology*.

Jeong, K.J., Park, I.Y., Kim, M.S., Kim, S.C., 1998. High level expression of an endoxylanase gene from Bacillus sp. In Bacillus subtilis DB104 for the production of xylobiose from xylan. Appl. Microbiol. Biotechnol. 50, 113–118. https://doi.org/10.1007/s002530051264

Jouzani, G.S., Taherzadeh, M.J., 2015. Advances in consolidated bioprocessing systems for bioethanol and butanol production from biomass: a comprehensive review. Biofuel Res. J. 5, 152–195. https://doi.org/10.18331/BRJ2015.2.1.4

Kalbarczyk, K.Z., Mazeau, E.J., Rapp, K.M., Marchand, N., Koffas, M.A.G., Collins, C.H. 2018. Engineering Bacillus megaterium Strains to Secrete Cellulases for Synergistic Cellulose Degradation in a Microbial Community. *ACS Synthetic Biology*, **7**(10), 2413-2422.

Kremling, A., J. Geiselmann, D. Ropers, and H. de Jong. 2015. "Understanding Carbon Catabolite Repression in Escherichia Coli Using Quantitative Models." *Trends in Microbiology*.

Kulkarni, V., Butte, K., Rathod, S., 2012. Natural Polymers – A Comprehensive Review.

Int. J. Res. Pharm. Biomed. Sci.

Li, M.F., Fan, Y.M., Xu, F., Sun, R.C., Zhang, X.L., 2010. Cold sodium hydroxide/urea based pretreatment of bamboo for bioethanol production: Characterization of the cellulose rich fraction. Ind. Crops Prod. 32, 551–559. https://doi.org/10.1016/j.indcrop.2010.07.004
López-Fonseca, R., Duque-Ingunza, I., de Rivas, B., Arnaiz, S., Gutiérrez-Ortiz, J.I., 2010. Chemical recycling of post-consumer PET wastes by glycolysis in the presence of metal salts. Polym. Degrad. Stab. https://doi.org/10.1016/j.polymdegradstab.2010.03.007

Lynd, L.R., Van Zyl, W.H., McBride, J.E., Laser, M., 2005. Consolidated bioprocessing of cellulosic biomass: An update. Curr. Opin. Biotechnol. https://doi.org/10.1016/j.copbio.2005.08.009

Lee, Q.A.-O., Li, H.A.-O. Photocatalytic Degradation of Plastic Waste: A Mini Review. LID - 10.3390/mi12080907 [doi] LID - 907. (2072-666X (Print)).

Lu, H., Diaz, D.J., Czarnecki, N.J., Zhu, C., Kim, W., Shroff, R., Acosta, D.J., Alexander, B.R., Cole, H.O., Zhang, Y., Lynd, N.A., Ellington, A.D., Alper, H.S. 2022. Machine learning-aided engineering of hydrolases for PET depolymerization. *Nature*, **604**(7907), 662-667.

Mboowa, D., Chandra, R.P., Hu, J., Saddler, J.N. 2020. Substrate Characteristics That Influence the Filter Paper Assay's Ability to Predict the Hydrolytic Potential of Cellulase Mixtures. *ACS Sustainable Chemistry & Engineering*, **8**(28), 10521-10528.

Mhatre, A., Kalscheur, B., McKeown, H., Bhakta, K., Sarnaik, A.P., Flores, A., Nielsen, D.R., Wang, X., Soundappan, T., Varman, A.M. 2022. Consolidated bioprocessing of hemicellulose to fuels and chemicals through an engineered Bacillus subtilis-Escherichia coli consortium. *Renewable Energy*, **193**, 288-298.
Mesa, L., González, E., Cara, C., González, M., Castro, E., Mussatto, S.I., 2011. The effect of organosolv pretreatment variables on enzymatic hydrolysis of sugarcane bagasse. Chem. Eng. J. https://doi.org/10.1016/j.cej.2011.02.003

Mtui, G.Y.S., 2009. Recent advances in pretreatment of lignocellulosic wastes and production of value added products. African J. Biotechnol. https://doi.org/10.4314/ajb.v8i8.60134

Montazer, Z., Habibi-Najafi, M.B., Mohebbi, M., Oromiehei, A. 2018. Microbial Degradation of UV-Pretreated Low-Density Polyethylene Films by Novel Polyethylene-Degrading Bacteria Isolated from Plastic-Dump Soil. *Journal of Polymers and the Environment*, **26**(9), 3613-3625.

Olson, D.G., McBride, J.E., Joe Shaw, A., Lynd, L.R., 2012. Recent progress in consolidated bioprocessing. Curr. Opin. Biotechnol.

https://doi.org/10.1016/j.copbio.2011.11.026

Okino, Shohei et al. 2008. "Production of D-Lactic Acid by Corynebacterium Glutamicum under Oxygen Deprivation." *Applied Microbiology and Biotechnology*.

Peng, C., Shi, C., Cao, X., Li, Y., Liu, F., Lu, F. 2019. Factors influencing recombinant protein secretion efficiency in gram-positive bacteria: Signal peptide and beyond. *Frontiers in Bioengineering and Biotechnology*, **7**(JUN), 1-9.

Raftery, J.P., Karim, M.N. 2017. Economic viability of consolidated bioprocessing utilizing multiple biomass substrates for commercial-scale cellulosic bioethanol production. *Biomass and Bioenergy*.

Rahman, M.A.-O., Hasan, M.A.-O., Nitai, A.A.-O., Nam, S., Karmakar, A.A.-O., Ahsan, M.S., Shiddiky, M.J.A., Ahmed, M.A.-O.X. Recent Developments of Carboxymethyl Cellulose. LID - 10.3390/polym13081345 [doi] LID - 1345. (2073-4360 (Electronic)).

Ramachandran, P., Tiwari, M.K., Singh, R.K., Haw, J.-R., Jeya, M., Lee, J.-K. 2012. Cloning and characterization of a putative β-glucosidase (NfBGL595) from Neosartorya fischeri. *Process Biochemistry*, **47**(1), 99-105.

Raut, S., Raut, S., Sharma, M., Srivastav, C., Adhikari, B., Sen, S.K. 2015. Enhancing Degradation of Low Density Polyethylene Films by Curvularia lunata SG1 Using Particle Swarm Optimization Strategy. *Indian Journal of Microbiology*, **55**(3), 258-268.

Ribitsch, D., Heumann, S., Trotscha, E., Herrero Acero, E., Greimel, K., Leber, R., Birner-Gruenberger, R., Deller, S., Eiteljoerg, I., Remler, P., Weber, T., Siegert, P., Maurer, K.H., Donelli, I., Freddi, G., Schwab, H., Guebitz, G.M. 2011. Hydrolysis of polyethyleneterephthalate by p-nitrobenzylesterase from Bacillus subtilis. *Biotechnology Progress*.

Roy, P.K., Titus, S., Surekha, P., Tulsi, E., Deshmukh, C., Rajagopal, C. 2008. Degradation of abiotically aged LDPE films containing pro-oxidant by bacterial consortium. *Polymer Degradation and Stability*, **93**(10), 1917-1922.

Roth, C., Wei, R., Oeser, T., Then, J., Föllner, C., Zimmermann, W., Sträter, N., 2014. Structural and functional studies on a thermostable polyethylene terephthalate degrading hydrolase from Thermobifida fusca. Appl. Microbiol. Biotechnol. https://doi.org/10.1007/s00253-014-5672-0

Sands, J.M., Fink, B.K., McKnight, S.H., Newton, C.H., Gillespie Jr, J.W., Palmese, G.R. 2001. Environmental issues for polymer matrix composites and structural adhesives. *Clean Products and Processes*, **2**(4), 0228-0235.

Schneewind, O., Missiakas, D.M. 2012. Protein secretion and surface display in Gram-positive bacteria.

Sowmya, H.V., Krishnappa, M., Thippeswamy, B. 2015. Degradation of polyethylene by Penicillium simplicissimum isolated from local dumpsite of Shivamogga district. *Environment, Development and Sustainability*, **17**(4), 731-745.

Sternberg, D., Vuayakumar, P., Reese, E.T. 1977. β-Glucosidase: microbial production and effect on enzymatic hydrolysis of cellulose. *Canadian Journal of Microbiology*, **23**(2), 139-147.

Sulaiman, S., Yamato, S., Kanaya, E., Kim, J.J., Koga, Y., Takano, K., Kanaya, S. 2012. Isolation of a novel cutinase homolog with polyethylene terephthalate-degrading activity from leaf-branch compost by using a metagenomic approach. *Applied and Environmental Microbiology*, **78**(5), 1556-1562.

Sang, T., Wallis, C.J., Hill, G., Britovsek, G.J.P., 2020. Polyethylene terephthalate degradation under natural and accelerated weathering conditions. Eur. Polym. J. https://doi.org/10.1016/j.eurpolymj.2020.109873

Sasaki, M., Jojima, T., Inui, M., Yukawa, H., 2008. Simultaneous utilization of d-cellobiose, d-glucose, and d-xylose by recombinant Corynebacterium glutamicum under oxygen-deprived conditions. Appl. Microbiol. Biotechnol. https://doi.org/10.1007/s00253-008-1703-z

Schneewind, O., Missiakas, D.M., 2012. Protein secretion and surface display in Gram-positive bacteria. Philos. Trans. R. Soc. B Biol. Sci. https://doi.org/10.1098/rstb.2011.0210
Schneewind, O., Model, P., Fischetti, V.A., 1992. Sorting of protein a to the staphylococcal cell wall. Cell. https://doi.org/10.1016/0092-8674(92)90101-H

Shen, Xi Hui, Ning Yi Zhou, and Shuang Jiang Liu. 2012. "Degradation and Assimilation of Aromatic Compounds by Corynebacterium Glutamicum: Another Potential for Applications for This Bacterium?" *Applied Microbiology and Biotechnology* 95(1): 77–89.

Shin, H.D., McClendon, S., Vo, T., Chen, R.R., 2010. Escherichia coli binary culture engineered for direct fermentation of hemicellulose to a biofuel. Appl. Environ. Microbiol. 76, 8150–8159. https://doi.org/10.1128/AEM.00908-10

Shosuke Yoshida, Kazumi Hiraga, Toshihiko Takehana, I.T., Hironao Yamaji, Yasuhito Maeda, Kiyotsuna Toyohara, K.M., †Yoshiharu Kimura, K.O., 2016. "a bacterium that degrades and assimilates poly(ethylene terephthalate) ". Science (80-.). 353, 759. https://doi.org/10.1126/science.aaf8305

Silva, C., Da, S., Silva, N., Matamá, T., Araújo, R., Martins, M., Chen, S., Chen, J., Wu,

J., Casal, M., Cavaco-Paulo, A., 2011. Engineered Thermobifida fusca cutinase with increased activity on polyester substrates. Biotechnol. J. https://doi.org/10.1002/biot.201000391

Singh, S., Cheng, G., Sathitsuksanoh, N., Wu, D., Varanasi, P., George, A., Balan, V., Gao, X., Kumar, R., Dale, B.E., Wyman, C.E., Simmons, B.A., 2015. Comparison of different biomass pretreatment techniques and their impact on chemistry and structure. Front. Energy Res. https://doi.org/10.3389/fenrg.2014.00062

Steen, E.J., Kang, Y., Bokinsky, G., Hu, Z., Schirmer, A., McClure, A., Del Cardayre, S.B., Keasling, J.D., 2010. Microbial production of fatty-acid-derived fuels and chemicals from plant biomass. Nature. https://doi.org/10.1038/nature08721

Sulaiman, S., Yamato, S., Kanaya, E., Kim, J.J., Koga, Y., Takano, K., Kanaya, S., 2012. Isolation of a novel cutinase homolog with polyethylene terephthalate-degrading activity from leaf-branch compost by using a metagenomic approach. Appl. Environ. Microbiol. 78, 1556–1562. https://doi.org/10.1128/AEM.06725-11

Sulaiman, S., You, D.J., Kanaya, E., Koga, Y., Kanaya, S., 2014. Crystal structure and thermodynamic and kinetic stability of metagenome-derived LC-cutinase. Biochemistry. https://doi.org/10.1021/bi401561p

Sun, Y., Cheng, J., 2002. Hydrolysis of lignocellulosic materials for ethanol production: A review. Bioresour. Technol. 83, 1–11. https://doi.org/10.1016/S0960-8524(01)00212-7

Taghavi, N., Zhuang, W.-Q., Baroutian, S. 2021. Enhanced biodegradation of non-biodegradable plastics by UV radiation: Part 1. *Journal of Environmental Chemical Engineering*, **9**(6), 106464.

Tang, Y., Shui, W., Myers, S., Feng, X., Bertozzi, C., Keasling, J. 2009. Central metabolism in Mycobacterium smegmatis during the transition from O2-rich to O2-poor conditions as studied by isotopomer-assisted metabolite analysis. *Biotechnology Letters*, **31**(8), 1233-1240.

Tang, Joseph Kuo Hsiang, Le You, Robert E. Blankenship, and Yinjie J. Tang. 2012. "Recent Advances in Mapping Environmental Microbial Metabolisms through 13C Isotopic Fingerprints." *Journal of the Royal Society Interface*.

Tang, Y., Shui, W., Myers, S., Feng, X., Bertozzi, C., Keasling, J. 2009. Central metabolism in Mycobacterium smegmatis during the transition from O2-rich to O2-poor conditions as studied by isotopomer-assisted metabolite analysis. *Biotechnology Letters*, **31**(8), 1233-1240.

Tang, Kuo Hsiang et al. 2010. "Carbon Flow of Heliobacteria Is Related More to Clostridia

than to the Green Sulfur Bacteria." *Journal of Biological Chemistry*.

Tiwari, P., Misra, B.N., Sangwan, N.S. 2013. β -glucosidases from the fungus Trichoderma: An efficient cellulase machinery in biotechnological applications. *BioMed Research International*.

Taherzadeh, M.J., Karimi, K., 2008. Pretreatment of lignocellulosic wastes to improve ethanol and biogas production: A review, International Journal of Molecular Sciences. https://doi.org/10.3390/ijms9091621

Tournier, V., Topham, C.M., Gilles, A., David, B., Folgoas, C., Moya-Leclair, E., Kamionka, E., Desrousseaux, M.L., Texier, H., Gavalda, S., Cot, M., Guémard, E., Dalibey, M., Nomme, J., Cioci, G., Barbe, S., Chateau, M., André, I., Duquesne, S., Marty, A., 2020. An engineered PET depolymerase to break down and recycle plastic bottles. Nature 580, 216–219. https://doi.org/10.1038/s41586-020-2149-4

V.Mahalakshmi, S.N.A. 2012. Assessment of Physicochemically treated plastic by fungi *Annals of Biological Research*, **3**(9), 4374-4381.

Valero-Valdivieso, M., Ortegon, Y., Uscategui, y.M.d.A.V.y.D., De, T.P.p.b., Isbn, t.d.l.i.p., pp, López, C.X.b.P., reológicas y aplicaciones, C., Bastioli, C.G.s.o.t.p.o., biobased packaging materials, S.-S., pp, Gross, R., Kalra, B.B.p., for the environment. Science, p., Novo, M.L.e.a.u.g., educación para el desarrollo sostenible, R.d., Educación, p., Novo, M.E.d.s.s.d., ambiental y educativa, E.U.M., España, I.p., Mejía. L, D.d.l.c.p., sintéticas, p.p.y.f.b., Bucaramanga, C.U.I.S.p., Y, D.N.P.A.i.p.l.p., Cadena, l.c.D.s., petroquímica, A.i.s.p., Vergara, B.L.M.y.P.F.U.p., Y, d.l.p.b.A., Perspectiva, p., Philp, J.C.R.R.J., Guy, K.B., plastics in a bioeconomy, T.B., pp, DiGregorio, B.E.B.p.b., Mirel, C.B.p., Moreno, N.C.m.d., Mucinas, b.f.e.c.c., Bogotá, C.U.N.d., Dyna, Colombia, P., Muniyasamy, S.M.R.M.M., Mohanty, A., Co-product, B.g.c.f.b., and poly, I., Crops, Products, p., Reddy, M.M.V.S.M.M., Bhatia, S.K., Mohanty, A.B.p.a., Opportunities, b.C.s., future, Progress in Polymer, S., Villada, H.S.y.A.H.A.B.n., usados en empaques biodegradables, T.A., pp, Bastioli, C.B.m.f.v., Special, a.B.G.A.a., Applications, S.A., S, A.I.A.D., Müller, R.J.B.o.p.R., and methods for testing, B.O.D.O.I., bpola, Lucas, N.B.C., Belloy, C.P., A, b.M., estimation techniques, review, C.p., Vilpoux, O., Averous, L.S.-b.p., Technology, U., Potentialities of Latin, A., Starchy Tubers, p., Yu, L.D.K., Li, L.P.b.a., composites from renewable resources, P.i.P., Science, p., Tabi, T.S.I.S.F.L.A., Kovacs, J., Its, C.s.o.a.p.a.a., relation to processing, E.P.L.p., Otey, F.H.y.D.W.M.C.X.I.c.f., Starch, E.S.C., technology, edition). San Diego: Academic Press, p., Avérous, L.B.m.s.b., on plasticized starch: A review, J.o.M., Science, P.C.P.R.p., Schroeter, J.O.t.m.p.o.n., starch granules, S.-S.p., Ratto, J.S.P., Auerbach, M.P., Thermoplastic, p., biodegradability of, a., aliphatic polyester/starch system, P.P., Desai, S.T.I.S.B., Devi, S., Elastomers, S.-p.r.i.p., containing starch as a crosslinker, P.E., Science, p., Seung, K.A.T.c.o.p., et al. 2013. Biopolímeros: Avances Y Perspectivas Biopolymers: Progress and Prospects. *Universidad nacional de Colomiba*.

Varman, A.M., He, L., You, L., Hollinshead, W., Tang, Y.J. 2014. Elucidation of intrinsic biosynthesis yields using ^{13}C-based metabolism analysis. *Microb Cell Fact*, **13**(1), 42.

Varman, Arul M et al. 2016. "Decoding How a Soil Bacterium Extracts Building Blocks and Metabolic Energy from Ligninolysis Provides Road Map for Lignin Valorization."

Varman, A.M., He, L., Follenfant, R., Wu, W., Wemmer, S., Wrobel, S.A., Tang, Y.J., Singh, S. 2016. Decoding how a soil bacterium extracts building blocks and metabolic energy from ligninolysis provides road map for lignin valorization. *Proc Natl Acad Sci U S A*, **113**(40), E5802-E5811.

Varman, A.M., He, L., You, L., Hollinshead, W., Tang, Y.J. 2014. Elucidation of intrinsic biosynthesis yields using ^{13}C-based metabolism analysis. *Microb Cell Fact*, **13**(1), 42.

Van Zyl, W.H., Lynd, L.R., Den Haan, R., McBride, J.E., 2007. Consolidated bioprocessing for bioethanol production using saccharomyces cerevisiae. Adv. Biochem. Eng. Biotechnol. https://doi.org/10.1007/10_2007_061

Vimala, P.P., Mathew, L. 2016. Biodegradation of Polyethylene Using Bacillus Subtilis. *Procedia Technology*, **24**, 232-239.

Wan, C., Zhou, Y., Li, Y., 2011a. Liquid hot water and alkaline pretreatment of soybean straw for improving cellulose digestibility. Bioresour. Technol. 102, 6254–6259. https://doi.org/10.1016/j.biortech.2011.02.075

Wan, C., Zhou, Y., Li, Y., 2011b. Liquid hot water and alkaline pretreatment of soybean straw for improving cellulose digestibility. Bioresour. Technol. https://doi.org/10.1016/j.biortech.2011.02.075

Wang, Chen et al. 2014. "Succinic Acid Production from Corn Cob Hydrolysates by Genetically Engineered Corynebacterium Glutamicum." *Applied Biochemistry and Biotechnology*.

Wiechert, Wolfgang. 2001. "13C Metabolic Flux Analysis." *Metabolic Engineering*.

Wahl, S.A., Dauner, M., Wiechert, W. 2004. New tools for mass isotopomer data evaluation in (13)C flux analysis: mass isotope correction, data consistency checking, and precursor relationships. *Biotechnol Bioeng*, **85**(3), 259-68.

Wei, R., Oeser, T., Schmidt, J., Meier, R., Barth, M., Then, J., Zimmermann, W. 2016. Engineered bacterial polyester hydrolases efficiently degrade polyethylene terephthalate due to relieved product inhibition. *Biotechnology and Bioengineering*, **113**(8), 1658-1665.

Xiao, Y., Feng, X., Varman, A.M., He, L., Yu, H., Tang, Y.J. 2012. Kinetic modeling and isotopic investigation of isobutanol fermentation by two engineered escherichia coli strains. *Industrial and Engineering Chemistry Research*, **51**(49), 15855-15863.

Yamada-Onodera, K., Mukumoto, H., Katsuyaya, Y., Saiganji, A., Tani, Y. 2001. Degradation of polyethylene by a fungus, Penicillium simplicissimum YK. *Polymer Degradation and Stability*, **72**(2), 323-327.

Yoshida, S., Hiraga, K., Takehana, T., Taniguchi, I., Yamaji, H., Maeda, Y., Toyohara, K., Miyamoto, K., Kimura, Y., Oda, K. 2016. A bacterium that degrades and assimilates poly(ethylene terephthalate). *Science*.

You, L., Page, L., Feng, X., Berla, B., Pakrasi, H.B., Tang, Y.J. 2012. Metabolic Pathway Confirmation and Discovery Through 13C-labeling of Proteinogenic Amino Acids. *J. Vis. Exp.*(59), e3583.

Young, Jamey D, Avantika A Shastri, Gregory Stephanopoulos, and John A Morgan. 2011. "Mapping Photoautotrophic Metabolism with Isotopically Nonstationary C Flux Analysis." *Metabolic Engineering* 13(6): 656–65. http://dx.doi.org/10.1016/j.ymben.2011.08.002.

Yim, S.S., Choi, J.W., Lee, S.H., Jeong, K.J., 2016. Modular Optimization of a Hemicellulose-Utilizing Pathway in Corynebacterium glutamicum for Consolidated Bioprocessing of Hemicellulosic Biomass. ACS Synth. Biol. https://doi.org/10.1021/acssynbio.5b00228

Yoshida, S., Hiraga, K., Takehana, T., Taniguchi, I., Yamaji, H., Maeda, Y., Toyohara, K., Miyamoto, K., Kimura, Y., Oda, K., 2016. A bacterium that degrades and assimilates poly(ethylene terephthalate). Science (80-.). https://doi.org/10.1126/science.aad6359

You, L., Page, L., Feng, X., Berla, B., Pakrasi, H.B., Tang, Y.J. 2012. Metabolic Pathway Confirmation and Discovery Through 13C-labeling of Proteinogenic Amino Acids. *J. Vis. Exp.*(59), e3583.

Zamboni, Nicola, Sarah Maria Fendt, Martin Rühl, and Uwe Sauer. 2009. "13C-Based Metabolic Flux Analysis." *Nature Protocols*.

Zamboni, Nicola, and Uwe Sauer. 2009. "Novel Biological Insights through Metabolomics and 13C-Flux Analysis." *Current Opinion in Microbiology*.

Zavrel, M., Bross, D., Funke, M., Büchs, J., Spiess, A.C., 2009. High-throughput screening for ionic liquids dissolving (ligno-)cellulose. Bioresour. Technol. https://doi.org/10.1016/j.biortech.2008.11.052

Zhang, X.Z., Sathitsuksanoh, N., Zhu, Z., Percival Zhang, Y.H., 2011. One-step production of lactate from cellulose as the sole carbon source without any other organic nutrient by recombinant cellulolytic Bacillus subtilis. Metab. Eng. 13, 364–372. https://doi.org/10.1016/j.ymben.2011.04.003

Zhang, W., Yang, M., Yang, Y., Zhan, J., Zhou, Y., Zhao, X. 2016. Optimal secretion of alkali-tolerant xylanase in Bacillus subtilis by signal peptide screening. (1432-0614 (Electronic)).

Zhang, X.Z., Sathitsuksanoh, N., Zhu, Z., Percival Zhang, Y.H. 2011. One-step production of lactate from cellulose as the sole carbon source without any other organic nutrient by recombinant cellulolytic Bacillus subtilis. *Metabolic Engineering*, **13**(4), 364-372.

Zhao, X.u., Li, Z., Chen, Y., Shi, L., Zhu, Y. 2007. Solid-phase photocatalytic degradation of polyethylene plastic under UV and solar light irradiation. *Journal of Molecular Catalysis A: Chemical*, **268**(1), 101-106.

APPENDIX A

13C FINGERPRINTING STUDIES

Introduction

The study of intracellular metabolic pathways has been a topic of interest. It gives useful information about bacterial metabolism and improves bacterial cells' performance to have applications in pharmaceuticals, biofuels, bioremediation, etc. Understanding cellular metabolism can be used to characterize different parameters like nutrient uptake, secretion rates, nutrient fixation in metabolic molecules, molecule synthesis, and pathway activities (Tang et al. 2012; Young et al. 2011). Isotope labelling has been widely used to study cellular functions. U-^{13}C labelling is an expedient method in helping the study of *in vivo* carbon transition in metabolites. After a particular U-^{13}C labelled substrate is fed to a microorganism, the label carbon is transferred through metabolites. It gets fixed in amino acids contributing to biomass or in the form of metabolites. As a result, some metabolites and amino acids carry the isotopic carbon fraction called isotopic fingerprints. Using this information, metabolic pathways of reactants to products can be predicted to develop the metabolic network. U-^{13}C fingerprinting information can be further combined with metabolic modeling information to estimate the reaction rates and the carbon flux in a metabolic pathway (Wiechert 2001; Zamboni et al. 2009; Zamboni and Sauer 2009).

Assimilation of different carbon sources by bacteria depends heavily on their native environments. Studying assimilation patterns in bacterial cells can help understand their growth, metabolomics and further help in engineering cells for various applications. Microorganisms found in soil can assimilate aromatics and other complex compounds, and studying these organisms helps in understanding their metabolic processes and to use them for industrial purposes (Shen, Zhou, and Liu 2012; Varman et al. 2016). *Corynebacterium glutamicum* is a gram-positive bacterium found in soil that prefers the assimilation of

aromatics compared to more widely favored carbon sources like glucose and xylose. *Corynebacterium glutamicum,* as the name suggests, has been extensively studied for its ability to secrete amino acids like glutamic acid. Recently this gram-positive candidate is also studied to produce a wide variety of products like lactate, Succinate, ethanol, etc. (Ahn, Jang, and Lee 2016; Inui et al. 2005; Okino et al. 2008; Wang et al. 2014). Increasing interest in this soil bacterium leads to the genomic study of this organism, and later it was known that it has genes essential for aromatics assimilation (Shen, Zhou, and Liu 2012). Hence, it is a potential candidate for biomass degradation and lignin processing fermentations.

Unlike *C. glutamicum,* a gram-negative bacterium widely explored because of its convenience of genetic manipulation in *Escherichia coli. E. coli* consumes simple sugars like glucose and xylose, but it cannot consume both the sugars at the same time; this is called Carbon Catabolite Repression (CCR) (Kremling et al. 2015). Different approaches have been used to assimilate hexose and pentose sugars at the same time. One of these approaches is using coculture consortia (Flores et al. 2020). In coculture consortia, two organisms grow symbiotically, helping each other by providing nutrients.

E. coli strains have been extensively explored mainly because of their convenience in genetic manipulation and the wide range of information about their genomics and proteomics. The stringent response is a phenomenon where *E. coli* cells limit certain cellular functions and give preference to essential functions in a state of fatty acid limitation, heat shock, amino acid limitation, etc. The stringent response has been extensively studied in the past decade, but not everything is known about the stringent

response (Brown et al. 2016; Chatterji and Kumar Ojha 2001; Jain, Kumar, and Chatterji 2006).

U-^{13}C fingerprinting studies can be used to study assimilation of aromatics in non-model organisms like *C. glutamicum,* Carbon assimilation in coculture consortia, and variation in assimilation patterns in stringent response. In the present study, we use U-^{13}C fingerprinting studies to understand the assimilation of different carbon sources in *C. glutamicum*, *E. coli* coculture, and *E. coli* mutants.
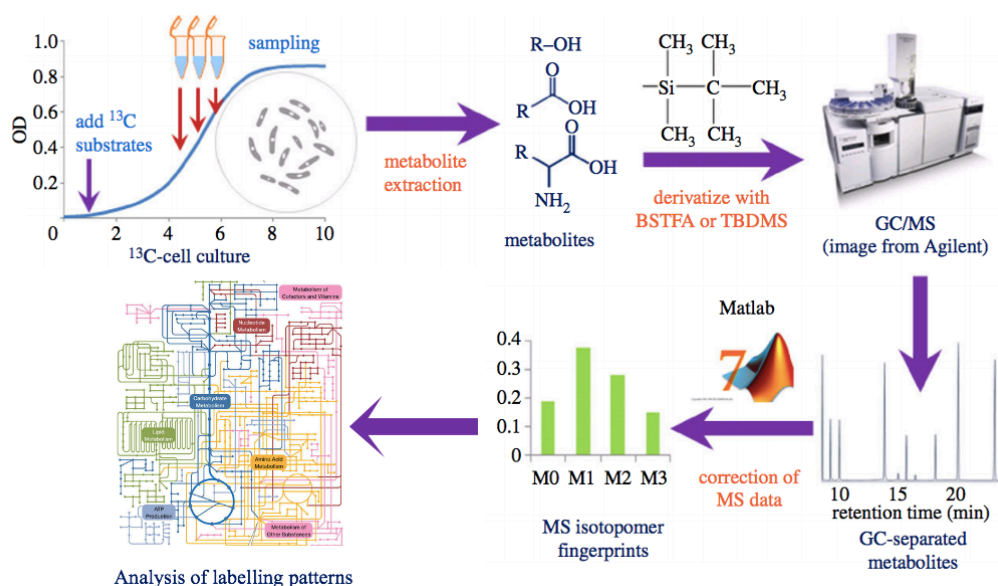
Figure A1: Overview of U-^{13}C fingerprinting analysis: Bacterial cultures were cultured in labelled sources and harvested at the late log phase and further derivatized in the presence of BSTFA/TBDMS. The derivatized samples were analyzed in GCMS equipment to get M/Z spectra corrected using a MATLAB code to obtain a Mass distribution vector (MDV). MDV variation was used to study metabolic pathways (Tang et al. 2012)

Materials and methods

Chemicals and reagents

Restriction enzymes, Q5 High-Fidelity DNA polymerase, and T4 DNA ligase were purchased from Fermentas or New England BioLabs. Oligonucleotides were purchased from Integrated DNA Technologies (San Diego, CA). All organic solvents, glucose, xylose, arabinose, aromatics, and other chemicals used in this study were purchased from Sigma-Aldrich (St. Louis, MO). U-^{13}C labelled glucose was purchased from Cambridge Isotope Laboratories (Tewksbury, MA).

Biomass growth for labelling studies

13C labelling studies to trace substrate assimilation patterns in *Escherichia coli* Mutants

The seed cultures were set up in minimal medium, as described previously. Cells were centrifuged and washed with minimal media to avoid any carryover of carbon substrates and media nutrients. For the labelling study, 50 µL of washed cells were inoculated into 5 mL of media tubes containing 5 g/L [U-^{13}C] glucose + CAS amino acids; 5 g/L [U-^{13}C] glucose + Acetate; Glucose + [1-^{13}C Acetate]. Bacterial cells were harvested after 24 hours, and the biomass was hydrolyzed to obtain proteinogenic amino acids.

Studying Carbon dioxide assimilation pattern in *E. coli* coculture consortia

E. coli coculture consisted of glucose to ethanol (G2S) producing strain and Xylose to Succinate producing strain (X2S) as shown in Figure 2. A dual-chamber experiment was

set up to obtain biomass for 13C analysis and study Co2 assimilation in X2S strain. 6 g/L of [U-^{13}C] glucose was added to G2S strain present in reactor 1, and labelled CO_2 passed from reactor 1 to reactor 2, which was assimilated along with unlabelled Xylose (Figure 2). The biomass sample in reactor 2 was centrifuged and washed to study for amino acid analysis. The G2E strain was enriched with ^{12}-C glucose (6 g/L) and U-^{13}C xylose (3 g/L) as a control to understand Xylose assimilation in the G2E strain. The biomass was further analyzed for amino acid analysis.
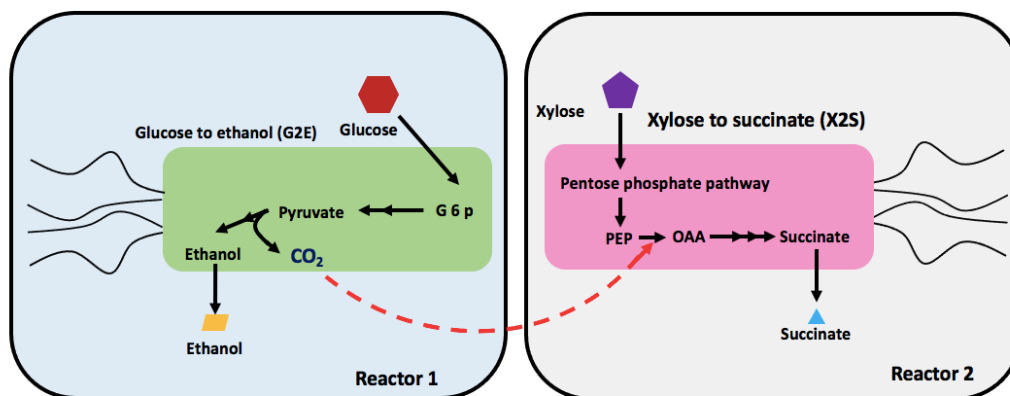
Figure A2: Overview of coculture consortia: Glucose to ethanol (G2E) culture in reactor 1 assimilates glucose via glycolysis and further produces ethanol as a product and carbon dioxide by-product. CO_2 present in the headspace is then transferred to reactor 2 wherein Xylose to Succinate (X2S) assimilates xylose as pentose sugar via pentose phosphate pathway to produce Succinate as a product.

Amino acid analysis

The amino acids were derivatized with TBDMS (N-(tert-butyldimethylsilyl)-N-methyl-trifluoroacetamide, Sigma-Aldrich) by following previously reported protocols (Varman et al., 2014; You et al., 2012). The derivatized amino acids were analyzed for their mass isotopomer abundance by GC-MS, as described elsewhere (Xiao et al., 2012; You et al., 2012). The m/z ion $[M-57]^+$ that corresponds to the entire amino acid was used to calculate the ^{13}C abundance in amino acids [m0 m1…. mn]. The m/z of $[M-15]^+$ was used for leucine and isoleucine alone since their $[M-57]^+$ overlaps with other mass peaks (Wahl et al., 2004). The natural abundance of isotopes, including ^{13}C (1.13%), ^{18}O (0.20%), ^{29}Si (4.70%), and ^{30}Si (3.09%) contributes noise to the mass isotopomer spectrum. This background noise was rectified in the calculation of ^{13}C fractions for amino acids using a published algorithm, and the detailed correction protocol can be found elsewhere (Tang et al., 2009).

Analytical methods

GC MS (Gas Chromatography Mass spectrometry) analysis was carried out to study amino acid profiles of derivatized biomass fraction. The sample (1ul) was injected in a GC system, having an oven temperature of 250 C passed through the column using a mass spectrometer detector.

Results and discussion

13C labelling studies to trace substrate assimilation patterns in *Escherichia coli* Mutants

E. coli mutants used in the present study were mutants that illustrated stringent response states even in rich media conditions. The stringent response is a state in which bacteria keep minimal cellular functions in starvation, heat shock, or other stress conditions. 13C fingerprinting study of this work was carried out to understand the active metabolic pathways in mutants.

CAS Amino acid assimilation pathway

CAS amino acids are casein hydrolysates rich in consortia of amino acids, making them a rich source of carbon for bacterial cells. In growth studies, mutants grew better in minimal media compared to CAS amino acids. [U-^{13}C] glucose + CAS amino acids were added in mutant and wild type strain to study the labelling pattern. Amino acids, mainly Methionine, Serine, Threonine, Phenylalanine, Aspartate, Glutamate, and Tyrosine, showed comparatively lesser reduction in Mn MDV (Mass Distribution Vector) values compared to wild type. The overall distribution of the MDV values showed wildtype strain shows better assimilation of CAS amino acids compared to the mutant strain (Figure 5). Higher assimilation of unlabelled carbon fraction in mainly Methionine, Threonine, Phenylalanine, Aspartate, Glutamate, Tyrosine in wildtype samples compared to mutants.
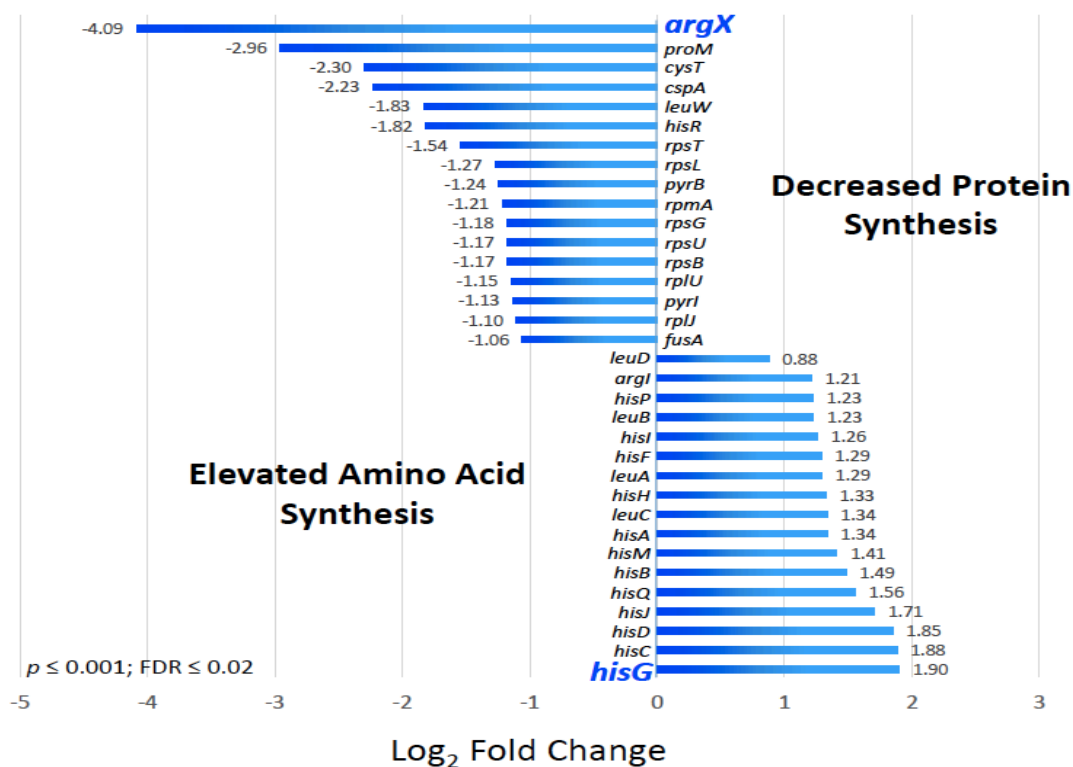
Figure A3: List of upregulated genes and downregulated genes in amino acid biosynthesis pathways. Genome sequencing of the mutants for estimation of upregulation of genes compared to wild type strain

[1-¹³C] acetate assimilation pathways in Mutant and Wildtype strain

[1-¹³C] acetate and glucose were added as the substrate in culturing wild type and mutant strains and processed for amino acid analysis. Amino acids in Mutant biomass, which showed an increase in M1 MDV values compared to wild type, were Leucine (20% increase), Valine (17% increase), and Isoleucine (27 % increase) (Figure 6). Also, Lysine, Histidine, and Tyrosine showed a minor increase in M1 MDV values. Histidine showed

the highest increase in M2 values with a 57.4% increase compared to wildtype, followed by Lysine (29%), Phenylalanine (14.71%), and Tyrosine (15%). Looking at Leucine, Valine, and Isoleucine biosynthesis pathways and gene upregulation will explain why such an increase in M1 values of these amino acids is evident.

	M (G)	WT (G)	M (CAS)	WT (CAS)
Alanine	0.991	0.991	0.837	0.769
Glycine	0.996	0.995	0.739	0.658
Valine	0.996	0.994	0.014	0.013
Leucine	0.844	0.834	0.003	0.005
Isoleucine	0.873	0.83	0.005	0.003
Methionine	0.988	0.855	0.225	0.016
Serine	0.992	0.995	0.912	0.849
Threonine	0.994	0.98	0.475	0.354
Phenylalanine	0.994	0.992	0.136	0.031
Aspartate	0.985	0.977	0.525	0.412
Glutamate	0.996	0.854	0.384	0.173
Lysine	0.997	0.835	0.048	0.008
Histidine	0.997	0.997	0.003	0.003
Tyrosine	0.993	0.997	0.803	0.710598

Scale:
1
0.8
0.6
0.4
0.2
0

Figure A4: Mn value distribution of MDV values in [U-^{13}C] glucose and unlabelled CAS amino acids in Wild type and Mutant (M) strains. M(G): Mutant strains cultured in 5 g/L [U-^{13}C] glucose; M(CAS): Mutant strains cultured in 5 g/L [U-^{13}C] glucose and CAS amino acids; WT(G): Wild type strains cultured in 5 g/L [U-^{13}C] glucose; WT(CAS): Wild Type strains cultured in 5 g/L [U-^{13}C] glucose and CAS amino acids. Scale 0 to 1 shows an increase in labelled fraction with 0 denoting no labelling and 1 denoting fully labelled fraction.

Leucine, Valine, and Isoleucine get one carbon labelling from pyruvate and threonine. Enzyme 2, 3 dihydroxy isovalerate dehydratase is the common enzyme in the biosynthesis of isoleucine, leucine, and valine, which contributes to forming 3-methyl 2 oxobutanoate and 3-methyl 2 oxo pentanoate pool, which can be a reason behind higher M1 values in specifically these three amino acids. The difference in M1 values in leucine, valine, and isoleucine only leads to an investigation of pathways that can biosynthesize these amino acids independently without carbon flow from the TCA cycle. One such pathway that could lead to these three amino acids' independent biosynthesis can be the citramalate pathway. According to Tang, 2012 as leucine and isoleucine have the same precursors; their labelling fraction should be the same for the citramalate pathway to be active. As shown in figure 7 there is a prominent difference in the MDV values of leucine and isoleucine; hence possibility of the citramalate pathway being active is unlikely. Also, Genes leuA, leu C, and leu B were upregulated, as shown in figure 4 involved in leucine biosynthesis. This explains higher M1 values in leucine.

	Mutant			Wildtype			
	M+0	M+1	M+2	M+0	M+1	M+2	
Alanine	0.421	0.534	0.034	0.434	0.530	0.031	
Glycine	0.426	0.563	0.012	0.443	0.533	0.024	
Valine	0.435	0.529	0.034	0.571	0.416	0.016	
Leucine	0.216	0.718	0.048	0.380	0.598	0.003	
Isoleucine	0.250	0.445	0.296	0.483	0.379	0.144	
Methionine	0.224	0.491	0.276	0.282	0.461	0.245	
Serine	0.420	0.570	0.018	0.442	0.533	0.026	
Threonine	0.940	0.000	0.000	0.786	0.000	0.231	1
Phenylalanine	0.228	0.243	0.343	0.285	0.246	0.299	0.8
Aspartate	0.153	0.517	0.308	0.196	0.535	0.260	0.6
Glutamate	0.142	0.324	0.480	0.191	0.335	0.438	0.4

Lysine	0.251	0.433	0.320	0.328	0.414	0.248		0.2
Histidine	0.436	0.378	0.137	0.534	0.346	0.087		0
Tyrosine	0.181	0.285	0.353	0.249	0.263	0.307		

Figure A5: M0, M,1, and M2 value distribution of MDV value in [1-^{13}C] Acetate and unlabelled Glucose in Wild type and Mutant (M) strains. M+0: Mass distribution vector denoting unlabelled fraction in the processed biomass; M+1: Mass distribution vector denoting one carbon labelled fraction in the processed biomass; M+2: Mass distribution vector denoting two carbon labelled fraction in the processed biomass. Scale 0 to 1 shows an increase in labelled fraction with 0 denoting no labelling and 1 denoting fully labelled fraction.
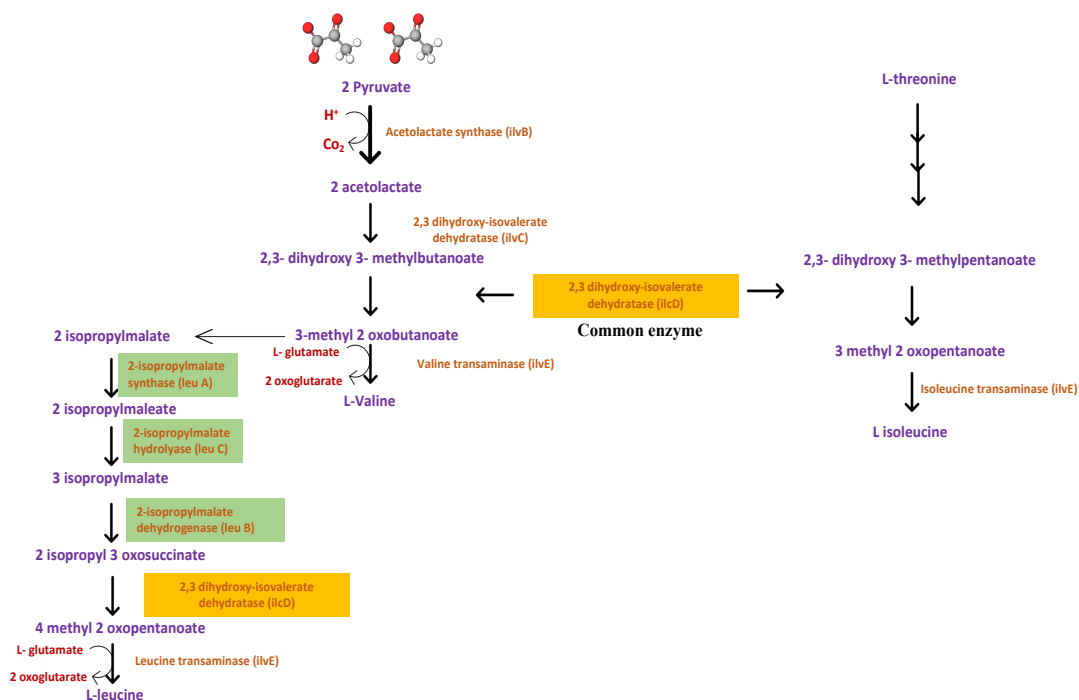
Figure a6: Leucine, Isoleucine, and Valine biosynthesis pathways. The green-colored enzymes shown in the figure are upregulated genes. Gene leuA, leu B, and leu C were upregulated, as shown in figure 2. The enzyme colored yellow is the common enzyme that drives both leucine, valine, and isoleucine biosynthesis pathways.

Increase in M2 MDV values in Histidine, Lysine (29%), and Aspartate (18.4%). Histidine synthesis genes, mainly hisA, hisM, hisB, hisQ, hisJ, hisD, hisC, and his G are upregulated, as shown in figure 4. This is in agreement with a 57% increase in M2 histidine values compared to wildtype. Histidine is considered to be an essential amino acid, and biosynthesis of Histidine in a state of stringent response is evident (Dozot, 2006)

In conclusion, the Mutant strain preferred minimal media and was in a state of stress, even in the presence of rich media. Labelling studies confirm that Mutant strain shows an increase in Acetate assimilation in Leucine, Valine, Isoleucine, Histidine, Phenylalanine, Aspartate, Glutamate, etc. Hence it can be concluded that mutant strain can perform better in minimal media.

Carbon dioxide assimilation in recombinant *Escherichia coli* cocultures

[U-^{13}C] substrates can be used beneficially in the determination of substrate preference in an organism. Utilization of labelled and unlabelled substrate combinations and studying the labelled fraction dilution has been extensively explored previously (Feng et al. 2010; Varman et al. 2013; Young et al. 2011). Feng et al. 2010 used [U-^{13}C] Glucose as a carbon enrichment in Cyanothece 51142 to confirm mixotrophy is cyanobacterial species. An increase in labelled fraction in all 5 studied amino acids confirmed percolation of labelled carbon in central metabolic pathways in Feng et al. 2010 study. Similarly, labelling

130

fractions in Glucose to Ethanol strain (G2E) biomass was cultured in unlabelled glucose substrate and labelled xylose as a control to confirm that there is no assimilation of xylose in glucose specialist strain. As shown in figure 8, M+0 values for all the mentioned amino acids are greater than 0.95, which shows all the carbons in these amino acids are unlabelled. All the amino acids with a high unlabelled fraction indicate no labelled carbon assimilation from xylose. This experiment was hence used to confirm that G2E strain does not consume xylose as a substrate.

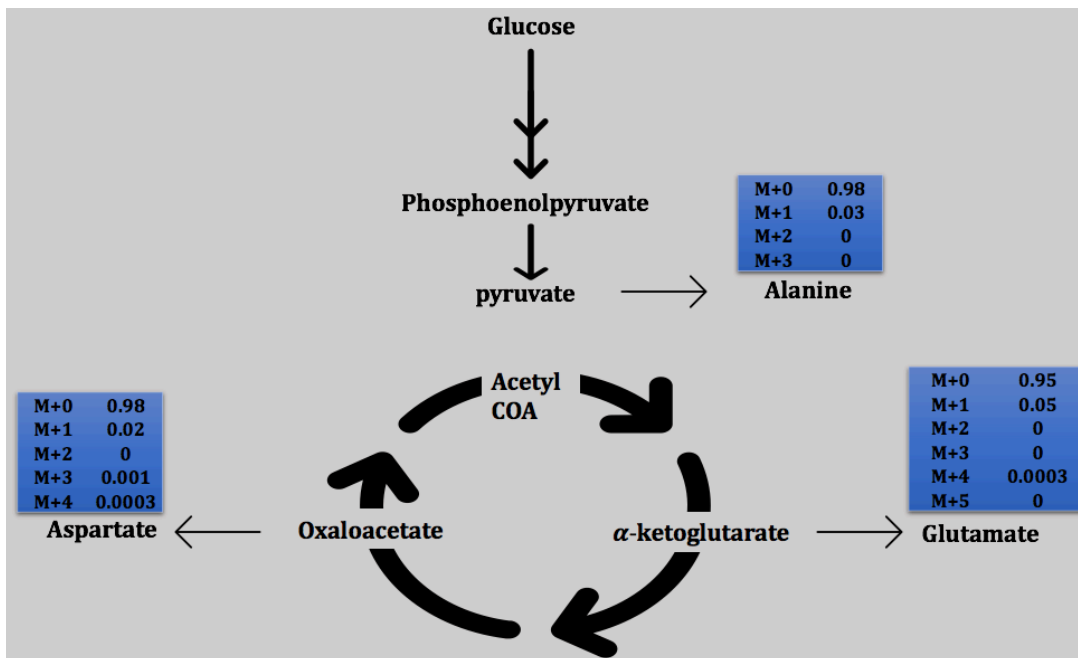Figure A7: Mass distribution vector (MDV) values obtained in G2E biomass after studying Alanine, Aspartate and glutamate biosynthesized in the central metabolic pathway: G2E strain was enriched with ^{12}-C glucose (6 g/L) and U-^{13}C xylose (3 g/L) to understand Xylose assimilation in G2E strain. M+0, M+1, M+2, M+3, M+4, and M+5 are MDV values wherein M+0: MDV value for unlabelled carbon; In Glutamate, M+1, M+2, M+3, M+4

are MDV values in partially labelled fractions, and M+5 is fully labelled fraction; In Alanine, M+1, M+2, are MDV values in partially labelled fractions, and M+3 is fully labelled fraction; In Aspartate, M+1, M+2, M+3 are MDV values in partially labelled fractions, and M+4 is fully labelled fraction.

The previous study mainly discussed how dilution in labelled fraction could be used to confirm substrate assimilation, but Isotopomer labelling analysis can also predict the exact position of the labelled carbons (Tang et al. 2010; Varman et al. 2016). U-^{13}C Isotopomer analysis showed M+2 values in the range of 0.15-0.18 in Aspartate, Isoleucine, Methionine, Lysine, and threonine (Figure 9). Oxaloacetate is the precursor to aspartate, followed by threonine and then lysine. As shown in the table, and as expected, all three have a broad labelling distribution (~50%, ~25% and ~15% for M+1, M+2, M+3, respectively).

Table A1: MDV values obtained in Isotopomer analysis in Aspartate, Threonine, and lysine

Reductive TCA Amino Acids ^{13}C-Labeling Distribution			
	M+0	M+1	M+2
Aspartate	0.28	0.56	0.16
Threonine	0.22	0.58	0.15
Lysine	0.34	0.51	0.12

This is consistent with the distribution observed for Succinate (24%, 57%, 16%) for M+0, M+1, and M+2, the respective presence of M+2 values in these amino acid indicates cate 2 labelled carbons in Oxaloacetate, Malate, Fumarate, and Succinate. The positions of labelled carbons were confirmed by comparing M-57 and M-159 MDV values. Reduction in M-159 values in M+2 MDV fractions in amino acids signifies labelled carbon at α and ß carboxylic ends of the metabolite. Feng et al. 2009 studied 1-^{13}C pyruvate as a carbon source in the central metabolite pathway. MDV values obtained in Feng et al. 2009 study

were similar to the pattern obtained in the present study, but $1\text{-}^{13}C$ pyruvate was not the source of labelled carbon in the present study.

The reductive TCA amino acid ^{13}C-labeling distribution provides evidence that oxaloacetate M+2 must be generated since malic enzyme and phosphoenolpyruvate carboxy kinase are known to be reversible, and in doing so, decarboxylate pyruvate. Pep-derived amino acids labelling pattern was examined. While the most abundant isotopomer was M+0 (~80%; xylose derived carbon), approximately 20% were found to be M+1 (transient-carbon-transition) in Alanine (Table 2).

Table A2: MDV values obtained in Isotopomer analysis in Aspartate, Threonine, and lysine

Pyruvate Precursor Amino Acids ^{13}C-Labeling Distribution			
	M+0	**M+1**	**M+2**
Alanine	0.80	0.19	0.006
Serine	0.87	0.12	0.006
Pyruvate Precursor Amino Acids ^{13}C-Labeling Distribution			
Phenylalanine	0.79	0.19	0.004

This implies that the transient-carbon-transition of pyruvate and PEP enables a second round of carboxylation, enabling oxaloacetate/malate M+2. 20% transient-carbon-transition of pyruvate and PEP is slightly higher than the M+2 reductive TCA amino acids (~15%).

Labelled carbon dioxide assimilates in Oxaloacetate and Malate via anaplerotic pathways is fixed at the carboxylic group of these metabolites, which adds to one carbon labelling in the Oxaloacetate and Malate. Decarboxylation of oxaloacetate and Malate to PEP and Pyruvate, respectively via Malate dehydrogenase enzyme leads to loss of labelled carbon.

However, Alanine labelling confirms the presence of labelled carbon at its carboxylic end (Table 2). Oxaloacetate and Malate need to have both their carboxylic ends labelled to prove active cataplerotic pathways from Malate to Pyruvate. Lindsay et al. 2019 showed the transition of carbon in the TCA cycle wherein the Fumarate to Malate reaction can lead to either of Malate isotopologues, and further Malate to Oxaloacetate reaction will lead to the formation of two possible Oxaloacetate isotopologues. Formation of isotopologues has 50% probability, and hence there is a 50% probability of labelled carbons at α carboxylic end and 50% carbons at β carboxylic ends. When Malate at α carboxylic end transitions combine with labelled Carbon dioxide to form oxaloacetate, this oxaloacetate has labelled carbon at both carboxylic ends (Figure 9b). Hence as Malate formed from Fumarate can form either of isotopologues because M+2 values were observed in Succinate and other TCA cycle amino acids.
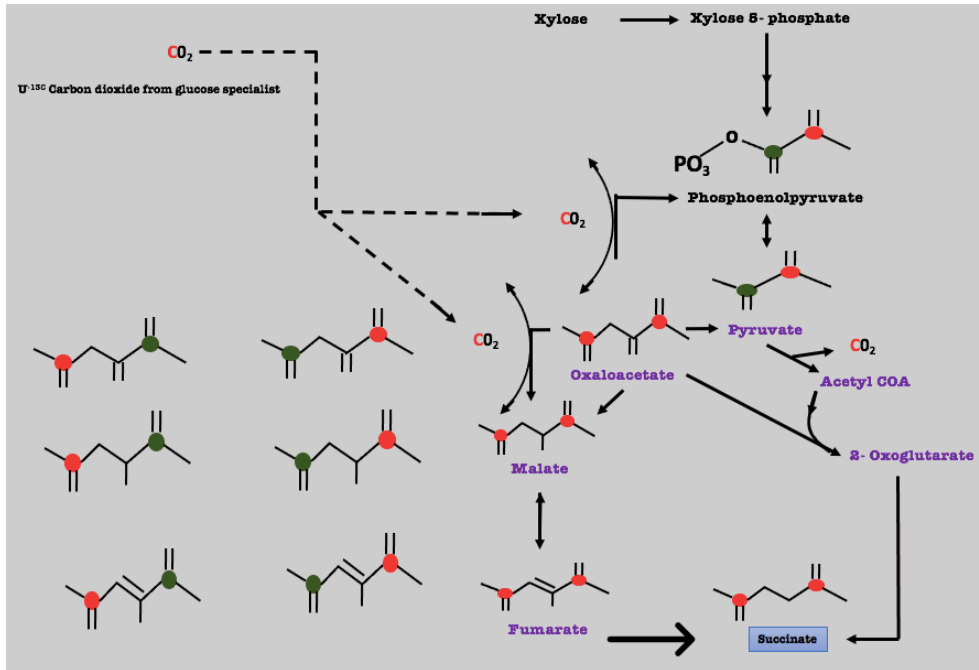
A)
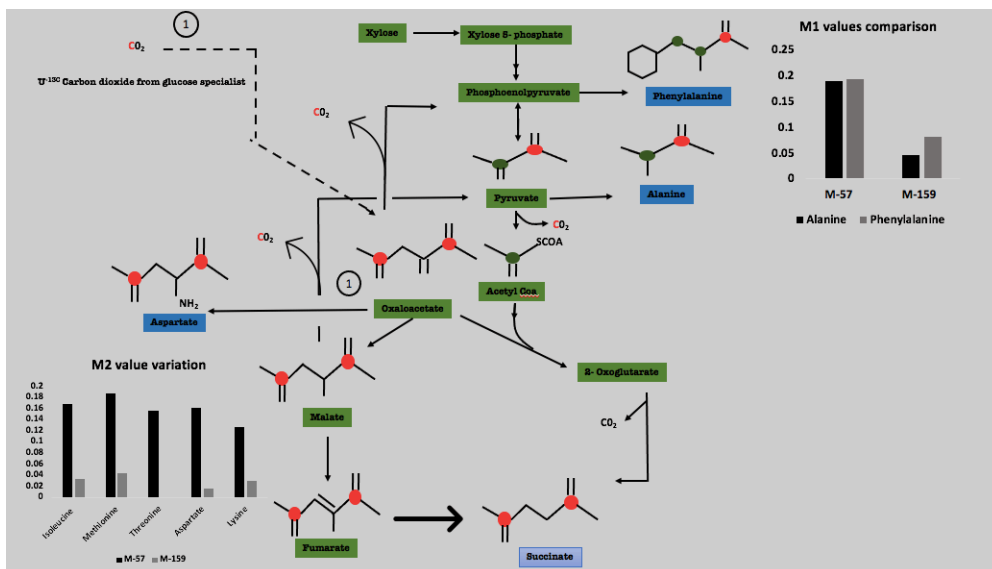
B)

Figure A8: Schematic of carbon transition in the central metabolic pathway. X2S strain was enriched with ^{13}-C Carbon dioxide entering from reactor 1 in the dual-chamber and ^{12}C xylose (3 g/L) added in reactor 2 to understand Xylose assimilation in G2E strain (Figure 2). M1 values are M+1 MDV values describing 1 carbon labelled fraction, and M2 values are M+2 MDV values denoting 2 carbon labelled fractions in biomass. A) Carbon labelling in central metabolic pathways based on MDV (M-159 and M-57) values obtained in Isoleucine, Threonine, Aspartate, Lysine, Methionine, Alanine, and Phenylalanine. B) Figure describing stereoisomeric metabolites contribute to two carbon values in TCA cycle amino acids.

3. 4. Conclusion

U-^{13}C Isotopomer studies can be effective tools in studying assimilation patterns, carbon transition in metabolic pathways, and studying active pathways in a state of stress. Aromatics assimilation was observed in *C. glutamicum.* Among different aromatic derivatives studied, coumaric acid showed the highest assimilation and hence highest dilution in labelling (67% and 48% reduction in glutamate and aspartate). Effect of stringent response was studied in *E. coli* mutants, which showed biosynthesis of essential amino acids like Histidine, which was coherent with the genome sequencing data. Also, U-^{13}C Isotopomer studies in *E. coli* coculture helped develop a carbon transition map in the central metabolic pathway.

References

Ahn, Jung Ho, Yu Sin Jang, and Sang Yup Lee. 2016. "Production of Succinic Acid by Metabolically Engineered Microorganisms." *Current Opinion in Biotechnology*.

Brown, Alan, Israel S. Fernández, Yuliya Gordiyenko, and V. Ramakrishnan. 2016. "Ribosome-Dependent Activation of Stringent Control." *Nature*.

Chatterji, Dipankar, and Anil Kumar Ojha. 2001. "Revisiting the Stringent Response, PpGpp, and Starvation Signaling." *Current Opinion in Microbiology*.

Feng, Xueyang et al. 2009. "Characterization of the Central Metabolic Pathways in Thermoanaerobacter Sp. Strain X514 via Isotopomer-Assisted Metabolite Analysis." *Applied and Environmental Microbiology* 75(15): 5001–8.

Flores, Andrew D. et al. 2020. "Catabolic Division of Labor Enhances Production of D-Lactate and Succinate From Glucose-Xylose Mixtures in Engineered Escherichia Coli Co-Culture Systems." *Frontiers in Bioengineering and Biotechnology*.

Inui, Masayuki et al. 2005. "Metabolic Engineering of Corynebacterium Glutamicum for Fuel Ethanol Production under Oxygen-Deprivation Conditions." *Journal of Molecular Microbiology and Biotechnology*.

Jain, Vikas, Manish Kumar, and Dipankar Chatterji. 2006. "PpGpp: Stringent Response and Survival." *Journal of Microbiology*.

Kremling, A., J. Geiselmann, D. Ropers, and H. de Jong. 2015. "Understanding Carbon Catabolite Repression in Escherichia Coli Using Quantitative Models." *Trends in Microbiology*.

Okino, Shohei et al. 2008. "Production of D-Lactic Acid by Corynebacterium Glutamicum under Oxygen Deprivation." *Applied Microbiology and Biotechnology*.

Shen, Xi Hui, Ning Yi Zhou, and Shuang Jiang Liu. 2012. "Degradation and Assimilation of Aromatic Compounds by Corynebacterium Glutamicum: Another Potential for Applications for This Bacterium?" *Applied Microbiology and Biotechnology* 95(1): 77–89.

Tang, Joseph Kuo Hsiang, Le You, Robert E. Blankenship, and Yinjie J. Tang. 2012. "Recent Advances in Mapping Environmental Microbial Metabolisms through 13C Isotopic Fingerprints." *Journal of the Royal Society Interface*.

Tang, Y., Shui, W., Myers, S., Feng, X., Bertozzi, C., Keasling, J. 2009. Central metabolism in Mycobacterium smegmatis during the transition from O2-rich to O2-poor conditions as studied by isotopomer-assisted metabolite analysis. *Biotechnology Letters*, **31**(8), 1233-1240.

Tang, Kuo Hsiang et al. 2010. "Carbon Flow of Heliobacteria Is Related More to Clostridia than to the Green Sulfur Bacteria." *Journal of Biological Chemistry*.

Varman, Arul M., Yi Yu, Le You, and Yinjie J. Tang. 2013. "Photoautotrophic Production of D-Lactic Acid in an Engineered Cyanobacterium." *Microbial Cell Factories* 12(1): 1–8.

Varman, Arul M et al. 2016. "Decoding How a Soil Bacterium Extracts Building Blocks and Metabolic Energy from Ligninolysis Provides Road Map for Lignin Valorization."

Varman, A.M., He, L., Follenfant, R., Wu, W., Wemmer, S., Wrobel, S.A., Tang, Y.J., Singh, S. 2016. Decoding how a soil bacterium extracts building blocks and metabolic energy from ligninolysis provides road map for lignin valorization. *Proc Natl Acad Sci U S A*, **113**(40), E5802-E5811.

Varman, A.M., He, L., You, L., Hollinshead, W., Tang, Y.J. 2014. Elucidation of intrinsic biosynthesis yields using ^{13}C-based metabolism analysis. *Microb Cell Fact*, **13**(1), 42.

Wahl, S.A., Dauner, M., Wiechert, W. 2004. New tools for mass isotopomer data evaluation in (13)C flux analysis: mass isotope correction, data consistency checking, and precursor relationships. *Biotechnol Bioeng*, **85**(3), 259-68.

Wang, Chen et al. 2014. "Succinic Acid Production from Corn Cob Hydrolysates by Genetically Engineered Corynebacterium Glutamicum." *Applied Biochemistry and Biotechnology*.

Wiechert, Wolfgang. 2001. "13C Metabolic Flux Analysis." *Metabolic Engineering*.

Xiao, Y., Feng, X., Varman, A.M., He, L., Yu, H., Tang, Y.J. 2012. Kinetic modeling and isotopic investigation of isobutanol fermentation by two engineered escherichia coli strains. *Industrial and Engineering Chemistry Research*, **51**(49), 15855-15863.

Young, Jamey D, Avantika A Shastri, Gregory Stephanopoulos, and John A Morgan. 2011. "Mapping Photoautotrophic Metabolism with Isotopically Nonstationary C Flux Analysis." *Metabolic Engineering* 13(6): 656–65. http://dx.doi.org/10.1016/j.ymben.2011.08.002.

You, L., Page, L., Feng, X., Berla, B., Pakrasi, H.B., Tang, Y.J. 2012. Metabolic Pathway Confirmation and Discovery Through 13C-labeling of Proteinogenic Amino Acids. *J. Vis. Exp.*(59), e3583.

Zamboni, Nicola, Sarah Maria Fendt, Martin Rühl, and Uwe Sauer. 2009. "13C-Based Metabolic Flux Analysis." *Nature Protocols*.

Zamboni, Nicola, and Uwe Sauer. 2009. "Novel Biological Insights through Metabolomics and 13C-Flux Analysis." *Current Opinion in Microbiology*.

APPENDIX B

CONSOLIDATED BIOPROCESSING OF HEMICELLULOSE TO FUELS AND
CHEMICALS THROUGH AN ENGINEERED BACILLUS SUBTILIS-ESCHERICHIA
COLI CONSORTIUM (SUPPLEMENTARY DATA)

Materials and methods

Determination of optimal pH of endo-1,4-β-xylanase producing strain supernatant
Recombinant strain SSL27 and wildtype WB800N strain was cultured overnight in 2xYT media. The seed was sub cultured the next day and induced at OD_{600} 0.8. The induced cultures were grown for 24 hours. The fermentation broth was centrifuged after 24 hours and the supernatant was isolated. The supernatant (20 µL) was added to beechwood xylan substrate (20 µL) made in citrate phosphate buffer (pH 3, 4, 5, 6, 7). After 60 mins of enzyme reaction, the reaction product was analyzed using DNSA assay as shown in the manuscript.

3M media used for *in situ* beechwood xylan depolymerization and coculture fermentation
Modifications in M9 media were made after optimal pH 6 was determined using previous results. The newly developed media is called 3M media. This media was mainly used in *in situ* beechwood xylan fermentation and sequential coculture fermentation. The media was customized for no sporulation, increased protein secretion, and optimal pH.

1. Supplementary figures
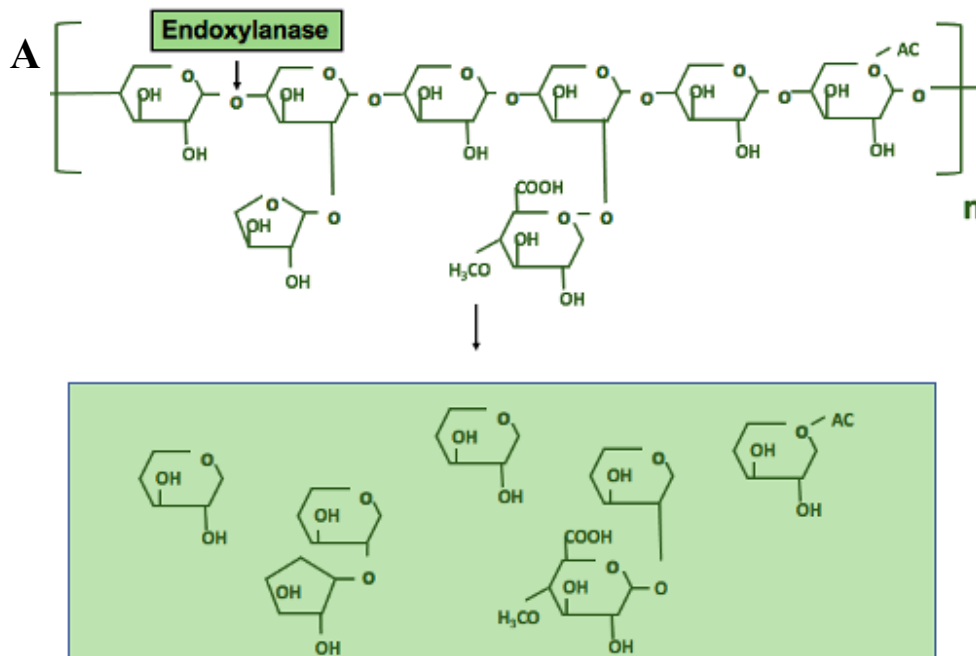
Fi   S1: Schematic drawing of the enzymatic reactions involved in the breakdown of hemicellulose and cellulose biopolymers by hydrolytic enzymes. A) Endo-1,4-β-xylanase enzyme cleaves glycosidic bonds forming the backbone of the xylan structure. Endo-1,4-β-xylanase breaks down the xylan structure into xylose and dimeric structures of xylose-acetyl groups, xylose-arabinose and xylose-glucuronic acid etc
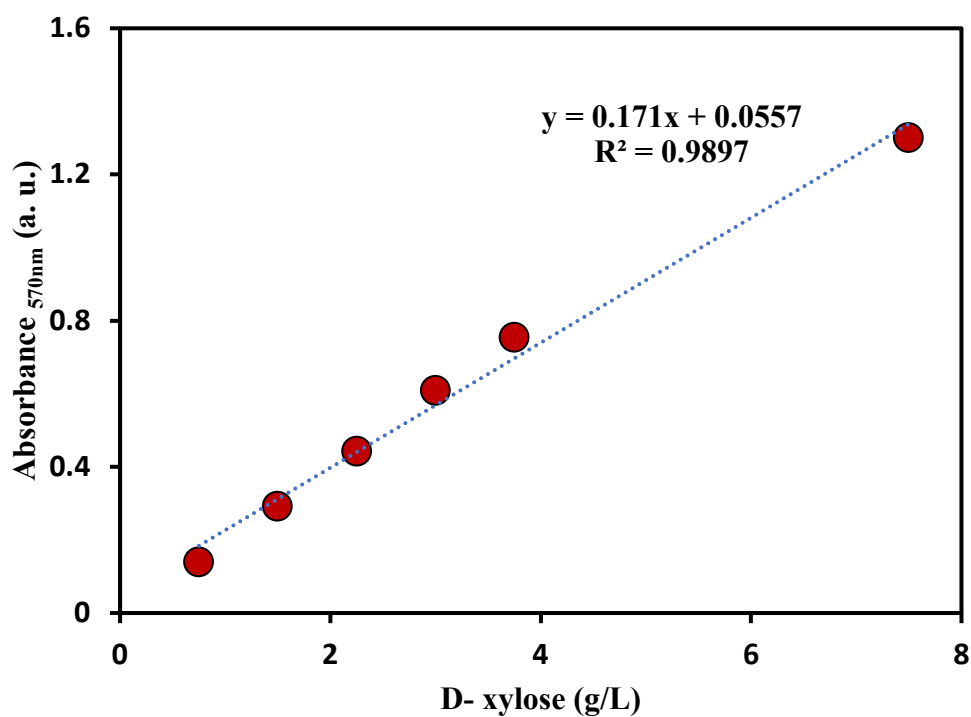
Figure S2: Calibration curve developed for D- xylose using varying D- xylose concentrations (g/L) denoted on the y axis and absorbance 570 nm denoted on the x-axis. Different D-xylose concentrations were developed in citrate phosphate buffer (pH 6) between the range 0.75 g/L to 7.5 g/L. Developed standards (40 μL) were added in DNS (160 μL) and the reaction was conducted for 20 mins at 100 °C.
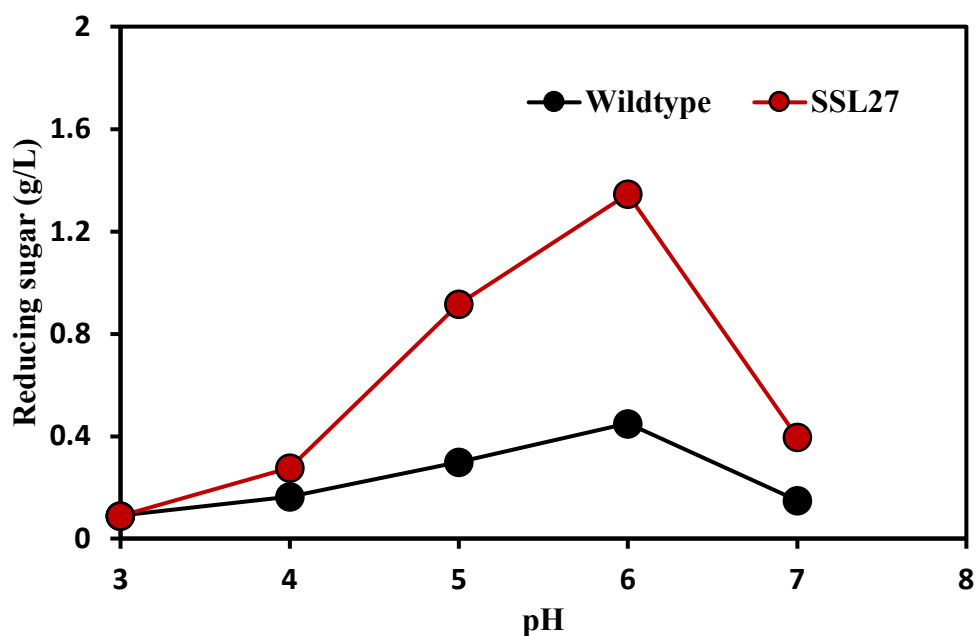
Figure S3: Reducing sugar (g/L) titer at different pH (3, 4, 5, 6, 7) between wildtype supernatant and SSL27 supernatant containing Xyn2. Supernatant samples obtained after induction (1 mM IPTG) were used in the enzyme reaction (1 % beechwood xylan substrate) at different pH to determine the optimal pH for further *insitu* experiments. The figure shows a significant difference in reducing sugar titer (g/L) between wild-type and SSL27 recombinant strain. The optimal pH observed in this experiment was 6 and it was further used to maintain pH 6 in 3M media used in *in situ* beechwood xylan depolymerization.
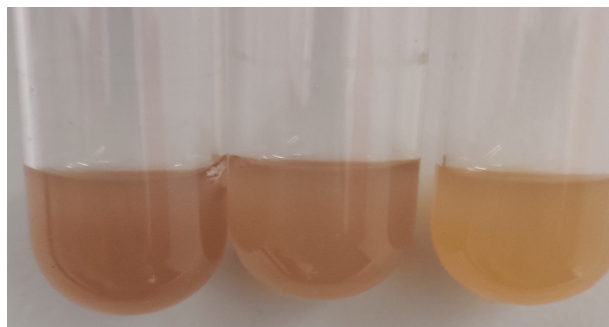
A
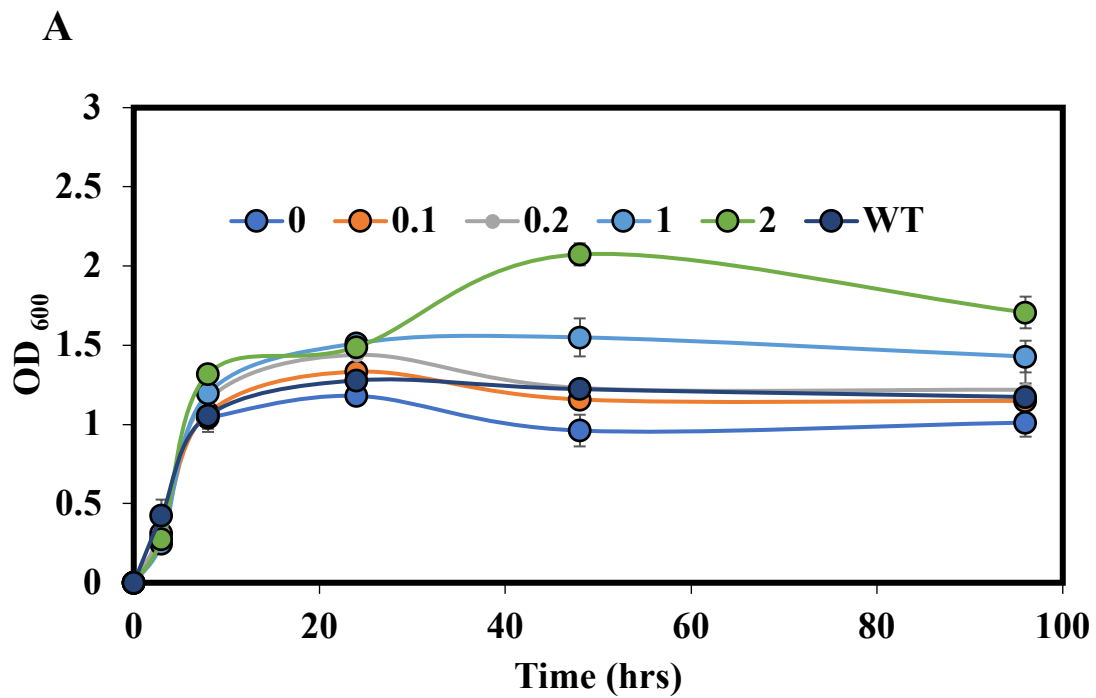
B

Figure S4: Variation in the growth of engineered SSL26 strains at varying IPTG concentrations A) Growth kinetics of SSL26 strain induced at different IPTG concentrations (0, 0.1, 0.2, 1, and 2 mM). SSL26 strain cultured in 3M media and induced at varying IPTG concentration at OD 600 of 0.8 and cultured further for 96 hours. The OD $_{600}$ readings were taken at 8, 24, 48, and 96 hours. B) Picture showing sporulation in higher IPTG concentrations (2 mM and 1 mM) wherein three tubes shown are SSL26 strains grown at 0.2 mM, 1 mM and 2 mM IPTG concentrations from right to left direction.
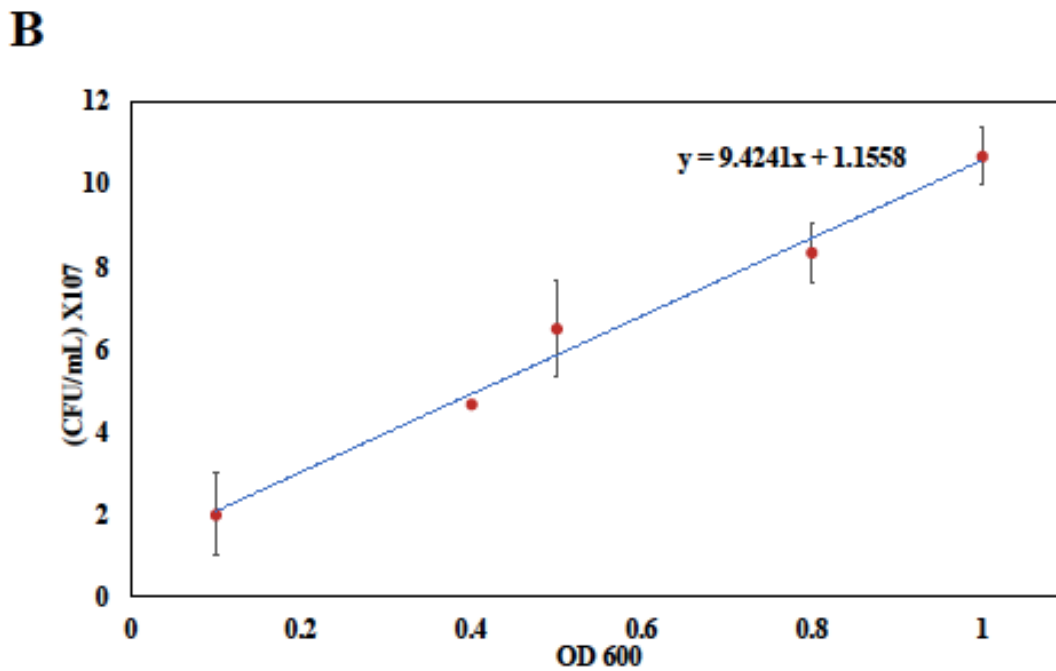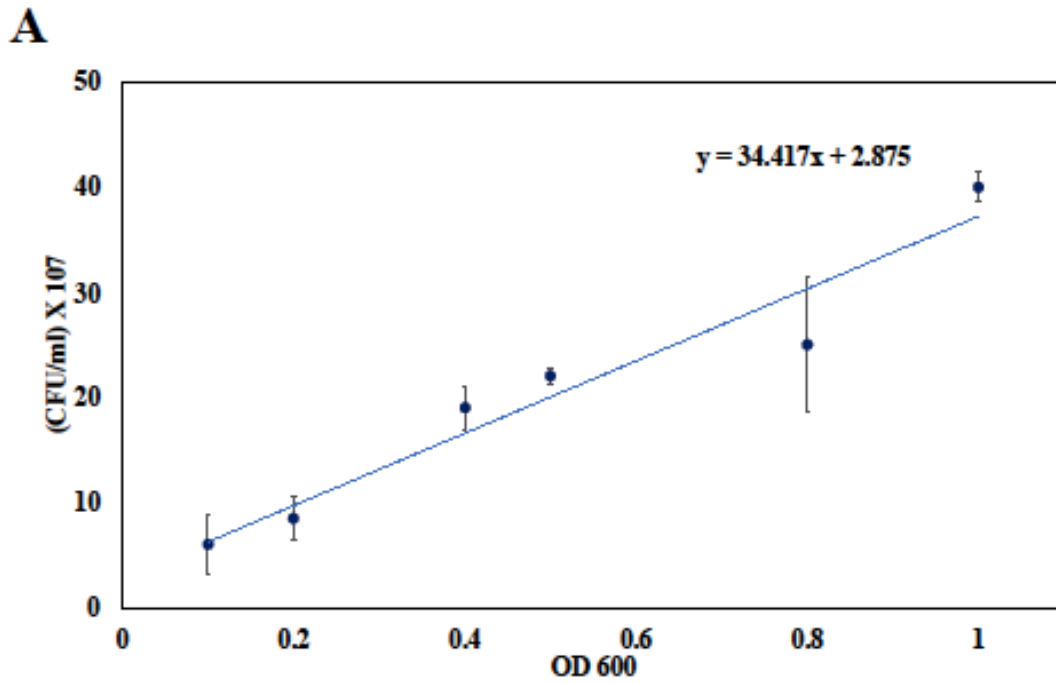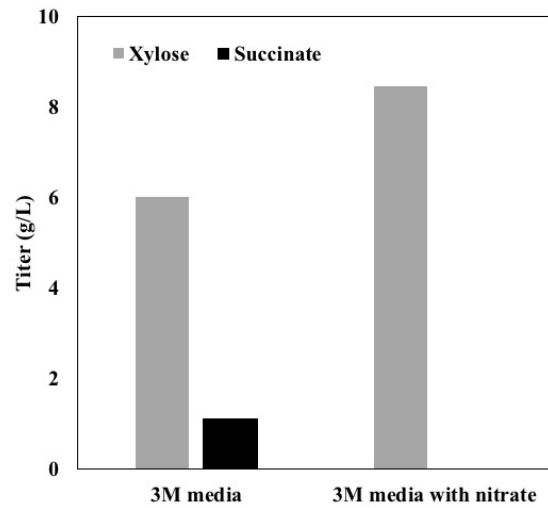
Figure S5: Calibration curve correlation between Colony forming units (CFU)/mL vs OD $_{600}$ A) Calibration curve correlating OD $_{600}$ vs CFU/mL for *E.coli* Dh5a strain (mean ± SD; n=3)

146

B) Calibration curve correlating OD $_{600}$ vs CFU/mL for *B. subtilis* WB800N strain (mean ± SD; n=3)
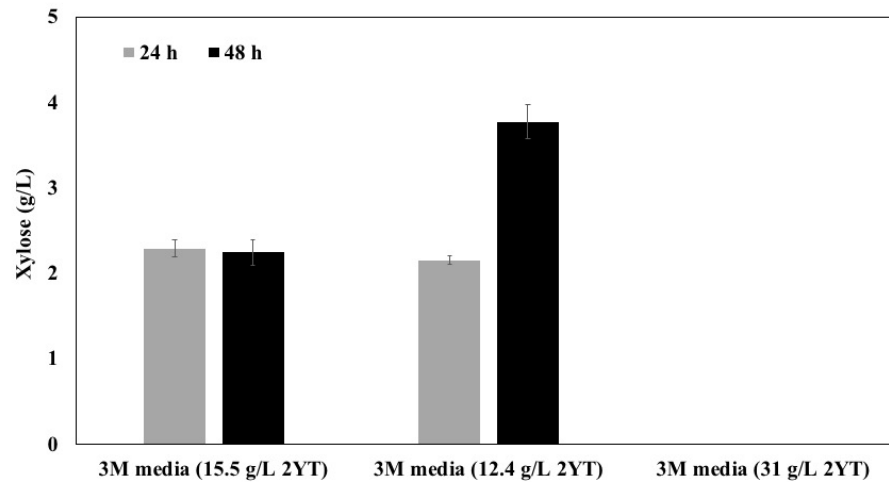
A

B

Figure S6: Effect of different media components on coculture fermentations. A) Effect of nitrate addition on xylose (g/L) and succinate (g/L) titres. B) Effect of 2xYT media concentrations on xylose production in 1% corn stover xylan fermentations.

Table S1: Oligonucleotide sequences used in present study

Primer name	Sequence	Description
pKB01_REV	GGTGATGAGCGACGTCGACTCTAGA TTATTGTCCAATCATCAGCTGGTTG	*ywmC$_{sp}$-xynA* insert reverse primer
pKB01_FWD	GCGGATAACAATTCCCATATAAAGG AGGAAGGATCCATGAAGAAAGATT TTCACTGATCATGATG	*ywmC$_{sp}$-xynA* insert forward primer
pKB02_FWD	GCGGATAACAATTCCCATATAAAGG AGGAAGGATCCATGAAGAAAGATT TTCACTGATCATGATG	*ywmC$_{sp}$-xyn2* insert forward primer
pKB02_REV	GGTGATGAGCGACGTCGACTCTAGA TTAGGACACCGTAATGCTTGC	*ywmC$_{sp}$-xynA* insert reverse primer
AMYE_FWD	GCGGATAACAATTCCCATATAAAGG AGGAAGGATCCATGTTTGCAAAACG ATTCAAAACCTCTTTACTGCCG	*amyE$_{sp}$* insert forward primer for pKB10
AMYE10_REV	CCCGCCAACAGAGACGTAAAAGATA CCATCAGCACTCGCAGCCGC	*amyE$_{sp}$* insert reverse primer
XYN210_FWD	GCGGCTGCGAGTGCTGATGGTATCTT TTACGTCTCTGTTGGCGGG	*xyn2* insert forward primer
XYN210_Rev	GATGGTGATGAGCGACGTCGACTCT AGATTAGGACACCGTAATGCTTGCG GAG	*xyn2* insert reverse primer
SacC_FWD	GAGCGGATAACAATTCCCATATAAA GGAGGAAGGATCCATGAAAAAGAG ACTGATTCAAGTCATGATCATGTTCA CCC	*sacC$_{sp}$* insert forward primer
SacC06_REV	CCCGCCAACAGAGACGTAAAAGATA CCATCTGCATCTGCCGAAAATGCCAT AGTCAAC	*sacC$_{sp}$* insert reverse primer
Xyn206_FWD	GTTGACTATGGCATTTTCGGCAGATG CAGATGGTATCTTTTACGTCTCTGTT GGCGGG	*xyn2$_{sp}$* insert forward primer
Xyn206_REV	GGTGATGAGCGACGTCGACTCTAGA TTAGGACACCGTAATGCTTGCGGAG C	*xyn2$_{sp}$* insert reverse primer

Table S2 Plasmids and strains

Plasmids/strains	Description	Source /reference
pHT254	Backbone plasmid used for development of all the constructs harboring ColE1 Ori, Cm^r and Amp^r	Mobitec, Inc
pKB01	Derived from pHT254 with $ywmC_{sp}$-$xynA$ and P$_{grac100}$ promoter	This study
pKB02	Derived from pHT254 with $ywmC_{sp}$-$xyn2$ and P$_{grac100}$ promoter	This study
pKB06	Derived from pHT254 with $sacC_{sp}$-$xyn2$ and P$_{grac100}$ promoter	This study
pKB10	Derived from pHT254 with amyE_{sp}-$xyn2$ and P$_{grac100}$ promoter	This study
Strains		
E. coli DH5α	Cloning host strain	New England biolabs
X2S	LP001 *Δ*galP glk::Km^r	[58]
X2E	LY180 ΔptsI ΔptsG ΔgalP glk::kan xylR*	[54]
X2L	TG114 ΔptsI ΔptsG ΔgalP glk::kan xylR*	[58]
B. subtilis	WB800N: *nprE aprE epr bpr mpr::ble nprB::bsr Δvpr wprA::hyg cm::neo*	Bacillus Genetic Stock Center
SSL26	*B. subtilis* P$_{grac100}$:: $ywmC_{sp}$-$xynA$::Cm^r	This study
SSL27	*B. subtilis* P$_{grac100}$:: $ywmC_{sp}$-$xyn2$::Cm^r	This study
SSL30	*B. subtilis* P$_{grac100}$:: $amyE_{sp}$-$xyn2$::Cm^r	This study
SSL33	*B. subtilis* P$_{grac100}$:: $sacC_{sp}$-$xyn2$::Cm^r	This study

APPENDIX C

STATEMENT OF CO-AUTHOR PERMISSIONS FOR MANUSCRIPT SHARING IN

THIS DISSERTATION INCLUDED AS CHAPTER 3

I, Apurv Mhatre, hereby declare that all co-authors of the manuscript titled "Consolidated bioprocessing of hemicellulose using *bacillus subtilis*: *escherichia coli* consortia for production of succinic acid", which is published in Renewable energy journal, have granted their permission for the sharing and dissemination of the manuscript in this dissertation as Chapter 3.

I'd like to let you know that each co-author named below has been informed about the intention to share the manuscript in this dissertation. Also, they have explicitly consented to the distribution of the manuscript in its entirety or in part, as deemed appropriate by the corresponding author, with the understanding that their intellectual contributions will be taken care of.

The following co-authors have granted their permissions for manuscript sharing:

1. Bethany Kalscheur

2. Haley Mckeown

3. Karan Bhakta

4. Aditya Sarnaik

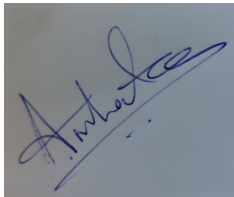5. Andrew Flores

6. David Nielsen

7. Xuan Wang

8. Thiagarajan Soundappan

9. Arul Varman

By signing this statement, I confirm that I have obtained explicit consent from each co-author and am authorized to act on their behalf regarding the sharing and dissemination the manuscript. I understand the responsibility for obtaining these permissions lies with me as the first author.

I want you to know that I acknowledge that this statement does not release me from any obligations or agreements with the journal. I will ensure compliance with all relevant policies, guidelines, and ethical considerations throughout the sharing and publication process.

Signed:

Apurv Mhatre

Arizona State University

06/26/2023